КОЛЛОИДНЫЙ ЖУРНАЛ

POSTMASTER:
IF NOT DELIVERABLE NOTIFY
Chemical Abstracts
OHIO STATE UNIV., COLUMBUS 10, O.
AND POSTAGE WILL BE SENT

REC'D. JUL 30 1958

WITHDRAWN

ABSTRACTOR:
PLEASE RETURN PROMPTLY TO
CHEMICAL ABSTRACTS
OHIO STATE UNIV., COLUMBUS 10, O.

COLLOID JOURNAL

(KOLLOIDNY ZHURNAL)

U.S.S.R.

IN ENGLISH TRANSLATION

VOL. 19 (1957) NO. 5

CONSULTANTS BUREAU, INC.
227 WEST 17TH STREET, NEW YORK 11, N. Y.
an agency for the interpretation of international knowledge

Soviet Research in ION-EXCHANGE CHROMATOGRAPHY
in English translation

Twenty papers by leading Soviet chromatographers covering certain theoretical problems of the application of ion-exchange chromatography, as well as original research and review papers on various applications of ion-exchange resins, particularly in the medicine and food industries. Papers were originally read at a session of the Commission on chromatography, Div. of Chem. Sci., Acad. Sci. USSR, in the fall of 1956, and published in Russian in 1957. English translation, 184 pages, $35.00

TITLES OF REPORTS

The Laminar Method For Approximate Calculation of Chromatograms.
Equations For Ion Exchange Isotherms and Their Experimental Verification.
Absorption of the Cations of Heavy Metals by Anion Exchange Resins.
Principles of Adsorption Technology.
Laws of Adsorption From Solutions Under Dynamic Conditions During Separation of Alkaloids by Means of Ion Exchange Resins.
Ion Exchange of Alkaloids on Synthetic Ion Exchange Resins.
Structure of Cation Exchange Resins, Their Suggested Chemical Structure, and Possible Breakdown Products.
Basic Problems in the Synthesis and Study of Ion Exchange Resins.
The Physicochemical Properties of Ion Exchange Resins.
The Properties of Some Cation Exchange Resins and the Possibility of Using Them in the Medical and Food Industries.
The Properties of Certain Anion Exchange Resins and the Possibility of Using Them in the Medical and Food Industries.
Purification of Certain Chemical Compounds by Means of Ion Exchange Sorbents.
The Possibility of Using Ion Exchange Resins for Obtaining Drinking Water From Water of High Mineral Content.
Purification of Lactic Acid by Means of Ion Exchangers.
Methods for Isolating Anabasine, Spherophysine, and Methyl Caffeine From Plant Raw Material and Mother Liquors by Means of Ion Exchangers.
Elution Curves of Morphine During Ion Exchange Chromatography on Cation Exchangers.
The Application of Ion Exchange Adsorbents in Pharmaceutical Analysis.
Absorption of Streptomycin by the Hydrogen and Hydrogen Salt Forms of Carboxylic Cation Exchangers.
The Use of Ion Exchange Sorbents for Preventing Blood Clotting.
Separation of Cadmium and Copper, Cadmium and Lead, and Cadmium and Bismuth by Ion Exchange Chromatography.

Consultants Bureau's translations by bilingual scientists. Clear reproduction by multilith process from IBM cold-type, including all diagrammatic and tabular material; books staple bound in durable paper covers.

CONSULTANTS BUREAU, INC.
227 West 17th Street, New York 11, N. Y.
Telephone: AL 5-0713 Cable: CONBUREAU NEWYORK

COLLOID JOURNAL

(KOLLOIDNYI ZHURNAL)

Journal of Theoretical and Applied Physics and
Chemistry of Colloids

Volume XIX

(Number 5, September-October, 1957)

Editor

A. V. Dumansky

Editorial Board

P. N. Antipov-Karataev, B. V. Deryagin, B. A. Dogadkin (Deputy Editor), A. V. Dumansky,
V. A. Kargin, S. M. Lipatov, P. A. Rebinder, I. P. Serdobolsky (Secretary), M. P. Volarovich

Publication of the Academy of Sciences of the USSR

IN ENGLISH TRANSLATION

Copyright, 1958

CONSULTANTS BUREAU, INC.
227 West 17th Street
New York 11, N. Y.

Printed in the United States

Annual Subscription . . . . $ 80.00
Single issue 20.00

Note: The sale of photostatic copies of any portion of this copyright translation is expressly prohibited by the copyright owners. A complete copy of any paper in this issue may be purchased from the publisher for $ 7.50.

SIGNIFICANCE OF ABBREVIATIONS MOST FREQUENTLY ENCOUNTERED IN SOVIET PERIODICALS

FIAN	Phys. Inst. Acad. Sci. USSR.
GDI	Water Power Inst.
GITI	State Sci.-Tech. Press
GITTL	State Tech. and Theor. Lit. Press
GONTI	State United Sci.-Tech. Press
Gosenergoizdat	State Power Press
Goskhimizdat	State Chem. Press
GOST	All-Union State Standard
GTTI	State Tech. and Theor. Lit. Press
IL	Foreign Lit. Press
ISN (Izd. Sov. Nauk)	Soviet Science Press
Izd. AN SSSR	Acad. Sci. USSR Press
Izd. MGU	Moscow State Univ. Press
LEIIZhT	Leningrad Power Inst. of Railroad Engineering
LET	Leningrad Elec. Engr. School
LETI	Leningrad Electrotechnical Inst.
LETIIZhT	Leningrad Electrical Engineering Research Inst. of Railroad Engr.
Mashgiz	State Sci.-Tech. Press for Machine Construction Lit.
MEP	Ministry of Electrical Industry
MES	Ministry of Electrical Power Plants
MESEP	Ministry of Electrical Power Plants and the Electrical Industry
MGU	Moscow State Univ.
MKhTI	Moscow Inst. Chem. Tech.
MOPI	Moscow Regional Pedagogical Inst.
MSP	Ministry of Industrial Construction
NII ZVUKSZAPIOI	Scientific Research Inst. of Sound Recording
NIKFI	Sci. Inst. of Modern Motion Picture Photography
ONTI	United Sci.-Tech. Press
OTI	Division of Technical Information
OTN	Div. Tech. Sci.
Stroiizdat	Construction Press
TOE	Association of Power Engineers
TsKTI	Central Research Inst. for Boilers and Turbines
TsNIEL	Central Scientific Research Elec. Engr. Lab.
TsNIEL-MES	Central Scientific Research Elec. Engr. Lab.—Ministry of Electric Power Plants
TsVTI	Central Office of Economic Information
UF	Ural Branch
VIESKh	All-Union Inst. of Rural Elec. Power Stations
VNIIM	All-Union Scientific Research Inst. of Meteorology
VNIIZhDT	All-Union Scientific Research Inst. of Railroad Engineering
VTI	All-Union Thermotech. Inst.
VZEI	All-Union Power Correspondence Inst.

Note: Abbreviations not on this list and not explained in the translation have been transliterated, no further information about their significance being available to us. — Publisher.

DEVELOPMENT OF COLLOID CHEMISTRY IN THE USSR

Prior to the Great October Socialist Revolution, only a relatively small number of people carried on systematic research in the field of colloid chemistry in Russia (A.V. Dumansky, V.V. Kurilov, P.P. Weimarn, N.P. Peskov, and N.A. Shilov. There were hardly any scientific institutions dealing with problems of colloid chemistry. Lectures in colloid chemistry were first given in 1912 by A.V. Dumansky in the University of Kiev. However, views on colloidal systems and their characteristics were advanced in Russia even in the earliest days of the science. For example, as long ago as 1869, Prof. I.G. Borshchov of Kiev University devised a more complete characterization of colloidal systems than had been produced abroad. The rheological properties of colloid solutions were studied in 1889 by Prof. F.N. Shvedov of Odessa University, who showed that dilute gelatin solutions do not obey the Maxwell relaxation equation but, in contrast to true viscous liquids, have a region of elastic deformations which persist for considerable periods.

After the October Socialist Revolution, the scientists of the Soviet Union were confronted with wide possibilities for free and full creative activity. Several scientific research institutes were established for rapid development of research and for training numerous scientific workers. The first Soviet groups of research workers in various branches of colloid chemistry were formed in the laboratories of N.A. Shilov, A.V. Dumansky, N.P. Peskov, A.I. Rabinovich, I.I. Zhukov, P.A. Rebinder and S.M. Lipatov. These laboratories were centers for the training of young specialists, many of whom became eminent scientists (V.A. Kargin, L.K. Lepin, and others). Simultaneously with this, numerous centers of research into topical problems directly related with the theory of colloid chemistry arose in many Universities and industrial undertakings of the Soviet Union (V.A. Naumov, S.I. Sokolov, B.A. Dogadkin, M.P. Volarovich, I.N. Antipov-Karataev, A.G. Pasynsky, A.I. Rabinerson, S.A. Voznesensky, V. I. Nazarov, S.G. Mokrushin, N. F. Ermolenko, S. S. Voyutsky, S. A. Glikman, and others).

The number of published papers on colloid chemistry rose sharply; between 1869 and 1917 only 234 papers were published by 50 authors, whereas between 1917 and 1952 6410 papers by nearly 1000 authors were published.

The most vigorous development of colloid chemistry in the Soviet Union was seen during the period of industrialization and during the early Five-Year Plans. During this period a number of applied problems of colloid chemistry was studied in addition to theoretical work. The number of laboratories increased both in the applied and in the fundamental scientific institutes.

In 1929 V.A. Kistyakovsky organized a colloido electrochemical laboratory, which was reorganized in 1935 as an institute under the same title. The extensive work of P.A. Rebinder on the physical chemistry of surface layers and disperse systems, and of B. V. Deryagin on the properties of thin liquid films and surface forces, has been developed in this institute.

The growth of the Colloid Chemistry Laboratory of the Voronezh Agricultural Institute was such that in 1932 it was reorganized as the All-Union Scientific Research Institute for Colloid Chemistry (Director A. V. Dumansky). The first All-Union Conference on the physical chemistry of colloids was held in 1934 in Voronezh at this Institute. The Conference indicated the course of the further development of colloid chemistry in the USSR, and approved A. V. Dumansky's proposals that a special colloid journal should be produced (this commenced publication in 1935) and that All-Union Conferences on colloid chemistry should be held periodically.

At that time the new synthetic rubber industry was beginning to develop in the Soviet Union. The first factory in the world for the production of sodium butadiene rubber, based on the classic researches of S. V. Lebedev, commenced production. Development of the synthetic rubber industry and of a number of other branches of industry (rubber, plastics, synthetic fibers and films) stimulated extensive colloidochemical and physicochemical researches on high polymers and their solutions.

In May 1937 a conference on lyophilic colloids was held in Moscow; attention was drawn to the importance of research on lyophilic systems, studies of interactions between the disperse phase and the medium, the structure of high polymers, and to the need for close coordination between physicochemical research on high polymers and the problems of organic chemistry and physics in this field.

The XVIIIth Congress of the All-Union Communist Party (Bolsheviks) presented the Soviet people with new important tasks for the further mighty development of the productive forces of the country. In consequence, numerous research institutes and universities, with highly qualified staffs available, directed their efforts to the solution of the most important theoretical and practical scientific problems. From that time research on colloid chemistry became increasingly closely associated with the demands of the national economy. New theoretical problems were studied in order to fulfill successfully the practical tasks of socialist industry.

During the years of the Great Patriotic War, Soviet scientists carried out numerous investigations relating to the defense industries and military needs.

After the end of the War, the scientific institutions for colloid chemistry started work on current problems directly related to restoration of the national economy. In 1945 a scientific conference on colloid chemistry in the food industry was held in Moscow. The number of publications grew rapidly. Colloid Journal, the publication of which was suspended during the War, resumed publication in 1946, under the Academy of Sciences USSR Press.

The organization of colloid and high polymer sections of the Moscow Section of the D.I. Mendeleev All-Union Chemical Society helped to unite scientists working in these respective fields.

In 1950 the Second All-Union Conference on Colloid Chemistry was held in Kiev; numerous papers were presented, mainly on the mechanical properties of disperse systems, the structure and properties of high polymers, solvation, properties of solvate layers, intermolecular forces, and stability of lyophobic colloids and suspensions. Conferences on high polymers, both on special aspects and on general questions of polymer chemistry, physics, and technology, have been regularly held.

The Third All-Union Conference on Colloid Chemistry was held in 1953 in Minsk. 62 papers were discussed, mainly on the following principal topics: the structure of disperse systems and their rheological properties, the stability of colloidal solutions, suspensions, and emulsions, the properties of thin layers at interphases, the properties of high polymers, and various applications of colloid chemistry in the national ecomy.

The successful development of colloid chemistry in the USSR is helped by direct contacts between many specialists in this field and industry, and the wide adoption of the results of scientific research in the national economy. In the place of the few laboratories of the prerevolutionary era, there are numerous laboratories in the universities and scientific research institutes in which vigorous work is done on colloid chemistry.

Let us examine some of the problems studied during the 40 years of Soviet power.

Most of our scientists were interested in the fundamental question of the stability of colloid systems. N. P. Peskov studied coagulation and aging of sols. He introduced the concepts of kinetic and aggregative stability. N. P. Peskov also attached great importance to questions of solvation. The problem of the stability of colloid systems was extensively studied by P. A. Rebinder and B. V. Deryagin.

A. V, Dumansky established that in the production of sols in chemical reactions micelle formation is preceded by formation of complex compounds, and that the micelle formed has an ionogenic complex based on these complex compounds. For a study of colloid systems from this viewpoint, a detailed investigation was made of the formation of hydrosols of heavy metal hydroxides in presence of hydroxy compounds and alkalies. A number of scientists cooperated in this research; S. I. Dyachkovsky, A. P. Buntin, A. G. Kniga, and S. E. Kharin worked in their respective departments on the stability and structure of sols. Several quantitative determinations of the water bound with the disperse phase were made, and the mechanism of water binding was examined. The heats of wetting (E.F. Nekryach, F. D. Ovcharenko), variations of dielectric constant (O. D. Kurilenko), and effects associated with the lyophilic properties of colloids were also studied. Original methods for preparation of metal organosols were developed, and the conditions for their stability were studied (E. M. Natanson).

Extensive work was done at the L. Ya. Karpov Physicochemical Institute by A. I. Rabinovich, V. A. Kargin, and their associates. The studies dealt mainly with electrochemical processes in lyophobic sols. This work led to a better understanding of the structure of micelles, and helped to develop the theory of coagulation in presence of electrolytes. A. I. Rabinovich and V. A. Kargin used the potentiometric titration method to make a detailed study of the coagulation mechanism of hydrophobic sols, and advanced and confirmed the view that the stability of hydrophobic sols and their selective sensitivity to different electrolytes are difficult to explain by physical models only; it is necessary to study chemical processes occurring between the disperse phase and the electrolytes of the dispersion medium during coagulation.

Interesting work has been done on highly purified sols and on electron microscopy of micelle structure at the instant of formation. It was shown that the particles of the disperse phase of a number of inorganic compounds originate from solutions in the form of amorphous spherical relatively large formations; these crystallize only later, and disintegrate into particles of colloidal dimensions.

V. A. Kargin, S. M. Lipatov, and B. A. Dogadkin began their investigations of the physicochemical properties of high polymers in the 1930 's.

I. I. Zhukov organized a scientific research laboratory for colloid chemistry in Leningrad University, and from 1926 he worked there with his pupils on the emulsifying properties of gelatin. Subsequent investigations dealt with synthetic rubbers, alginic acid, and its derivatives. The extensive work of Zhukov and his school on electrokinetic phenomena is particularly important.

S. M. Lipatov has worked systematically on problems of the lyophilic nature of disperse systems since 1925. It was shown that the syneresis effect is associated with a tendency of the system to reach a state of thermodynamically stable equilibrium. The work of S. M. Lipatov and his associates (A. A. Morozov, I. N. Putilova) has provided explanations for many processes of gel formation and gel structure. These authors consider that lyophilic colloidal systems –high polymers – are complex polydisperse systems consisting of a number of adsorptively interacting fractions.

The work of N. F. Ermolenko on swelling in high polymer systems should also be mentioned.

It was later established, by the work of B.A. Dogadkin, V.A. Kargin and their associates (A. A. Tager and S. P. Papkov) that polymers form true solutions which are thermodynamically stable systems.

P. A. Rebinder and his associates (A. B. Taubman, E. K. Venstrem, K. F. Zhigach, N. N. Serb-Serbina, and others) have carried out numerous important investigations in a variety of directions; in general these are all associated with the influence of surface phenomena on disperse systems and their stability. Extensive investigations on the wetting of solid surfaces have led to the concept of selective wetting, and have shown that this quantity is a quantitative characteristic of the molecular nature of the solid phase. Investigations of all aspects of the influence of surface layers on the properties of suspensions, emulsions, foams, and colloidal systems, carried out by means of new methods, were used for stydying the possibility of regulating technological processes. Studies of the influence of the medium on the mechanical properties of solids have great significance. In this field, the effect of adsorptional decrease of strength was discovered. In recent years, the work of P.A. Rebinder and his school (N.E. Segalova, N. N. Serb-Serbina, B. Ya. Yampolsky) has been directed toward studies of the eleasticoplastic properties of a great variety of structurized systems.

Mention should be made of the work of A.A. Trapeznikov on the elasticoviscous properties of monolayers of various compounds and the effects of various factors on their structural and mechanical properties.

N. A. Figurovsky developed convenient methods of sedimentation analysis, which have been extensively adopted.

In the field of rheology, mention must be first made of the investigations of M.P. Volarovich and his associates (D. M. Tolstoi, A. M. Gutkin, V. L. Valdman, and others), who developed new methods for measurement of viscosity and flow limit of highly viscous and viscoplastic bodies, and studied the structuromechanical properties of a number of different disperse systems. Their methods have been widely adopted.

B. A. Dogadkin and his associates (M. M. Reznikovsky, K. A. Pechkovskaya, Z. N. Tarasova, A. S. Novikov, V. E. Gul) have carried out investigations on rubber. The viscosity, structure formation, and structuromechanical properties of rubbers with and without fillers have been studied in detail.

G. V. Vinogradov and his associates designed original instruments for studying flow processes in lubricant greases at various velocities and temperatures, and also hydrophobization of clays and other mineral adsorbents. D. S. Velikovsky, M. P. Volarovich, G. I. Fuks, and others studied colloidochemical processes in lubricating materials. Problems of adsorption have been successfully studied by M.M. Dubinin and his school and by A. V. Kiselev.

The large number of investigations on high polymers has already been mentioned. Here we will refer only to certain studies of latexes, of general significance in colloid chemistry (B. A. Dogadkin, S. S. Voyutsky, D. M. Sandomirsky, A. A. Yurzhenko). Extensive work on rubber and other polymers has been done by P. P. Kobeko, A. P. Aleksandrov, Ya. I. Frenkel, S. E. Bresler, and others. Soil colloids have been studied by I. N. Antipov-Karataev, A. F. Tyulin, and others.

B. V. Deryagin's studies, commenced in 1932, on liquid films at solid surfaces are of great significance for colloid chemistry. These studies provide explanations of the stability of sols, emulsions, and suspensions. In his study of the so-called disjoining action effect (discovered jointly with E. V. Obukhov, M. M. Kusakov, and others), Deryagin concluded that a solid surface exerts an influence at a considerable distance on the properties and thermodynamic state of adjacent liquid layers. In particular, Deryagin and Landau jointly developed a theory of the stability of lyophobic sols, which has gained wide acceptance. It was applied by Yu. M. Glazman and I. M. Dykman to the problem of ionic antagonism. Direct determinations of molecular forces, carried out by B. V. Deryagin and I. I. Abrikosova, confirmed the validity of the physical principles of Im. M. Lifshits's theory of molecular forces. Original methods for measuring forces and energy of adhesion have been developed, and an electrical theory of adhesion was put forward (jointly with N. A. Krotova). Interesting work has been done by S. G. Mokrushin and N. Demenev on the formation of solid films on the surfaces of aqueous solutions.

During the period under review, estensive and important work on aerosols was initiated and continued by N. A. Fuks and I. V. Pteryanov, and by B. V. Deryagin and his associates (I. S. Artemova, P. S. Prokhorov, G. Ya. Vlasenko, A. G. Amelin, O. M. Todes, and G. L. Natanson).

The above far from complete review* shows that dozens of scientific research institutes, and hundreds of laboratories in the universities and technical colleges, opened and equipped for research by the Soviet Government, have attracted thousands of scientists, and have helped to establish important scientific schools and to raise work on colloid chemistry to a level which has given a leading position to Soviet colloid chemistry.

A. V. Dumansky

---

*A more detailed review will be found in A. V. Dumansky's published monograph: "Bibliographical Review of the Development of Russian Colloid Chemistry", in three parts, published by the Academy of Sciences, Ukrainian SSR.

ANTIFRICTION~~AL~~ PROPERTIES OF DISPERSE PHASE~~S~~ OF METAL ORGANOSOLS

M. L. Barabash and E. M. Natanson

It has been established by a series of investigations that the antifrictional properties of many metals and alloys are primarily determined by the fact that at the time of first contact highly disperse particles are liberated at the points of friction and form a more or less stable suspension in the lubricating oil. When such a suspension is formed in the gap at the point of friction, the wear and the coefficient of friction of the contacting metallic surfaces are sharply diminished [1-3].

On this basis, we suggested [4] the introduction of lubricating oils containing colloidal metal additives into the gaps at points of friction. Use was made of the principle that the antifrictional properties of rubbing surfaces largely depend on the physicochemical state of these surfaces and of the layer of oil in the gap at the point of friction. In absence of colloidal metal additives, a lubricating oil usually forms adsorbed solvate layers only on the surfaces of contacting metals [5-7]. In such cases the lubricating oil interlayer consists only of two solvate layers and a thin interlayer of free oil between them. On addition of a colloidal metal, nearly all the lubricating oil is in a solvated state owing to the formation of a solvate layer on the surface of each particle. Thus, if a colloidal metal is present in the lubricant, instead of two solvate layers of oil, polysolvate layers appear in the gap, which should have a favorable effect in lowering the coefficient of friction and wear of the metals.

The organosols of iron, bismuth, and other metals in various lubricating oils, which were subsequently named metallocolloidal lubricants, have been studied in many scientific research institutions and undertakings. Some of the results are given in the present communication.

Tests of wear with various frictional pairs were made with a disk friction machine of special design, in which it was possible to measure the frictional moment, the temperature of friction, the rotational speed, the frictional path, and the current consumption of the machine motor (Fig. 1). The operating time of the machine could be automatically varied between 30 seconds and 12 minutes. A frequent start-stop procedure was used in the experiments. In such "impulse" conditions it is possible to shorten considerably the testing time, which is usually very long in presence of high-quality lubricants. The effects of pressure variations (between 6 and 60 kg/cm^2), sliding velocity (from 0.67 to 7.5 m/second), friction path (from 2,000 to 30,000 m), and of an electric current passing through the friction pair were studied. The wear was estimated from the change in weight, the running-in time being deducted.

Four friction pairs were chosen for study: 1) bronze OTsS on steel 45; 2) globular gray iron on steel 45; 3) metal compact (based on iron powder) on steel 45; 4) the same metal compact on globular gray iron. The first two pairs are often used at points of friction, while the two latter are of definite interest in relation to the prospects of their wide adoption in machine construction.

In addition, specimens of conducting contacts used in town trolley cars were studied: aluminum, a copper-graphite composition, and a metal compact, both with and without graphite and sulfur. The wear resistance of all the specimens was studied in presence of a number of lubricating oils in pure form and in the form of organosols of iron and other metals. The latter were made by the electrolytic [8] and flotation [9] methods, based on formation of colloidal metal particles in an aqueous medium followed by their transfer into an organic medium by means of surface active substances.

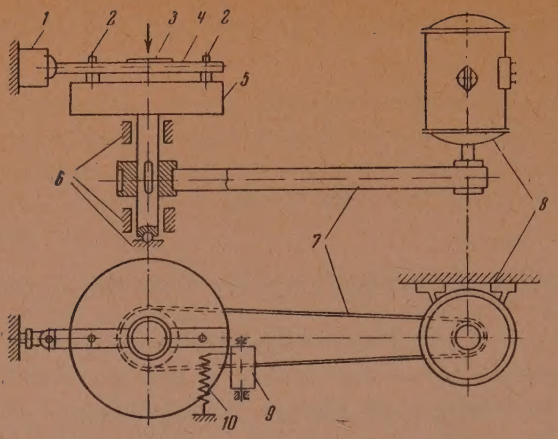

Fig. 1. Diagram of KADI-02 machine for studying friction and wear; 1) universal joint for machine arm; 2) specimen holders; 3) load pan; 4) arm carrying the specimen holders; 5) machine disk and shaft; 6) shaft bearigns; 7 belt drive; 8) electric motor; 9) recording device; 10) spring dyanmometer.

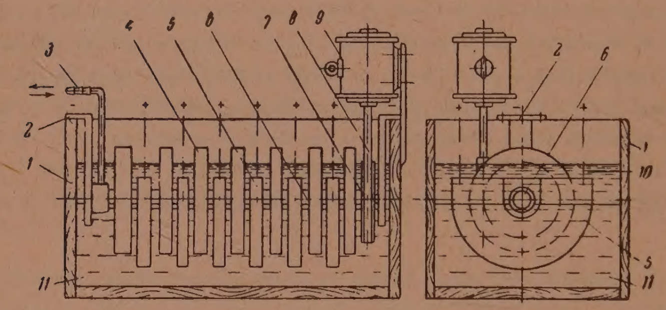

Fig. 2. Electrolytic cell with rotating cathode, for production of iron organosols on the semimanufacturing scale: 1) cell casing; 2) cathode shaft supports; 3) inlet and outlet tubes for water cooling the cathode shaft; 4) internally cooled cathode disk; 5) anode plates; 6) hollow cathode shaft; 7) worm gear; 8) worm shaft; 9) electric motor; 10) organic medium; 11) electrolyte.

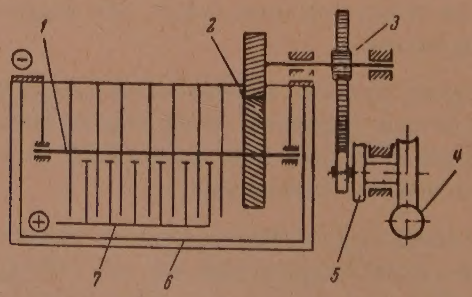

Fig. 3. Electrolytic cell with rocking cathode for production of iron organosols: 1) cathode shaft; 2) drive for rocking cathode shaft; 3) rocking mechanism; 4) worm reducing gear; 5) eccentric; 6) cell casing; 7) anode plates.

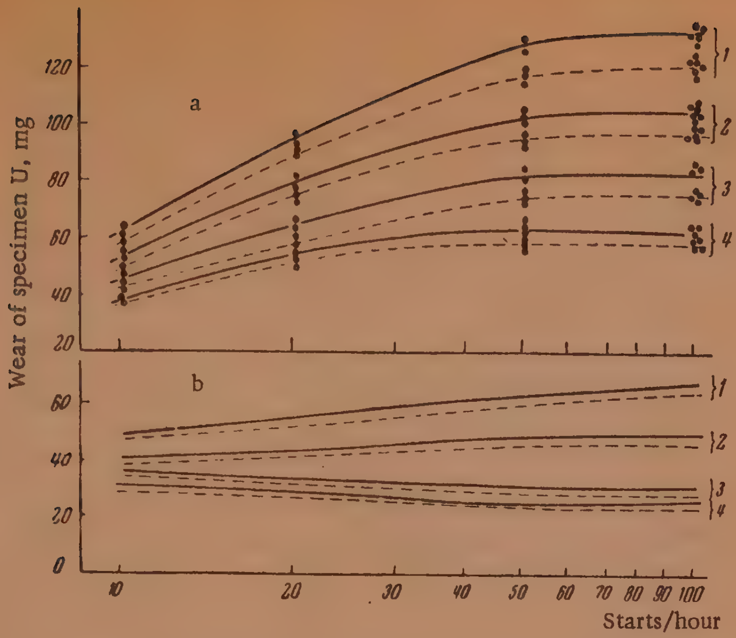

Fig. 4. Effect of the number of starts and stops of the testing machine on wear: a) with lubrication by a mixture of Avtol 10 (50%) and Solidol T (50%); b) with the same lubricant with addition of 2% iron organosol in Avtol 10. Friction pairs: 1) bronze OTsS on steel 45; 2) globular gray iron on steel 45; 3) metal compact on steel 45; 4) metal compact on globular gray iron. Continuous lines – with removal of products of wear; broken lines – without removal of products of wear. Test conditions: pressure 60 kg/cm^2; sliding velocity 0.67 m/second; sliding path 5000 m.

The electrolysis was usually carried out in a two-layer electrolytic bath, the lower layer of which was an aqueous solution of a salt of the metal in question, and the upper layer consisted of various lubricating oils containing small amounts of surface active agents. The cathode was a rotating horizontal shaft with a system of disks at the boundary between the oil and water phases. The anodes (fixed) were plates of the appropriate metals.

This principle was the basis for the design of electrolytic cells of various types, suitable for production of metal organosols in lubricating oils on the semimanufacturing scale and under factory conditions. After tests of a number of the most suitable cells for this purpose, we chose a cell with a cathode internally cooled (Fig. 2) by running water, so that it was possible to perform the electrolysis at relatively high current densities without any great increase of the cell temperature. It was found, however, that cells with rotating cathodes have a considerable disadvantage owing to the presence of a sliding contact in the cathode circuit, causing sparking and undesirable loss of potential. To avoid this fault, we designed a cell with a rocking cathode (Fig. 3), to operate at 1500 amp. One such cell is used as the main unit in the section producing metallocolloidal lubricants based on iron organosols.

The results of tests on the above systems are given in Figs. 4 and 5. It is seen in Fig. 4, a and 4, b that the wear of the specimen pairs is proportional to the number of starts of the machine, between 10 and 50 starts per hour. The wear is less with a lubricant containing 2% disperse iron organosol. A decrease of wear was also found when the products of wear were not removed from the friction surface of the machine disk.

The best results were obtained for the powdered metal compact against a disk of globular gray iron. This pair was subjected to further tests in order to study the effects of pressure, sliding velocity, and sliding path on wear. In all these experiments the number of stops and starts of the machine was automatically kept at 20 starts per hour.

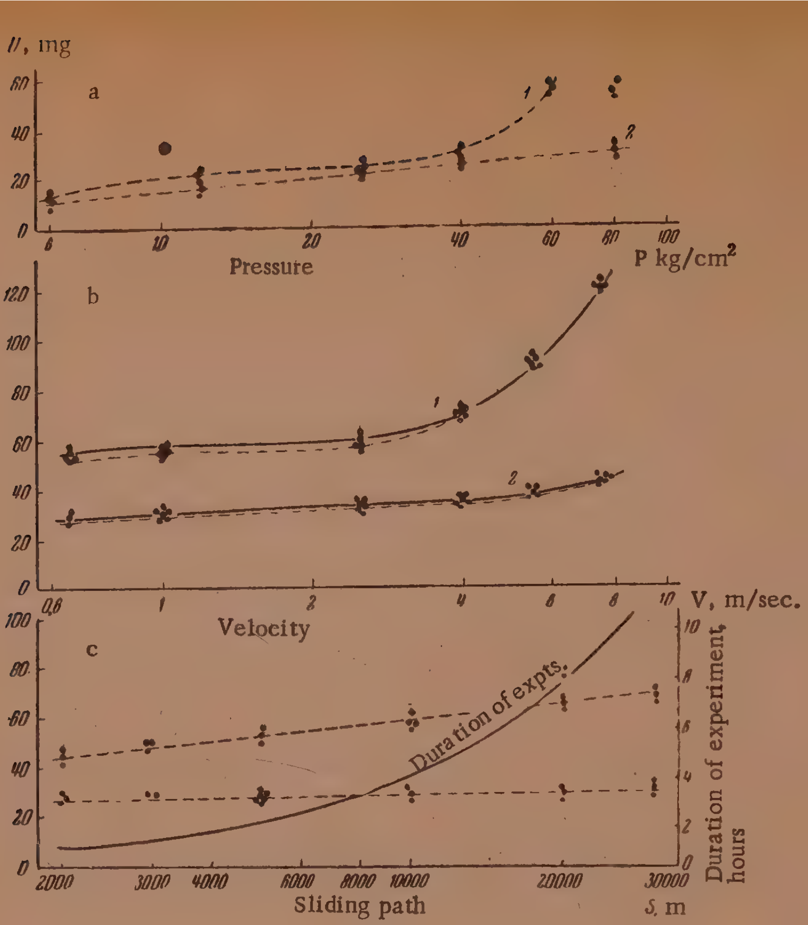

Fig. 5. Effects of pressure (a), sliding velocity (b) and sliding path (c) on wear of powdered metal compacts rubbed against globular gray iron: 1) lubricant – Avtol 10 and Solidol T (1:1); 2) the same, with addition of 2% iron organosol. Continuous lines – with removal; broken lines – without removal of the products of wear.
Test conditions: a) sliding velocity 0.67 m/second; sliding path 5000 m with 20 starts of the machine per hour; b) pressure 60 kg/cm²; sliding velocity 0.67 m/second with 20 starts of the machine per hour.

The results of these investigations, presented in graphical form (Fig. 5) show that addition of 2% iron organosol in Avtol decreases the wear in this pair considerably. Verification of these results under industrial conditions is of considerable interest. A study of the effects of additions of organosols to lubricating oils on the wear resistance of a worm wheel and crown wheel – the principal parts of the reducing gear on the rear platform of a trolley car – was carried out on a special test stand constructed to the design of M. L. Barabash, B. S. Veneraki, A. A. Ruklyadev, G. P. Litvak, and others. The results of these tests, shown in Fig. 6, confirm the great effectiveness of additions of iron and especially of bismuth organosols to lubricants, in lowering wear in these machine parts.

Similar results were obtained in a study of the wear resistance of sliding contacts, widely used in electrical transport (trolley cars, etc.). Experiments showed that additions of iron organosol to the lubricant used for impregnation of the metal compact inserts increase their wear resistance 2 to 3-fold.

Valchuk's investigations [10] have shown that additions of colloidally dispersed metals to MS-20 lubricating oil decrease wear, coefficient of friction, (= C of F) and specific work of friction over a definite range of pressures and friction paths. Some of these results are given in Fig. 7.

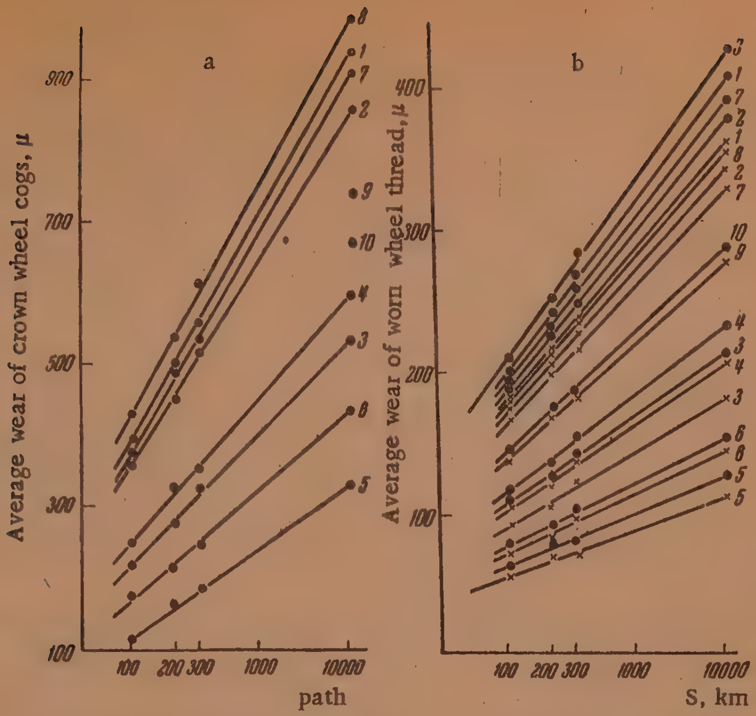

Fig. 6. Effect of type of lubricant on the wear of reducing gear crown wheel cogs a) and of thread of reducing gear worm wheel (b) of a trolley car ; 1-6) bronze crown wheel;
7-8) ditto, cast iron; 9-10) Rusanov's data.
1) cylinder oil;
2,10) EZN-2 oil;
3,7) ditto + 0.1% colloidal iron;
4,8) ditto + 0.2% " " ;
5) ditto + 0.25% " bismuth;
6) cylinder oil + 0.25% "
9) EZN-3 oil.

Fig. 7 shows that at a pressure P = 25 kg/ cm^2 the least wear was found with the use of MS-20 oil with added colloidal bismuth. Additions of colloidal iron or graphite had less effect. Under a pressure P = 100 kg/ cm^2 the least wear is again found with additions of colloidal bismuth. In this case colloidal iron and graphite accelerate running-in.

Variations of the C. of F. of steel 45 against cast iron MSCh 38-60 with different types of lubricants, pressure, and friction path are shown in Fig. 8. It is seen that under a pressure P = 25 kg/cm^2 the lowest C. of F. is found for a lubricant containing colloidal iron. It is significant that the C. of F. remains almost unchanged for 200,000 cycles. Additions of colloidal bismuth at this pressure result in a higher C. of F. than is found for oil with added colloidal iron. The situation changes when the pressure is increased to P = 100 kg/cm^2: the lowest C. of F. is found with additions of colloidal bismuth; additions of colloidal iron and graphite give approximately the same C's. of F., somewhat higher than for pure MS-20 oil. It is interesting to note that addition of colloidal graphite to MS-20 oil gives the highest C. of F., higher than for pure MS-20 oil, at P = 100 kg/cm^2. It is also noteworthy that the C. of F. is decreased for the lubricant containing colloidal bismuth when the pressure is raised from 25 to 100 kg/cm^2 .

Fig. 9 shows variations of the specific work of friction for some of the pairs studied (steel 45 on steel 45 and MSCh 38-60 on MSCh 38-60 cast iron) with lubrication by pure MS-20 oil and the same oil with additions of colloidal brass. In the latter case the addition of the colloidal metal decreases the specific work of friction sharply as compared with the value found for pure MS-20 oil, for the whole pressure range from 25 to 112.5 kg/ cm^2.

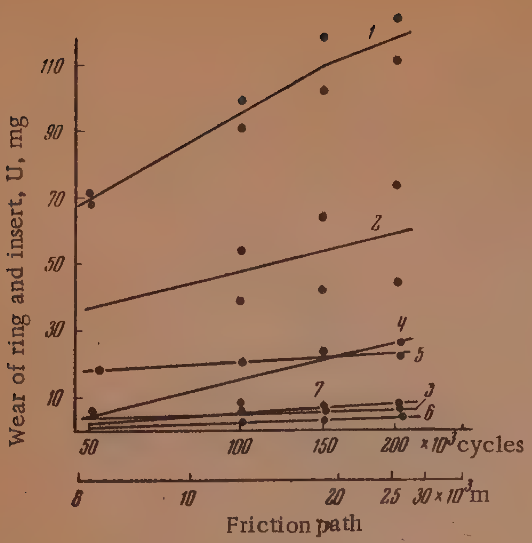

Fig. 7. Variation of the wear of steel 45, rubbed against MSCh 38-60 cast iron, with type of lubricant, pressure, and friction path. Lubrication with MS-20 oil with additions of: 1,4) colloidal iron; 2,5) colloidal graphite; 3,6) colloidal bismuth; 7) pure MS-20 oil; 1-3 and 7) pressure 100 kg/cm²; 4-6) pressure 25 kg/cm².

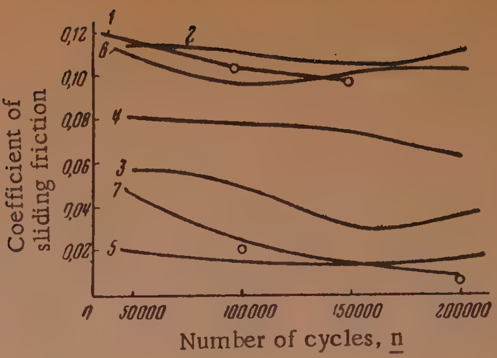

Fig. 8. Variation of the coefficient of friction of steel 45 on MSCh 38-60 cast iron, with type of lubricant, pressure, and friction path. Lubrication with MS-20 oil with additions of: 1,5) colloidal iron; 2,6) colloidal graphite; 3,7) colloidal bismuth; 4) pure MS-20 oil; 1-4) pressure 100 kg/cm²; 5-7) pressure 25 kg/cm².

It should be noted that with the use of a lubricant containing the colloidal metal, the specific work of friction changes little in the course of the tests for both pairs, whereas with the use of pure MS-20 oil in prolonged trials it shows a tendency to continuous increase over more than 500,000 cycles.

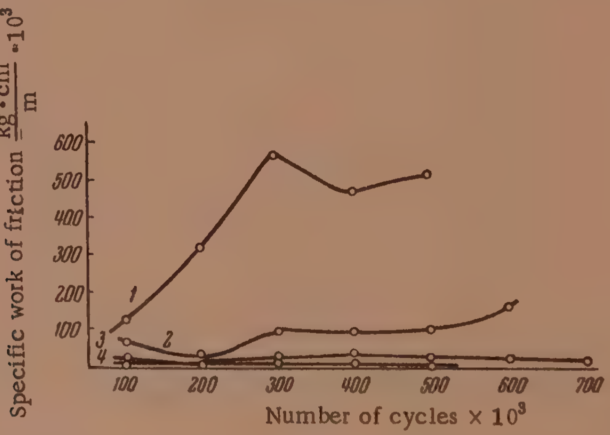

Fig.9.Variation of the specific work of friction of steel 45 on steel 45 (2), and cast iron MSCh 38-60 on cast iron MSCh 38-60 (1,3,4), with type of lubricant, pressure, and friction path. Lubrication with MS-20 oil (1,3); lubrication with MS-20 oil with addition of colloidal brass (2, 4); 1, 2, 4) pressure 112.5 kg/cm²; 3) pressure 25 kg/cm².

SUMMARY

1. The antifriction properties of organosols of iron, bismuth, and other metals in ordinary lubricating oils have been studied, and the technology of their preparation is briefly described.

2. Laboratory tests have shown the high effectiveness of these systems in increasing the wear resistance of the following friction pairs:

a) steel 45 on bronze OTsS; b) steel 45 on globular gray iron; c) powdered iron compact on steel 45; d) powdered iron compact on globular gray iron; e) steel 45 on modified gray iron MSCh 38-60; f) modified gray iron MSCh 38-60 on MSCh 38-60, and others.

3. Tests of these results under operational conditions in a number of points of friction: reducing worm gear in the rear platform of a trolley car, conducting contact inserts, etc., confirmed the suitability of organosols of certain metals (iron, bismuth, and others) for increasing the wear resistance at a number of points under heavy frictional load in modern machines.

We express our gratitude to the management of the Kiev Trolleybus and Trolley Car Administration and of the Dzerzhinsky factory for their cooperation in the tests under operational conditions, for organization of the experimental production of metallocoloidal lubricants, and active participation in work on adoption of the materials.

Institute of General and Inorganic Chemistry
Academy of Sciences, Ukrainian SSR, Kiev
The Kiev Automobile and Road Institute

Received July 4, 1956.

LITERATURE CITED

[1] M.P. Slavyansky and R.N. Bordovsky, in Symposium, "Tin-Free and Low-Tin Babbitts", No. 1 1935; No. 2 1937.

[2] G.A. Kashchenko, Principles of Metallography (Metallurgy Press, Leningrad-Moscow, 1950) p. 640.

[3] M. L. Barabash, in Symposium "Increase of Wear Resistance and Service Life of Machines" (Mashgiz, Kiev 1953) p. 352.

[4] M. L. Barabash, and E. M. Natanson, Authors' Certif. No. 104098.

[5] P.A. Rebinder and N.A. Kalinovskaya, in Symposium "Investigations in the Field of Applied Physical Chemistry of Surface Phenomena"(Izd. AN SSSR, Moscow-Leningrad 1936); P. A. Rebinder and N. N. Petrova, in Symposium "Friction and Wear in Machines" vol. 1, (Izd. AN SSSR, Moscow 1939).

[6] B. V. Deryagin, in Symposium "Friction and Wear in Machines" vol. 4, (Izd. AN SSSR, Moscow -Leningrad, 1951).

[7] A. S. Akhmatov, in Symposium "Friction and Wear in Machines", vol. 3, (Izd. AN SSSR, Moscow -Leningrad, 1949).

[8] E.M. Natanson, Mem. Inst. Chem. Acad. Sci. Ukrainian SSR, 7, 311 1040; Colloid J., 9, 191 1947; Authors' Certif. No. 538521.

[9] E. M. Natanson, Colloid J., 9, 428 1947.

[10] M. L. Barabash, G. I. Valchuk, and E. M. Natanson, Trans. Inst. Constr. Mechanics Acad. Sci. Ukrainian SSR, No. 22 1956.

MODIFICATION OF POLYAMIDE PROPERTIES BY THE INCLUSION METHOD*

A.N. Bykov, M.I. Ivanova and A.B. Pakshver

It was shown in the previous communication [1] that by means of inclusion it is possible to change the properties of high polymers, and in particular to increase their reactivity.

Recently a single paper has been published [2] on the effect of "intermediate swelling" on the sorptive properties of cellulose. The term "intermediate swelling" was applied to preliminary treatment of cellulose with alkali with subsequent replacement of the alkali by water and alcohol, i.e., inclusion. The molecular structure of the cellulose, loosened by swelling in alkali, became fixed by the alcohol. After such treatment the cellulose had a considerably higher sorptive power for dyes and iodine.

The present paper deals with modification of the properties of polyamide fibers by the inclusion method, and in particular the increase of polyamide reactivity in sorption of dyes, acids, and phenol. The effects of the degree of drying of the treated specimen, and of the duration and temperature of the inclusion treatment on fiber reactivity were also studied. The rate of restoration of the polyamide structure after swelling, the equilibrium sorption of phenol after inclusion treatment, and the kinetics of sorption of phenol by treated specimens were studied.

Drawn and undrawn capron yarn was used for the experiments. Benzene was used as the inclusion substance. The results of the inclusion treatment were studied by experiments on the sorption of 0.01 N acetic acid, acid chrome brown dye at pH 3.0, and phenol from solutions of various concentrations, by the polyamide fibers. The amounts of acid, dye, and phenol taken up were determined as follows: for acid, from the decrease of the acid concentration, found by titration with 0.01 N NaOH solution before and after the sorption; for the dye, by means of the Kol-1 M concentration colorimeter; and for phenol, iodometrically by the bromide–bromate method.

The inclusion treatment was performed as follows: a 2.0 g sample of the fiber was treated for 15 minutes with a substance which causes swelling and weakens interaction between the polymer macromolecules. A solution of phenol, at a concentration of 20 g/liter, was used for this purpose. The sample was pressed out after the treatment, and the swelling liquid was replaced by the inclusion substance–benzene. The replacement was effected consecutively in the sequence: phenol → water → alcohol → benzene.

Effect of the degree of drying of the inclusion-treated sample on the reactivity of the polyamide. The sorption of acid and dye by inclusion-treated drawn capron yarn was determined under the following conditions: without drying, after drying in air for 1 hour, after drying in a drying oven for 1 hour, and after drying in a drying oven to constant weight. The oven drying was effected at 60-70°.

The results are given in Table 1 (the sorption of the untreated sample is taken as 100%).

These results show that the drying conditions after the inclusion treatment do not affect the change of reactivity which results from swelling and treatment with the inclusion substance. The samples remain highly reactive even when dried to constant weight.

Effect of duration of inclusion treatment. The results of a study of the effect of duration of the inclusion treatment on the sorption of acid and dye by inclusion-treated capron fiber are given in Table 2.

---

* Communication 2 in the series on inclusion processes in high polymers.

TABLE 1

Effect of Degree of Drying of Inclusion-Treated Polyamide on the Sorption of Acid and Dye*

Degree of drying of inclusion-treated polyamide	Sorption of acid, %	Sorption of dye, %
Without drying	149	198
After drying for 1 hour in air	148	192
After drying for 1 hour in drying oven	146	201
After drying to constant weight	151	199

* The sorption of acid and dye by an untreated sample was taken as 100%.

TABLE 2

Effect of Duration of Inclusion Treatment on Polyamide Reactivity

Duration of inclusion treatment, min.	Sorption of acid, %	Sorption of dye, %
10	145	198
30	148	198
60	146	198
180	—	193

TABLE 3

Effect of Temperature of Inclusion Treatment on Polyamide Reactivity

Treatment temperature, °C	Sorption of acid, %	Sorption of dye, %
20	158	198
25	158	195
30	159	200
35	159	199
40	160	198

It is seen from Table 2 that increase of the inclusion treatment time does not affect the sorption of acid or dye by the treated fiber. 10 minutes is sufficient for the inclusion substance to penetrate into the loosened structure and fix it.

The reactivity is largely determined by the degree of swelling, i.e., loosening of the intermolecular structure of the polymer, as was shown previously [1].

Effect of temperature of the inclusion treatment. The treatment was carried out at different temperatures in order to find whether the treatment temperature has any effect on the increased reactivity of the polyamide resulting from inclusion treatment (Table 3).

It follows from Table 3 that the temperature, like the duration of the inclusion treatment, does not influence the increased reactivity of the treated polyamide. The inclusion substance is already able at 20° to replace the swelling substance and to fix the structure at an adequate rate.

Restoration of polyamide structure after swelling. Throughout the investigation the treatment was carried out in the following sequence:

phenol → water → alcohol → benzene*

Parallel experiments were carried out on the replacement of water and alcohol by benzene in the sequence:

phenol → acetone → benzene

---

* The mechanical properties of treated and untreated fiber samples were determined. The tensile strength decreased by 3% and the elongation at break increased by 3% as the result of the treatment of capron yarn; thus, the mechanical properties changed little.

The purpose of this substitution was the better preservation of the increased reactivity of the inclusion-treated polyamide, since the more rapid the replacement of the swelling substance by the inclusion substance, the higher should be its reactivity. This is confirmed by the data in Tables 4 and 5.

TABLE 4

Influence of Intermediate Steps in Inclusion Treatment on Polyamide Reactivity

Treatment sequence	Sorption of acid, %	Sorption of dye %
Phenol — water — alcohol — — benzene	148	190
Phenol — acetone — benzene	157	202

TABLE 5

Restoration of Polyamide Structure After Swelling

Treatments	Sorption of phenol %	Sorption of dye, %
Swelling in phenol solution for 15 min. without washing	—	231
Swelling for 15 min., 3 water washings in 30 min., drying	158	216
Inclusion treatment and drying	172	228
Inclusion treatment after three days of storage	175	—

The data in Tables 4 and 5 show that the reactivity increases with increasing speed with which the swelling substance is replaced by the inclusion substance. Any additional operations which prolong the interval between the state of maximum loosening of the structure and the instant of fixation decrease fiber reactitivity. The highest reactivity is found when the sorption of the dye takes place immediately after swelling.* Washing with water does not retard the formation of new intermolecular bonds, broken during swelling, and the reactivity decreases. Inclusion treatment with nonpolar or weakly polar liquids halts the formation of intermolecular bonds, fixing the loosened structure, and the reactivity is therefore higher.

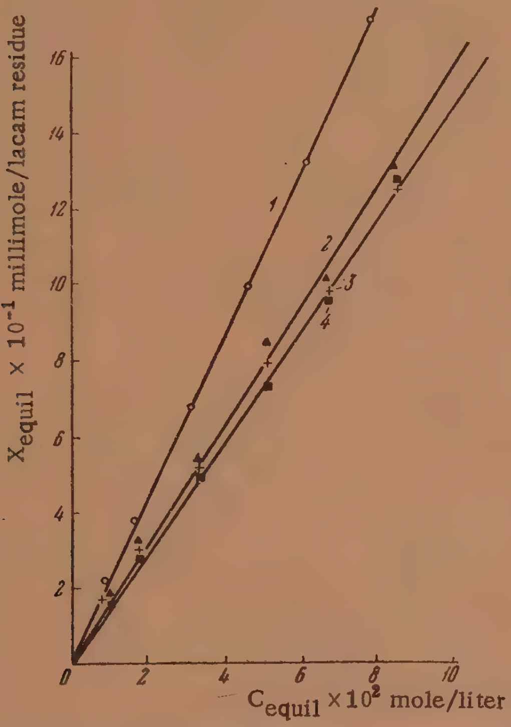

Fig. 1. Sorption isotherms for capron yarn: 1) original undrawn; 2) inclusion-treated drawn; 3) swollen and washed, drawn; 4) original drawn.

The inclusion-treated fibers retain their high reactivity even after three days of storage, i.e., after the inclusion treatment the fixed loosened structure does not become dense again, at least for a considerable time. To determine the degree of change of the polyamide fiber structure by inclusion treatment, experiments were carried out on the equilibrium sorption of phenol and on the kinetics of phenol sorption.

Equilibrium sorption of phenol. For determination of the equilibrium sorption of phenol, 0.5 g samples of polyamide fiber were placed in 25 ml lots of phenol solution, of 1, 2, 4, 6, 8, and 10 g/liter. The flasks were firmly stoppered and held at 20° in a thermostat until equilibrium was reached. The state of equilibrium was indicated by equal values for the sorption by three samples after different times in the thermostat. Sorption isotherms were plotted for the original drawn and undrawn capron yarn, inclusion-treated samples, and fibers swollen and washed in water (Fig. 1).

Fig. 1 shows that undrawn yarn has a higher value than drawn yarn for the equilibrium sorption of phenol; this is explained by differences in their structure. The values for the equilibrium sorption by the original untreated, swollen and washed, and inclusion-treated samples are practically the same. This is explained by the fact that the changes occurring in the structure of the polyamide as the result of inclusion treatment are not as deep as those produced by drawing.

---

* In these conditions the dye is sorbed only by the end groups, while phenol interacts with the amide groups of the polyamide.

The integral heats of solution of untreated and inclusion-treated polyamide fiber samples were also practically equal, confirming the above supposition.

Integral heat of solution in cal./g	
Untreated yarn	14.70
Inclusion-treated yarn	14.66

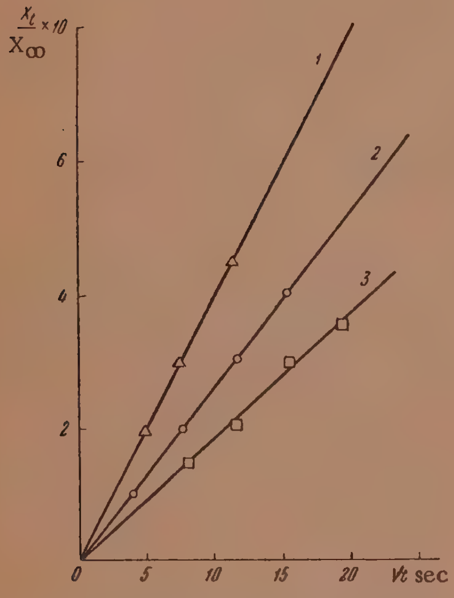

Fig. 2. Kinetics of sorption by capron yarn: 1) inclusion-treated; 2) swollen and washed; 3) original.

TABLE 6

Values of k and Diffusion Coefficient D for Different Samples of Polyamide Fibers

Fiber sample	$k \cdot 10^2$	$D \cdot 10^{12}$
Not treated	1.82	147.0
Swollen and washed	2.58	295.0
Inclusion-treated	4.00	710.0

Kinetics of the sorption of phenol by inclusion-treated polyamide fiber. The kinetic studies were carried out as follows: samples of drawn capron yarn (0.5 g) after various treatments were immersed in 25 ml of phenol solution at a concentration of 1 g/liter at 20°. The time from the immersion to the extraction of the sample was noted. The amount of sorbed phenol was determined iodometrically.

Fig. 2 shows the relationship

$$x_t / x_\infty = f(\sqrt{t}),$$

where x_t is the sorption of phenol at time t; x_∞ is the sorption at equilibrium.

For diffusion processes, this relationship is represented by a straight line, from the slope of which it is possible to determine the value of k in the equation.

$$x_t / x_\infty = k\sqrt{t}, \qquad k = 4/r\sqrt{D/\pi},$$

where r is the fiber radius.
This method was used to calculate the coefficients of diffusion of phenol into the fibers

$$D = k^2 r^2 \pi/16; \; r = 1{,}5 \cdot 10^{-3} \text{ cm}.$$

The applicability of this equation to the sorption of phenol by polyamide fibers was demonstrated earlier by Pakshver and Mankash [3], who showed that the sorption of phenol by capron is determined mainly by internal diffusion of phenol into the fiber.

Values of k and the diffusion coefficient D are given in Table 6.

These values show that diffusion of phenol into inclusion-treated yarn proceeds at almost 5 times the rate for the original, untreated yarn. Previous swelling of the polyamide fibers, without fixation of the loosened structure, only doubles the diffusion rate. The inclusion treatment is therefore of special significance in processes the rate of which is determined by internal diffusion, such as dyeing.

SUMMARY

1. The increase of polyamide reactivity produced by inclusion treatment does not depend on the time of drying of the inclusion-treated fiber for given conditions, time, and temperature of the treatment.

2. The more rapid the replacement of the substance causing swelling by the inclusion substance, the higher is the reactivity of the treated fiber.

3. Inclusion treatment results in a several-fold increase of the rate of diffusion of reagents into the fibers, and is especially important for acceleration of processes determined by internal diffusion.

The Ivanovo Institute of Chemical Technology

Received October 13, 1956

LITERATURE CITED

[1] A. N. Bykov and A. B. Pakshver, Colloid J., 19, 27 1957.*

[2] Messik Klara, Szabo Kalman, Faserforshchung und Textiltechnik 2, 89 1956.

[3] A. B. Pakshver and E. K. Mankash, J. Phys. Chem., 25, No. 4, 468 1951; J. Appl. Chem., No. 10, 1200, 1953.

---

* Original Russian pagination. See C. B. translation.

STUDIES OF ELECTROÖSMOSIS IN BINARY POWDER MIXTURES CONSISTING OF PARTICLES OF DIFFERENT CHEMICAL NATURE

O.N. Grigorov and K.P. Tikhomolova

Investigations of electroosmosis in complex capillary sustems heterogeneous in composition and structure are of considerable interest in relation to extension of the field of application of this method. In many instances of the use of electroosmosis as a method for determining zeta potential or for removal of water from various comminuted substances one deals with materials containing particles of different chemical nature. The known laws for electroosmotic effects in homogeneous capillary systems may prove inapplicable to systems of this type. Unfortunately, very little information on this subject is available in the literature. The only work known to us on electroosmosis in mixed powder diaphragms consisting of different types of particles is that of Reshetnikov [1]. On the assumption that the electrokinetic potential should be definitely determined by the nature of the solid partition for a solution of given composition and concentration, Reshetnikov derived a number of relationships which aid in determining the specific surfaces of powders composed of different substances. In particular, for determining the specific surface of porous adsorbents, Reshetnikov finds it convenient to determine those surface properties of the adsorbent which would vary, when it was mixed with another adsorbent (with known specific surface), in the composition–property diagram additively with variations of the composition of the binary mixture. The property chosen by Reshetnikov is the electrokinetic potential, which depends on the nature of the surface in interaction with the liquid medium, and is independent of the total surface or mass of the substance. As a result, he derives the following equation for the zeta potential of the mixture:

$$\zeta_m = \frac{\zeta_1 x + \zeta_2 k (1 - x)}{x + k (1 - x)},$$

where x and 1 − x are the fractions of the components present; k is the ratio of the specific surfaces of the components of the mixture; ζ_1 and ζ_2 are the zeta potentials of the individual components.

On the condition that the properties of the mixture are additive, the variation of the zeta potential of a binary mixture with the ratio of the components present should be represented on a composition – zeta potential diagram by a curve which satisfies the condition $\zeta_1 > \zeta_n > \zeta_2$ when k = constant. For the particular case, when k = 1, the curve becomes a straight line. Reshetnikov considers that the above equation can be used to determine the true specific surface of one component if the specific surface of the other is known or can be determined, and also to find the relative specific surface of oen of the components if the specific surface of the other is taken as unity. To confirm his views, Reshetnikov carried out a series of experiments on electroosmosis in mixtures; the substances used were ground quartz sand and Khotkovo tripoli earth roasted at various temperatures. The above equation proved to be valid for this mixture, and the nature of the zeta potential – composition curve was as predicted.

In our opinion, however, Reshetnikov's experiments do not provide a quantitative verification of his theory, since both tripoli and sand particles are irregular in shape, and moreover tripoli has a considerable internal surface owing to the fine pores permeating its particles. In other words, tripoli powder has two types of capillaries: within and between the particles. The conditions for motion of the liquid are different in these types of capillaries, and it is doubtful whether the foregoing theory is applicable in principle to the use of electroosmosis as a method for determining the electrokinetic potential.

To verify this view, we carried out experiments on mixed powders of spherical polystyrene particles in the pure state and with added Sudan III dye. The original powders in 0.01 N KCl solution ($\kappa - 9.3 \cdot 10^{-4}$ $ohm^{-1} \cdot cm^{-1}$) had zeta potentials of 15 mv for pure polystyrene and 33 mv for polystyrene with Sudan III. Fractions of the powders with narrow particle size ranges were obtained by prolonged sedimentation in distilled water; microscopical dispersion analysis was used as a check. The apparatus described in the previous communication [2] was used for the electroosmotic transport determinations. The apparatus was filled as follows: a definite fraction was first settled in it, and the height of its column was measured; it was then covered with another fraction, and the height of the column of the latter was measured. The percentage composition was found from the ratio of the column heights (the cross section of the apparatus was constant). The fractions were then mixed thoroughly and the electroosmotic transport determinations were carried out.

The results for mixtures of different compositions were represented graphically in the form of plots of the zeta potential, calculated by means of the usual Helmholtz-Smoluchowski equation, against the compositions of the binary mixtures.

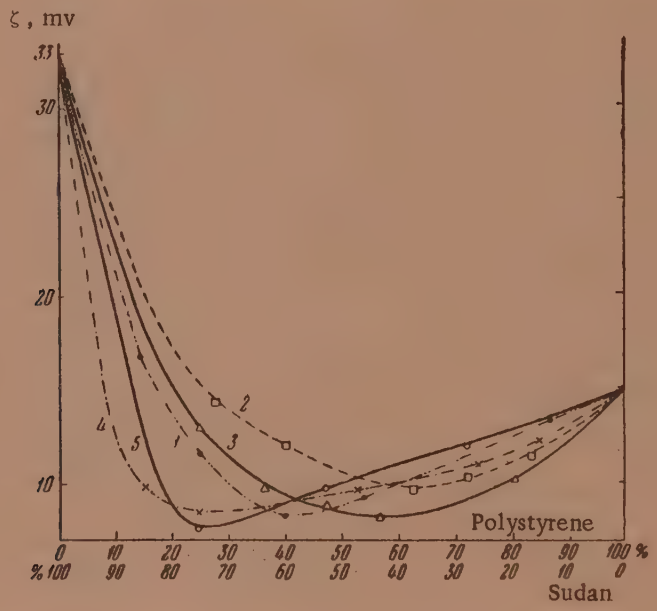

Variation of zeta potential with binary mixture composition

Particle diameter			Particle diameter
1) Polystyrene	8.3 μ +	polystyrene and Sudan	55 μ
2) "	34.1 μ +	" "	55 μ
3) "	53.7 μ +	" "	55 μ
4) "	53.7 μ +	" "	38.5 μ
5) "	53.7 μ +	" "	13 μ

The value of k for a system of spherical particles is easily calculated, as the ratio of the specific surfaces of the spheres in the mixture must be equal to the inverse ratio of their radii. However, if k is calculated from Reshetnikov's equation, not only is there no agreement with the experimental data, but for most values of the zeta potential of the above mixture such calculations cannot be made at all. The graph shows that the zeta potential of the mixture decreases sharply with small additions of the other component, and assumes values smaller than the electrokinetic potential of the less active component, in this instance pure polystyrene.

Comparison of Curves 1 and 2 shows that a decrease of the particle size of the less active component leads to a steeper descent of the curve in the region where the percentage content of the less active component is low. The position of the minima on the curves is also shifted into this region. If the particle size of the more active component is greater than that of the other component, a decrease of the particle size of the former results in a less steep descent of the curve (Curves 4 and 5).

The great discrepancy between the results for powder mixtures with spherical particles and the results which should be obtained on the basis of Reshetnikov's theory shows that this theory is erroneous. The zeta potential of binary mixtures determined by electroosmosis cannot be assumed to be an additive property. The electroosmotic transport effect in a real capillary system is much more complex than Reshetnikov assumes. In considerations of the mechanism of liquid flow in the pore channels of such mixed diaphragms the rate of liquid flow cannot be taken as constant, as the regions over which the flow conditons change are comparable in size to the lengths of the capillaries. Changes in the liquid flow rates along the pore channels, caused by variations in the mosaic structure of the walls, and also by possible changes in the direction of the flow, may result in disturbances of steady laminar flow in such a system, with a resultant decrease of the volume of liquid transported.

Therefore, Reshetnikov's views concerning the applicability of the additivity principle to variations of a definite surface property of a binary mixture of substances in the disperse state are not confirmed by the results of determinations of electroosmotic transport of a liquid.

SUMMARY

1. Electroosmotic transport values through powder diaphragms consisting of mixtures of spherical particles of pure polystyrene and of polystyrene with additions of Sudan III dye, having different zeta potentials, have been determined.

2. The values of the zeta potential plotted as functions of the binary mixture composition have sharply defined minima, owing to deviations from steady laminar flow of the liquid in such mixed systems.

3. The results show that the additivity principle is not applicable to variations of the electrokinetic potential (determined by electroosmosis) as a function of the composition of a binary mixture of particles with charges of different magnitudes.

The A. A. Zhdanov State University, Leningrad

Received November 6, 1956

LITERATURE CITED

[1] M. A. Reshetnikov, Colloid J., 7, 537 1941.

[2] O. N. Grigorov and K. P. Tikhomolova, Colloid J., 19, No. 4, 406 1957.*

---

* Original Russian pagination. See C. B. translation.

THE INFLUENCE OF INTERMOLECULAR INTERACTION ON THE PROPERTIES OF RUBBER SOLUTIONS

V.E. Gul and V.A. Berestnev

As has already been shown, the nature of the intermolecular interaction is one of the basic factors determining a number of properties of rubbers and vulcanizates [1]. The effects of intermolecular action on molecular light scattering in solutions of nitrile rubbers have also been studied [2]. In the present investigation, the influence of intermolecular interaction on the properties of polymer solutions has been studied by viscosimetric and swelling determinations*.

In order to study the influence of intermolecular interaction on the properties of polymers and their solutions, it is necessary to have a series of polymers which differ in the degree of intermolecular interaction but with all the other structural characteristics constant. For example, if the light scattering method is used, the chain length and branching should be the same for all the polymers. If the swelling method is used, the degree of cross linking should be the same in all the polymers. Finally, for viscosimetric determinations the polymers should also have the same molecular weight and degree of branching.

Four types of intermolecular interaction in polymer solutions are usually considered: 1) between regions of the same polymer chains; 2) between individual polymer molecules; 3) between molecules of the polymer and solvent; 4) between the solvent molecules.

The first and third of these types of interaction have the predominant influence on the viscous properties and molecular light scattering of rubber solutions, while in swelling the principal role is played by the second type of interaction. Thus, studies of the properties of polymers by light scattering, viscosimetry, and swelling provide a complete picture of the influence of intermolecular interaction on the properties of polymers and their solutions. Interaction between the solvent molecules does not seem to be significant in investigations like ours, although there are indications [3] that it must be taken into account in some cases.

Guided by the foregoing considerations, we chose standard butadiene – acrylonitrile copolymers (SKN--18, SKN-26, and SKN-40), containing different proportions of acrylonitrile, as the materials, and these were studied by the viscosimetric and swelling methods.

The polymers were purified and fractionated for the viscosimetric determinations. The purification was effected by double reprecipitation by dehydrated methyl alcohol from solutions in benzene, in an atmosphere of pure nitrogen. The fractionation consisted of fractional precipitation of the polymers from benzene solutions with cooling to 0°. The fractions were dried in nitrogen and dissolved in methyl ethyl ketone. These solutions were used for determinations of the molecular weights of the fractions and for the viscosimetric measurements. The molecular weights of the fractions were determined by the light scattering method described previously [2]. The results of these determinations are given in Table 1.

For studying intermolecular interaction by the swelling method, the polymers were converted into unfilled vulcanizates of the following composition (in parts by weight):

Rubber	100
Sulfur	2
Sulfenamide BT	1.8
Zinc oxide	5
Stearic acid	2
Neozone "D"	1

---

* The swelling data were obtained jointly with L. A. Oksentyevich.

The density ρ by the double weighing method, and the equilibrium elasticity modulus E_{∞} by a dynamometer of the Polanyi type, were determined for these vulcanizates, and the molecular weights of the chains M_c were then calculated by means of the equation [4]:

$$M_c = N_a \cdot 3k \cdot T\rho / E_{\infty}, \tag{1}$$

where N_a is the Avogadro number; k is the Boltzmann constant; T is the absolute temperature.

TABLE 1
Molecular Weights of Different Fractions of Nitrile Rubbers

Rubber	Molecular weights of fractions			
	I	II	III	IV
SKN-18	148 000	57 100	19 250	—
SKN-26	—	312 000	87 800	48 200
SKN-40	148 000	100 000	46 700	28 400

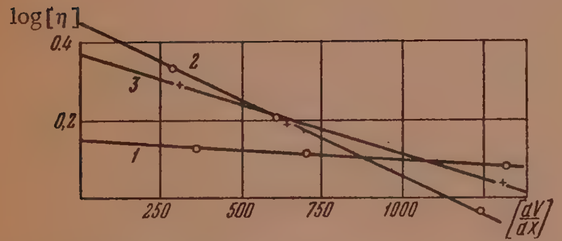

Fig. 1. Variation of intrinsic viscosity with limiting velocity gradient for fractions of similar molecular weight: 1) SKN-18 (M-57,000); 2) SKN-26(M-48,200); 3) SKN-40 (M-46,700)

The greatest deviation between the values of M_c was only 6%. Therefore the degree of cross linking was practically the same in all three vulcanizates; this satisfies the above condition for the applicability of the swelling method.

The viscosimetric determinations were carried out with three efflux velocity gradients in a special capillary viscosimeter [5], the measuring portion of which consisted of three balls arranged vertically. The efflux velocity gradient dv/dx is caluculated by means of the equation

$$\frac{\partial v}{\partial x} = \frac{A}{\eta / d}, \tag{2}$$

where A is a constant found by calculation; η / d is the kinematic viscosity, determined from the equation

$$\eta / d = \alpha (t - \beta / dt), \tag{3}$$

where α and β are constants for the apparatus; t is the efflux time.

The constants α and β were found by determinations of the viscosity of water; the efflux time was measured by a seconds clock to an accuracy of 0.2 second. The efflux times were used to calculate the specific viscosity η_{sp}, the reduced viscosity η_{sp}/c, and the velocity gradient. The following relationships were plotted for each ball of the viscosimeter, situated at a definite height:

1) η_{sp}/c against the concentration c. Extrapolation to $c \to 0$ gave the intrinsic viscosity $[\eta]$;

2) logarithm of the efflux velocity gradient against the concentration. This was also extrapolated to $c \to 0$ to determine the efflux velocity gradient at zero concentration [dv/dx].

The values found for $[\eta]$ and [dv/dx] were used to plot the logarithm of the intrinsic viscosity against the velocity gradient. Extrapolation of this graph to zero velocity gradient gave values for the viscosity at zero concentration and zero efflux velocity gradient, i.e., values which were entirely independent of the experimental conditions.

Fig. 1 shows log $[\eta]$ plotted against [dv/dx] for fractions of different nitrile rubbers of approximately the same molecular weight (Table 1). The relationships are linear, and conform to the equation:

$$\lg [\eta] = \lg [\eta]' - B [\partial v / \partial x], \tag{4}$$

where log $[\eta]'$ corresponds to the intrinsic viscosity at zero velocity gradient and zero concentration. The coefficient B differs for the different polymers used, and depends on the acrylonitrile content, i.e., on the intermolecular interaction (Table 2), characterized by the square root of the cohesive energy density [6]. The values of the slope factor (B) in Equation (4), the equilibrium swelling (Q), the slope factors of the molecular light scattering curves, taken from an earlier paper [2], and the cohesive energy densities ($\sqrt{E/V}$) for the rubbers studied are given in Table 2. The data in Table 2 show that the factor B does not vary steadily with $\sqrt{E/V}$. The probable reason is that changes of polymer polarity are accompanied by changes in the difference between the nature of intermolecular interaction in the solvent and in the polymer. The less this difference is, the stronger will be the polymer-solvent interaction. With increase of this interaction the polymer molecules become more flexible, the dependence of log $[\eta]$ on $[dv/dx]$ becomes more pronounced, and the absolute value of B in Equation (4) increases. If the polarity of the polymer is increased further, the nature of the interaction between the polymer molecules will change so much that it will again differ from the nature of the interaction between the solvent molecules. This will diminish polymer-solvent interaction and therefore decrease the absolute value of B, as the polymer molecules will become more rigid and will be deformed less by flow of the solution.

TABLE 2

Variation of Slope Factors of Viscosimetric and Light Scattering Curves and Equilibrium Swelling with Degree of Intermolecular Interaction

Polymer	$B \cdot 10^3$	Q in%	$B_\tau \cdot 10^3$	$\sqrt{\frac{F}{V}}$
SKN-18	1.12	210	0.67	8.86
SKN-26	4.89	215	3.86	9.22
SKN-40	3.24	207	1.94	9.52

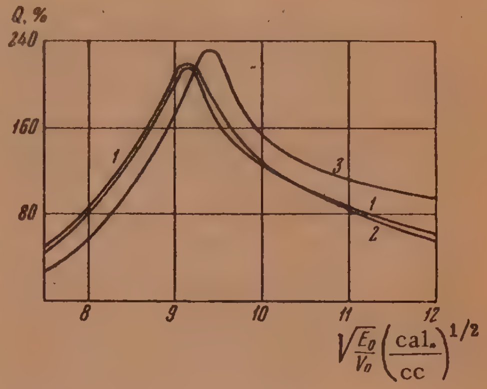

Fig. 2. Variation of degree of swelling of nitrile rubbers with cohesive energy density of the solvent: 1) SKN-18; 2) SKN-26; 3) SKN-40.

To estimate the energy of intermolecular interaction, the equilibrium swelling was found by extrapolation of the plot of the degree of swelling Q against time t to t ⟶ 0. Several solvents with increasing values of cohesive energy density were chosen for these experiments: ethyl ether, n-amyl acetate, n-propyl acetate, butyraldehyde, ethyl acetate, methyl ethyl ketone, ethyl formate; methyl acetate, acetone, and acetonitrile. The values of the cohesive energy density for the polymers studied were at about the middle of this series. The values for the cohesive energy densities of the solvents were taken from Gee's paper [6].

These values were used to plot the equilibrium swelling of the three polymers against the cohesive energy densities of the solvents, as shown in Fig. 2. These smoothed curves were used for determining the degree of swelling of nitrile rubbers in solvents with known values of $\sqrt{E_0/V_0}$. The results show that the maximum is displaced toward lower values of Q and $\sqrt{E_0/V_0}$ with decreasing $\sqrt{E/V}$ for the polymer.

It follows from the data in Table 2 that such properties as viscosity, swelling, and molecular light scattering of divinyl-acrylonitrile polymers in methyl ethyl ketone do not vary smoothly with intermolecular interaction, and vary with the polarity of the rubber, passing through a maximum.

SUMMARY

1. A study has been made of the viscosities of divinyl-acrylonitrile rubber solutions, and of the equilibrium swelling of vulcanizates of these rubbers with the same degree of cross linking, in various solvents.

2. It was found that the viscosity and light scattering characteristics of the solutions, and swelling of the vulcanizates of divinyl-acrylonitrille rubbers, are not steady functions of the degree of intermolecular interaction, represented by the difference of the square roots of the cohesive energy densities of the polymer and the solvent, and pass through a maximum with variations in the polarity of the rubber.

The M. V. Lomonosov Institute of Fine
Chemical Technology Moscow

Received September 5, 1956.

LITERATURE CITED

[1] B. A. Dogadkin and V. E. Gul, Proc. Acad. Sci. USSR, 70, 6, 1017 1950; V. E. Gul, Colloid J., 13, 2, 99 1951; V. E. Gul, T. V. Dorokhina, and B. A. Dogadkin, Colloid J., 13, 5, 339 1951; V. E. Gul, N. Ya. Sidneva, and B. A. Dogadkin, Colloid J., 13, 6, 422 1951.

[2] V. E. Gul and G. S. Klitenik, Colloid J., 16, 3, 37 1954.*

[3] J. G. Kirkwood, R. J. Goldberg, Chem. Phys. 18, 1, 54 1950.

[4] G. M. Bartenev and L. A. Vishnitskaya, J. Tech. Phys., 20, 7, 858 1950.

[5] Krigbaum, P. Flory, J. Pol. Sci. 11, 1, 37 1953.

[6] G. Gee, Chemistry of Large Molecules, Vol. 1, (IL, 1948).

---

* Original Russian pagination. See C. B. translation.

THE POSSIBILITY OF SURFACE ACTIVATION AND PASSIVATION OF NUCLEI IN WATER VAPOR CONDENSATION

G.I. Izmaĭlova, P.S. Prokhorov, and B.V. Deryagin

It is known that atmospheric condensation nuclei play the principal role in processes of cloud and mist formation, and therefore in precipitation. By artificially introducing hygroscopic $CaCl_2$ nuclei into clouds, Fedoteev succeeded, for the first time in history, in inducing artificial precipitation. Studies of the activity of different kinds of atmospheric condensation nuclei should assist in the development of the theory of cloud formation and precipitation. It appears even more attractive to develop means for varying the activity, and hence the "activity spectrum", of atmospheric condensation nuclei, as this may make it possible to influence the dispersivity of the forming cloud, and hence the precipitation conditions.

For a study of this range of problems, we began by developing a method for estimation of the activity of condensation nuclei by measurement of the degree of supersaturation at which the condensation nuclei "appear", i.e., can be observed visually. This degree of supersaturation can be termed the "nominal critical supersaturation", as it depends to a considerable extent on the experimental and observation conditions*.

The most convenient of the very few existing methods for determining the critical supersaturation is Amelin's flow method [2]. The principle of this method is that when a free vapor-air stream mixes with the surrounding air (or in general, when any gases differing considerably in temperature and humidity are mixed), there is a definite optimum mixing ratio n, which depends only on the temperatures and humidities of the mixing gases, and which corresponds to the maximum supersaturation given by:

$$S = \frac{p_1 + p_2 bn}{(1 + bn)\, p_s}, \qquad (1)$$

where p_1 and p_2 are the water vapor pressures in the stream and the air volume; b is the ratio of the molecular weights of the vapor-air mixture in the stream and the volume, M_1/M_2; n is the mixing ratio, equal to the ratio of the weights of the mixing volumes, g_2/g_1; p_s is the saturated vapor pressure of water at the temperature of mixing.

By gradually varying the temperature of the stream and recording the temperatures and moisture contents of the mixing volumes at the instant of mist formation, it is possible to use the above equation to calculate the corresponding supersaturation, which is also the critical value. If condensation could be observed at the first instant of new phase formation, this method would give quite exact results. In fact, however, there is some lag in recording the start of condensation. It may happen that before this occurs some droplets will leave the zone of maxium supersaturation, at which condensation began, and will start to evaporate; this will evidently give a high value for the measured critical supersaturation. This disadvantage may be avoided by mixing two streams, with a volume flow ratio exactly equal to the optimum mixing ratio n_{opt} which gives the maximum supersaturation S_{max} at the given temperatures and moisture contents of the streams. In such a case, if the corresponding S_{max} is equal to the critical supersaturation for the condensation nuclei introduced into one of the streams, droplet growth will not cease even after complete mixing, once it has started. At the same time there is no longer any risk that the measured critical supersaturation is below the true value, as it is impossible for a region to be formed in the mixing zone where the supersaturation is greater than it would be on complete mixing, and accordingly greater than S_{max}. To diminish errors due to condensation of moisture on the walls, the mixing streams can be directed countercurrent, as the supersaturation zone is then formed in the central region of the cell.

---

* It may be noted, however, that the theoretical value of the critical supersaturation in the theories of Volmer, Beaker and Doring, Zeldovich, Frenkel [1] and others also depends on an arbitrary boundary value of the rate of formation of viable nuclei, although in practice this uncertainty is not very important.

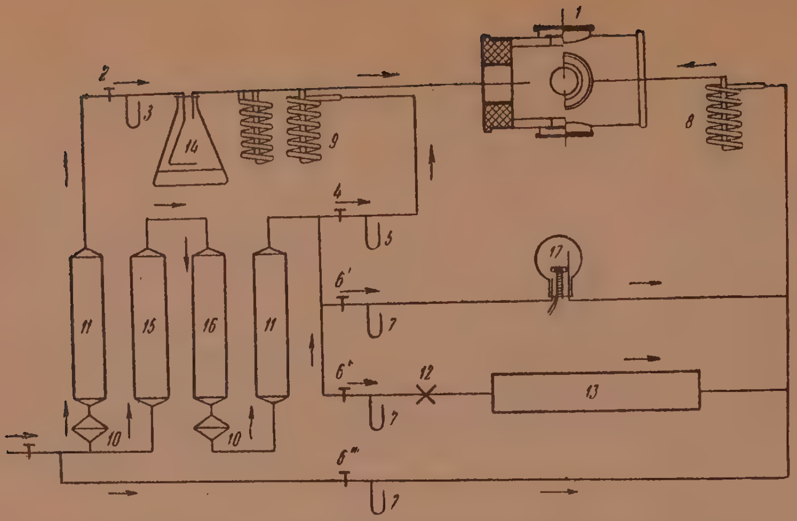

Fig. 1. Diagram of apparatus for measurement of critical supersaturation: 1) cell; 2-4-6^{I}-6^{II}-6^{III}) micro-taps; 3-5-7) flow meters; 8-9) thermostats; 10) glass gas filter; 11) filter filled with absorbed degreased cotton wool; 12) atomizer; 13) oven with drying agent; 14) humidifier for hot stream; 15) $CaCl_2$ column; 16) activated alumina column; 17) device for sublimated nuclei.

The apparatus is shown schematically in Fig. 1. Two streams are mixed in the cell 1; one is a hot stream of variable moisture content, passing through the micro-taps 2 and 4, and flow meters 3 and 5, where the flow rate is measured. The second is a dry cold stream, with condensation nuclei introduced into it; this passes through the micro-tap 6 and is measured in the flow meter 7. The temperature of the cold stream is regulated by means of the thermostat 8. The hot stream is humidified in the evaporator 14. Condensation nuclei are fed into the cold stream as required; atmospheric nuclei (micro-tap 6^{III}), by sublimation (micro-tap 6^{I}), and from a solution atomized in the atomizer 12 (micro-tap 6^{II}), the solvent being absorbed in the drying oven 13. The air is filtered through glass and cotton wool gas filters. Moisture is absorbed from the air in calcium chloride and activated alumina to a dew point ≈ - 50°.

The determination procedure is as follows: n_{opt} * corresponding to the given characteristics of the cold and hot streams is calculated. The cold dry stream containing the condensation nuclei, and the warm stream of variable humidity, are then fed into the cell in a ratio equal to n_{opt}. The moisture content of the warm stream is then smoothly varied by addition of a stream saturated with water vapor to it, at a constant total flow rate. At the instant of visible mist formation in the cell the moisture content of the warm stream and the temperature of the mixture are recorded, and the results are used to calculate the critical supersaturation from Equation (1).

It should be noted that n_{opt} does not remain constant with increase of the moisture content of the warm stream, as the specific heat and molecular weight vary accordingly. However, it is easy to make the appropriate corrections.

---

* If the first derivative of S with respect to n is equated to zero and the equation solved for n, we have:

where $a = \frac{C_2}{C_1}$ is the specific heat ratio; L is the latent heat of vaporization in cal./g.

TABLE 1

Critical Supersaturation (S_c) as a Function of the Size of the Condensation Nuclei

Weight concentration of solution in g per 100 g of solution	Area of rectangle, cm² • • 28,000	Nominal radius, cm	S_c, experimental	S_c' theoretical, calculated by [2]
0.3	0.96	$2 \cdot 10^{-5}$	0.84	1.000
$0.3 \cdot 10^{-2}$	0.34	$1 \cdot 10^{-5}$	0.92	1.001
$0.3 \cdot 10^{-4}$	0.1	$6 \cdot 10^{-6}$	1.1	1.002
$0.3 \cdot 10^{-6}$	0.04	$3.6 \cdot 10^{-6}$	1.33	1.005

TABLE 2

Critical Supersaturation for NaCl Nuclei Modified by Vapors of Surface Active Substances

Surface active substance	Critical supersaturation			$\frac{\overline{S}_c^{\times}}{\overline{S}_c}$
	before modification $\overline{S}_c$	modified $\overline{S}_c^{\times}$	after modification $\overline{S}_c$	
Formaldehyde	1.6	2.38	1.77	1.4
$Si(C_2H_5)_2$	1.34	1.25	1.38	0.9
$[(C_2H_5)_3Si]_2O$	1.33	1.15	1.33	0.82
Acetone	1.16	0.9	1.16	0.8
Isoamyl alcohol	1.47	1.09	1.47	0.7

The method described above was used to determine the critical supersaturation for small (average radius $r = 3.6 \cdot 10^{-6}$ cm) crystals of sodium chloride as a function of crystal size. A solution of NaCl in distilled water was atomized by a dry filtered stream of air in a glass atomizer. The resultant fairly monodisperse mist, with droplet size $\sim 0.1\,\mu$ was first passed through a heated tube, where the drops dried and the water vapor was then absorbed in phosphoric anhydride, while the air stream containing the crystals was cooled in a thermostat and entered the cell. The crystal size can be regulated by variation of the solution concentration. At the entry into the cell the crystals were caught on a gauze and then photographed under the electron microscope after chrome shadowing *. The photographs were used to determine the crystal size in mutually perpendicular directions, and the nominal radius of a nucleus was calculated from the average of several such measurements. Nuclei consisting of silica were studied next. The starting material was silica powder of the following chemical composition:

$$Na_2CO_3 \text{ not } > 2\%$$
$$CaCO_3 \text{ not } > 8\%$$
$$SiO_2 \text{ and } H_2O \text{ not } < 90\%$$

The specific surface of the powder was 100 m²/g.

The SiO_2 nuclei were fed in by the same procedure as the NaCl nuclei, the only difference being that a suspension of SiO_2 in distilled water was atomized rather than a solution.

The results obtained for NaCl nuclei are given in Table 1.

The activity of the condensation nuclei – NaCl crystals – was modified by the action of vapors of certain surface active substances. To a stream containing the nuclei a small amount of vapors of the surface active

---

* The electron micrographs were kindly taken by Yu. M. Polukarov, to whom we express our gratitude.

substances. To a stream containing the nuclei a small amount of vapors of the surface active substances was added, penetrating into the system by diffusion from a vessel connected by a tap, and the surface active substances were adsorbed on the nuclei. The accuracy of the determinations was checked by comparison of the values for the critical supersaturation at the nuclei before introduction of the vapors, and after their supply had been cut off. If these values agreed, there were no errors in the determination. The results are given in Table 2.

Silica was chosen as a material for study as its surface properties can be easily modified by heat treatment [3]. The SiO_2 nuclei were modified in a tubular quartz furnace through which they were passed, and the temperature of which could be varied by variation of the heater voltage. The treatment time was 2-3 minutes. The temperature, which was varied between 120 and 732°, was measured by means of a thermocouple placed in the aerosol stream at the furnace exit.

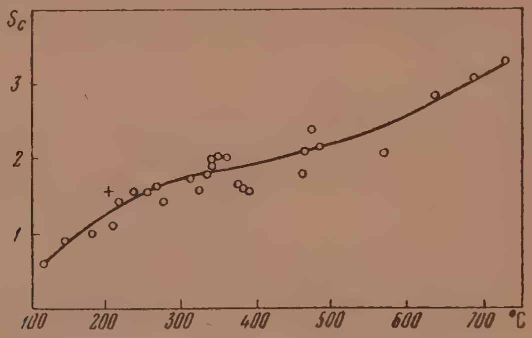

Fig. 2. Variation of the critical supersaturation for SiO_2 condensation nuclei with the temperature of heat treatment.

The relationship obtained between S_c for water vapor and the temperature of heat treatment of the condensation nuclei is shown graphically in Fig. 2. To test whether the thermal modification was reversible, SiO_2 powder was heated in a muffle furnace at 750° for 4 hours, cooled, introduced into the cell by the usual method, and S_c for it was determined (the result is indicated on the graph by a cross). It is seen that the thermal modification is reversible, the initial surface properties being restored.

DISCUSSION OF RESULTS

Our experimental values of S_c for different sizes of the NaCl nuclei were compared with theoretical values of S'_c calculated with the influence of curvature (Kelvin) and of vapor pressure variations over solutions of variable concentrations (Raoult) taken into account [4]. The values found for S'_c are given in Table 1.

The experimental values for condensation nuclei 0.1-0.2 μ in size are rather lower than the calculated values, which is probably because the large nuclei can reach 0.4 μ in diameter, which corresponds to the threshold of visibility by equilibrium humidification before the maximum on the supersaturation – droplet size curve is reached.

For nuclei of the order of 10^{-6}cm the deviations between the experimental and theoretical values are considerable. The probable reason for this discrepancy is that the theoretical calculations are primarily based on the assumption that the condensation process is fairly slow, whereas in our case the process is very rapid. In consequence, our measured values must be regarded as nominal supersaturation.

Calculations show that in our apparatus the droplets should grow to 0.4μ in 0.5 second, and the mist formed can then be observed visually. It is interesting to compare our values of S_c for NaCl with previously published data [5].

In the investigation cited, the authors used a diffusion chamber and obtained a value of 1.09-1.2 for S_c for NaCl nuclei with minimum diameter 10^{-6} cm, which is fairly close to our value for $6 \cdot 10^{-6}$ cm nuclei (see Table 1). However, the kinetic factor to which reference was made earlier should have an effect in this case also.

The results of experiments on modification of the condensation nuclei, either by vapors of surface active substances in the case of NaCl, or by heat treatment, show that it is possible in practice to vary the measured nominal critical supersaturation at condensation nuclei.

The dehydration mechanism of the SiO_2 surface (as a result of modification) probably involves impedance to the formation of donor-acceptor bonds between molecules on the surface and molecules of condensing water [3], which evidently influences the condensation process. The results obtained for NaCl nuclei modified by surface active vapors indicate that the surface of the condensation nuclei is changed owing to formation of adsorption layers. The formation of adsorption layers is accompanied by a change in the interaction between the surfaces of the condensation nuclei and the molecules of condensing water, i.e., in the general case the hydrophilic nature of the surface is changed and it may become hydrophobic.

SUMMARY

1. It is shown that it is possible to vary the "activity" of NaCl and SiO_2 condensation nuclei toward water vapor, as shown by increase or decrease of the nominal critical supersaturation S_c.

2. The change of "activity" can be effected by adsorption of vapors of surface active substances on the nuclei in the case of NaCl, or by dehydration in the case of SiO_2.

3. The mechanism of this effect probably consists of modification of the surface properties of the condensation nuclei, leading to changes in the condensation rate owing to variation of the accommodation coefficient.

Institute of Physical Chemistry Academy of Sciences
USSR Moscow

Received January 24, 1957

LITERATURE CITED

[1] M. Volmer, Kinetic der Phasenbildung, Leipzig, 1939; Beaker, Doring., Ann. Phys. 24, 719 1935; Ya. B. Zeldovich, J. Exp. Theoret. Phys., 12, 525 1942; Ya. I. Frenkel, The Kinetic Theory of Liquids (Izd. AN SSSR 1945).

[2] A. G. Amelin, Theoretical Principles of Mist Formation in Chemical Industries (Goskhimizdat, 1951).

[3] S. P. Zhdanov, Proc. Acad. Sci. USSR, 68, 99; 100, 1115 1955.

[4] W. E. Howell, J. Meteorol., 6, 134-149 1949; B. V. Kiryukhin, Trans. Chief Geophys. Observatory, No. 24, 86 1950; B. V. Deryagin, S. S. Dukhin, M. L. Mikelson, and V. I. Kagener, The Struggle Against Silicosis (Izd. AN SSSR 1955) p. 22.

[5] D. Schiff, H. J. Schilf, P. R. Gendron, Canad. J. Chem. 31, No. 11, 1108 1953.

ADSORPTION OF WATER VAPOR BY SILICA AND HYDRATION OF ITS SURFACE*

A.V. Kiselev and G.G. Muttik

Investigations of the adsorptive properties of coarsely porous silica gels and various specimens of quartz show that the adsorptive properties per unit surface of these adsorbents are similar [2-7]. This is the consequence of the similarity of the chemical surface structure of these substances if their degrees of hydration are similar. Differences in the packing of the silicon-oxygen tetrahedra in the amorphous particles of the silica gel skeleton and in quartz crystals have no significant influence on the adsorptive properties. Silica xerogels, since they originate from hydrogels, carry silicic acid hydroxyls on the surface. These hydroxyls can be removed by calcination [8, 9]. Hydration of the surface of calcined silica gels again leads to formation of surface hydroxyls, bound to the skeleton by valency bonds [10-12]. These acid hydroxyl groups act as electron acceptor centers of the surface, and may form donor-acceptor bonds with molecules having electron donor properties [5, 7, 13, 14]; water molecules are bound to the surface hydroxyl groups by hydrogen bonds, and these are the bonds which primarily determine adsorption on hydrated silica gel and quartz surfaces. It is therefore of interest to study the concentration of hydroxyl groups on silica gel surfaces, and the bonds between adsorbed molecules and these groups. In adsorption of water vapor, each molecule can be bound to the surface hydroxyls by means of one or of two hydrogen bonds. Electrostatic and dispersional interaction also depend on the degree of hydration, as the electostatic field of the surface and the distances between the adsorbed molecules and the atoms of the lattice vary with changes in the concentration of the hydroxyl groups. On the other hand, the view has been put forward that other adsorption centers are present on silica gels, differing from hydroxyl groups by having considerably higher activity in adsorption of water and alcohol vapors [15].

Most workers who studied adsorption on silica gel and quartz used adsorbents with surfaces hydrated to various extents. In the case of silica gels, the surface hydration depends on the method used for their preparations from hydrogels; the various specimens of quartz, rock crystal, porous glass, and other silica specimens were usually subjected to prolonged contact with water and their surfaces were hydrated. However, in most of the cases described in the literature** the adsorbents were heated in vacuum at 150-500°, and were thereby dehydrated to various extents; this affected the adsorptive surface properties. It has been established [10-12] that after adsorption of water vapor followed by evacuation at temperatures not higher than 200° the surfaces of different specimens of silica gel and quartz are hydrated to approximately the same extent. The isotherms for adsorption of water vapor per unit area of such similar surfaces coincide [5, 11, 12]. The surfaces of such specimens are almost completely hydrated, i.e., all the silicon atoms on the surfaces are bound to hydroxyl groups. Heating in a vacuum at 200-300° has little effect on the degree of surface hydration. At maximum hydration, all the silicon atoms emerging on the surface are bound with one or two hydroxyl groups [5, 12].

In the present investigation the adsorption of water vapor was studied on a silica specimen which did not come into contact with water during preparation, and which was therefore not so strongly hydrated as silica gels.

---

* A preliminary communication of the results of this investigation was made at the Jubilee Conference of the Moscow State University, April 20, 1955 [1].

** See [11, 12] for the literature.

Specimens and Determinations

Silica. The starting specimen of silica was prepared by G. V. Vinogradov, by combustion of organosilicon compounds; to remove residual carbon the specimen was heated at 900-1000° for several hours*; its specific surface was 185 m^2/g [16]. A part of the original specimen was covered with water and dried at 90-100° after 6.5 months of exposure to water. The specific surface of this hydrated specimen, also determined by nitrogen adsorption, was 135 m^2/g**. Investigations of the adsorption-desorption isotherms for benzene vapor on these specimens showed that they are heterogeneously porous [19]; combustion and calcination resulted in irregular sintering, but the surfaces of the specimens were quite accessible even to benzene molecules. The hydroxyl group contents on the surfaces of the evacuated specimens were determined from the weight loss after calcination at 1100°. For the original specimen, evacuated at 200°, the hydroxyl group content was 3 micromoles/m^2, while for the specimen hydrated by exposure to water and then evacuated at 115° it was 11 micromoles/m^2. This latter value is close to the limiting hydroxyl content on silica surfaces, which is ~ 13 micromoles/m^2 [12].

Adsorption determinations. The choice of the method of adsorption determination was guided by the following considerations: 1) it was necessary to determine with fair accuracy very small values of adsorption with small degrees of surface filling, especially on dehydrated specimens; 2) it was also necessary to determine very large values of adsorption on the same specimens at high relative pressures of water vapor; 3) it was very desirable to follow the course of slow hydration of the surface of the original specimen. To satisfy these requirements, we used an automatic recording vacuum balance specially designed for such determinations [20]. To ensure a fairly large total surface of the specimen, the balance takes loads up to 10 g; the weighing range is 1.2 g; the sensitivity over the whole weighing range is at least $1 \cdot 10^{-4}$ g. The zero position should not be appreciably displaced during an adsorption – desorption experiment, which usually lasted several months.***

A diagram of the vacuum adsorption apparatus with the recording balance, used in our investigation, is shown in Fig. 1.

The specimen is placed in the bucket 1, suspended from the front end of the beam 2 by means of a tungsten wire 18 μ in diameter. The beam is suspended, from similar vertical tungsten wires 3, inside the glass T-tube 4. The opposite end of the beam carries an iron core 5. By varying the current strength in the electromagnet 6 by means of the rheostats R_1 and R_2 the beam may be brought into the horizontal position. Changes in the weight of the specimen can be found from changes in the current strength, measured by the milliammeter 7. The horizontal position of the beam is indicated by the position of the end of the pointer 8. By varying the current in the electromagnet 6 between 0 and 30 ma, an increase of 0.1 g in the weight of the specimen can be compensated; if the weight increase is greater than this, the rider 9 is moved along the notches of the beam with the aid of an auxiliary magnet****. For each of the 12 positions of the rider, a calibration curve is plotted showing the current strength in the coil of the electromagnet 6 as a function of the load on the front end of the beam; the calibration is carried out with the aid of microanalytical weights and by an aerostatic method [25].

Changes in the weight of the specimen can be recorded automatically. A light beam from the source 10 is directed on the mirror 11, attached to the beam. The reflected light is distributed between the photocells of the differential photorelay***** in a manner which depends on the deflection of the beam; the amplifier 13 receives a positive or negative signal, and the pen of the recording device moves to the right or left, simultaneously displacing the sliding contact of the rheostat. As a result the current strength in the electromagnet 6 is altered, and the beam again assumes the horizontal position*.

---

* We take this opportunity to thank G. V. Vinogradov for supplying this specimen.

** The decrease of specific surface after exposure to water is probably the consequence of reconstruction of the silica particles owing to solution of the smallest particles, which comprise an appreciable fraction of the total surface. A similar change of specific surface on treatment of xerogels by hot water vapor occurs very rapidly (see [17, 18]).

*** The vacuum balances described in the literature do not satisfy all the above requirements. The most sensitive vacuum balances [21-23] can only take considerably smaller loads, and their weighing range is considerably narrower. Gregg's balance [24] is free from these faults, but is too complicated.

**** Displacement of the rider by one notch corresponds to 0.1 g change in weight.

***** For the photorelay circuit, see [26].

The glass T-tube of the balance is separated from the ampoule containing the adsorbate by an electromagnetic valve 14, which admits the adsorbate vapor into the working part of the apparatus. The construction of the valve is shown in Fig. 1. A moving iron core 23 with a Teflon lining is pressed against the central opening by the spring 24 – in the normal position the valve is shut. If a current is passed through the electromagnet 25, the core 23 is attracted to the stationary part 26, and the tubes 27 become connected. The coil of the electromagnet is enclosed in the iron yoke 28 in order to increase the magnetic flux in the gap between cores 23 and 26.

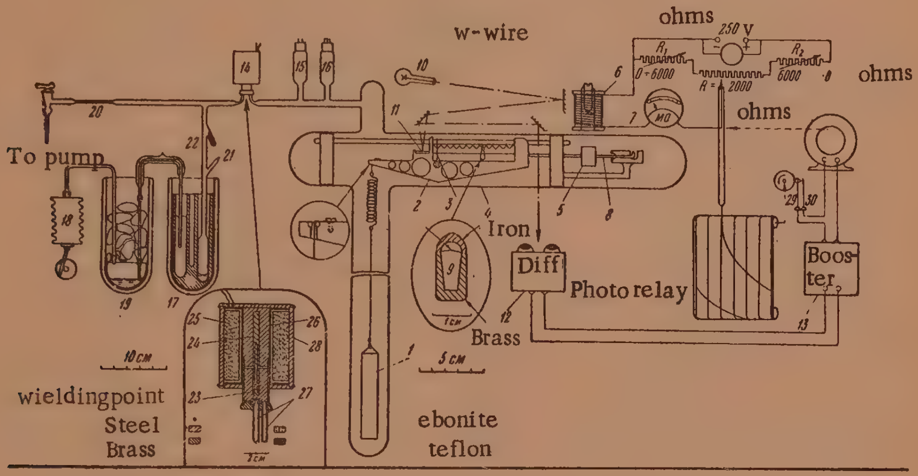

Fig. 1. General diagram of apparatus: 1) specimen; 2) balance beam; 3) tungsten suspensions; 4) glass T-tube; 5) iron core; 6) electromagnet; 7) milliammeter of 0.1 class; 8) pointer; 9) rider; 10) light source; 11) beam mirror; 12) photorelay; 13) booster for recording EPP-09 potentiometer; 14) electromagnetic valve; 15) tube of LT-1 thermocouple vacuum gauge; 16) tube of LM-2 ionization manometer; 17) aluminum block; 18) pneumatic pump; 19) cold storage cell of cryostat; 20) capillary tube; 21) branch tube; 22) glass membrane; 23) core of valve; 24) spiral spring; 25) electromagnet winding (wire 0.3 mm in diameter); 26) stationary iron core of valve; 27) outlet tubes; 28) yoke of electromagnet; 29, 30) cut-out contacts.

The vacuum is measured during evacuation of the adsorbent by means of a Pirani manometer 15 and an ionization manometer 16. The ampoule with the absorbent is placed in a K-1 cryostat**. The aluminum block 17 of the cryostat is cooled at a temperature of +20 to -60° by methanol, which is pumped by the pump 18 from the cold storage cell 19, where it is cooled by solid carbon dioxide. At lower temperatures, liquid nitrogen is used for cooling. In such cases the cold storage cell 19 is replaced by a Dewar flask (Fig. 2) 1 liter in capacity. The block 17 is then cooled by liquid nitrogen entering along the tube 2, as in Henning's cryostat [28, 29]. Instead of a contact thermometer, a resistance thermometer 3, which is an arm of a Wheatstone bridge supplied by an alternating current at 2 v through the transformer 12, is inserted into the block 17. The disbalance potential is fed from the bridge to the booster 4 of an EPD-17 recording potentiometer***. A variable resistance R_1 (type SP-2) and a mercury valve 5 are attached along the axis of the recording instrument slide wire. The cryostat is regulated to the required temperature by means of the resistance box R_2. If the temperature of the block 17 is higher than required, the bridge is out of balance, and the recorder motor closes the valve 5.

---

* For a more detailed description of the vacuum balance, see [20].

** Described in [27], manufactured by the "Platinopribor" works.

*** EPD-07 or EPP-09 may be used, or balanced bridges with electronic boosters.

Evaporating nitrogen cannot then escape from the vessel 7 and liquid nitrogen therefore passes along the tube 2 into the block 17 and cools it. When the block has reached the required temperature, the sign of disbalance in the bridge changes, the motor opens the valve 5, and flow of nitrogen into the block 17 stops. This low-temperature cryostat was used at temperatures below – 60°, down to – 195°, with a thermostatic accuracy of ± 1°.

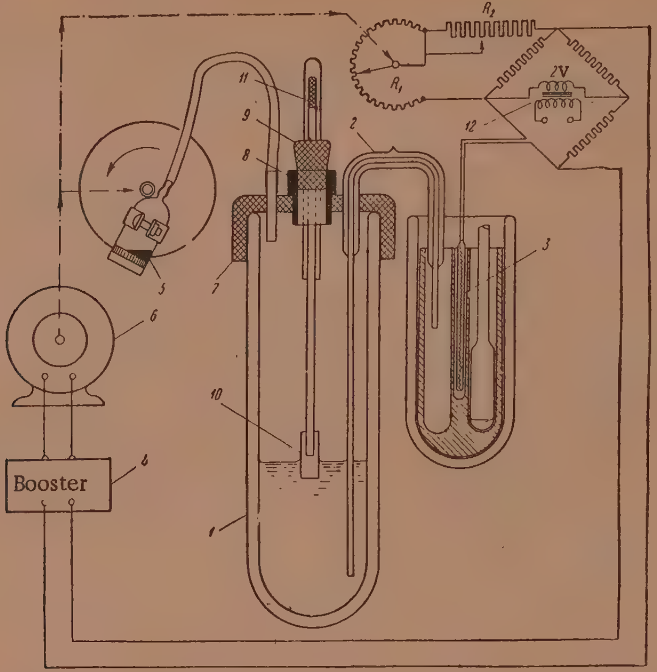

Fig. 2. Cryostat for temperatures between – 60 and – 195°: 1) cold storage cell with liquid nitrogen; 2) siphon tube; 3) resistance thermometer (nickel wire 0.07 mm in diameter); 4) booster of EPD-17 recording instrument; 5) mercury valve with porous glass partition (No.2 filter); 6) motor; 7) rubber cover; 8) tube for adding nitrogen; 9) bung; 10) float; 11) nitrogen level indicator; 12) transformer.

By keeping the block 17 at the required temperature by means of one of these cryostats, the desired vapor pressure of the adsorbate can be maintained in the apparatus. The apparatus therefore has no greased taps (the constriction 20 is sealed off after evacuation of the apparatus), mercury seals, or mercury manometers, so that it is possible to work with organic vapors soluble in vacuum grease, and no mercury vapor is present.

The evacuation is effected by an MM-40A oil diffusion pump and a VN-494 rotary pump. The apparatus was separated from the pumps by a trap with liquid nitrogen. Dissolved gases were removed from the adsorbate through the side tube 21 in a separate apparatus. After evacuation of the apparatus the ampoule membrane 22 was broken, and the adsorbate vapor was able to enter the intermediate part of the apparatus. A thermostat was placed under the lower end of the glass T-tube 4 (see Fig. 1), by means of which the specimen could be thermostatically controlled between 10 and 450° to an accuracy of ± 0.1°.

DISCUSSION OF RESULTS

Adsorption of water vapor on the original silica specimen. Fig. 3 shows the isotherm for adsorption of water vapor on the original specimen, after evacuation at 2–5 $\cdot 10^{-5}$ mm Hg and 200° for 20 hours. The weight loss was small (< 3 mg per 1 g silica) although the original specimen was exposed to air after preparation.

Despite the large specific surface of the original specimen (185 m^2/g), the adsorption is very slight in the initial part of the isotherm, indicating that the activity of this silica specimen in adsorption of water vapor

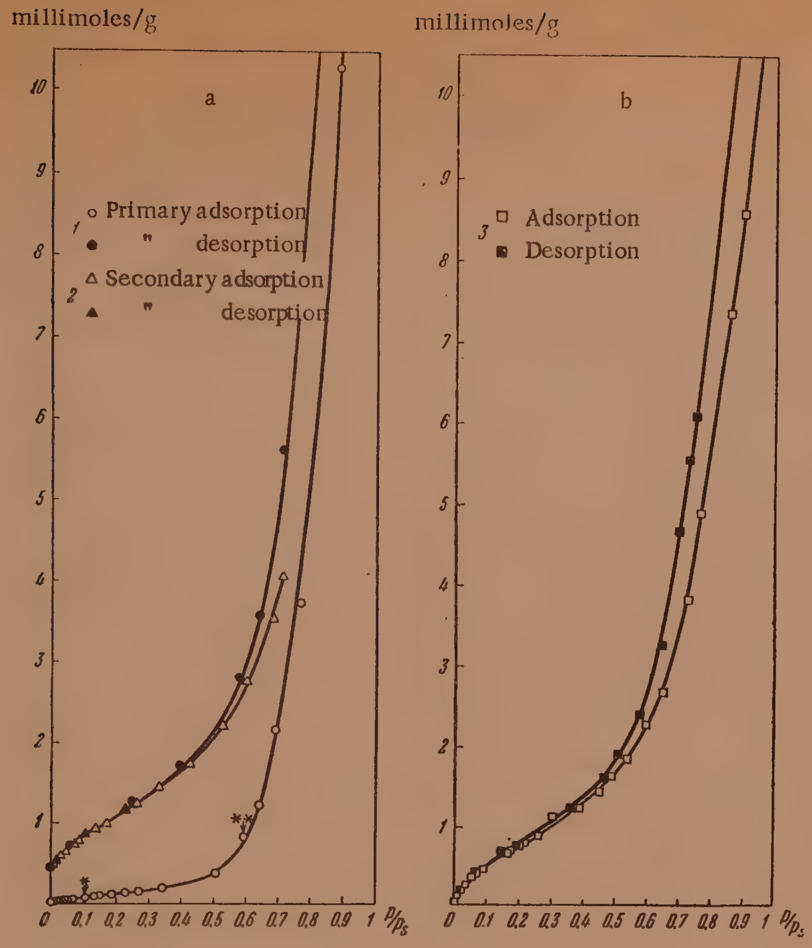

Fig. 3. Isotherms for adsorption and desorption of water vapor: 1) on the original specimen; 2) specimen hydrated in water vapor; 3) specimen hydrated in liquid water.

is very low in comparison with silica gels. At a relative water vapor pressure $p/p_s = 0.2$ the specimen adsorbed only 0.6 micromole/m^2, whereas a silica gel with a hydrated surface at the same p/p_s adsorbed 6.5 micromoles/m^2, [11]. The initial region of the isotherm for this specimen is concave; equilibrium was established rapidly (within 1-2 hours) in this region. This indicates that the interaction is confined to physical adsorption of water vapor. However, at relative pressure of 0.4-0.6 and over, the amount of adsorbed water increased sharply, and equilibrium at each point of this region of the isotherm was only reached after 30-60 hours*. Fig. 4 shows the corresponding kinetic curves for the original specimen at $p/p_s \approx 0.1$ and at $p/p_s \approx 0.6$. The nature of the curves in Figs. 3 and 4 indicates that in the region of high p/p_s slow chemisorption leading to hydration of the silica surface takes place in the original specimen, in addition to capillary condensation and physical adsorption.

2.5 months was necessary for studying the region of the isotherm in the p/p_s range between 0.4 and 0.95. Thus for ~1800 hours the specimen was in an atmosphere of water vapor at relative pressures between 0.4 and 0.95. Total saturation ($p/p_s = 1.0$) was not reached in this experiment, but despite this, as Fig. 5 shows, the desorption and adsorption branches did not coincide down to the lowest water vapor pressures. After evacuation at 25° for 2 weeks, ~0.42 micromole of water per 1 g, or 1.8 micromole/m^2, remained bound with the silica surface. The secondary adsorption branch determined after this coincided with the desorption branch up to $p/p_s =$ $= 0.3$ (to the start of capillary condensation); it resembles in shape the usual convex isotherm for adsorption of water vapor on silica gels and quartz. Thus, after prolonged exposure of the specimen to water vapor at high values of p/p_s, when a liquid water film accelerating hydration was formed on the surface, the isotherm became reversible.

---

* In analogous cases capillary condensation on silica gels with hydrated surfaces is much more rapid.

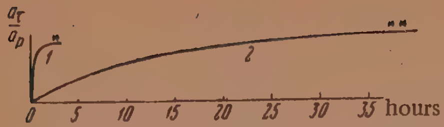

Fig. 4. Comparison of the kinetics of water vapor adsorption at low and high relative pressures. The curves lead to the equilibrium points marked by asterisks in Fig. 3: 1) one asterisk; 2) two asterisks.

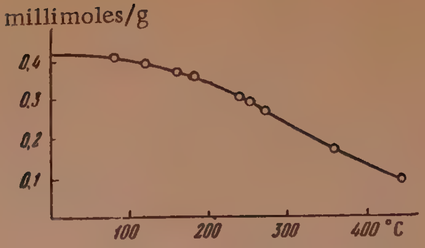

Fig. 5. Graph showing loss of weight on heating of a specimen hydrated in vapor, i.e., after an adsorption-desorption cycle.

After a second adsorption was carried out up to $p/p_s = 0.7$, a desorption experiment demonstrated the reversibility of the isotherm. The specimen was further evacuated on heating consecutively to temperatures of 80, 120, 160, 180, 240, 250, 270, 360 and 450°. The evacuation was continued for 6 hours at each temperature, with 20 hours at 450°. In this way the specimen was brought to practically constant weight at each temperature. Fig. 5 shows the amounts of water retained by this specimen at different evacuation temperatures. It is seen that heating in a vacuum to 200° dehydrates the surface of this silica specimen only slightly. The water adsorbed by the original specimen during the adsorption experiment cannot be completely removed even by heating to 450° in vacuum.

The fact that the desorption branch and the primary adsorption branch for adsorption of water vapor do not coincide in the initial region of the isotherm has been noted earlier for porous glasses and silica gels heated to 300° before the adsorption experiments. However, in these experiments the amount of irreversibly bound water was relatively small and the primary adsorption branch remained convex (see [11]). The primary adsorption isotherm was concave only for adsorption of water vapor by porous glass and silica gel heated at 650° in vacuum [12, 30]. In such cases the action of capillary-condensed water on the surface freshly dehydrated by heating also restored the original convex form of the isotherm, and ~ 5 micromoles/ m^2 of water again remained irreversibly bound to the surface.

In our case the adsorption took place on a specimen which was still less hydrated, and therefore the amount of irreversibly bound water proved very large.

Adsorption of water vapor on a hydrated silica specimen. Isotherms for adsorption and desorption of water vapor on a silica specimen kept under water for 6.5 months are given in Fig. 3, b. The specimen was evacuated at 115° before the experiment. The initial region of the isotherm for primary adsorption of water vapor is convex in this instance, and differs sharply in this respect from the concave initial region of the isotherm for the original specimen (Fig. 3, a). The isotherm in Fig. 3, b resembles the isotherms for adsorption of water vapor on silica gels [11]. The secondary adsorption branch is close to the primary adsorption branch.

The initial regions of the adsorption isotherms, calculated per unit surface, are compared in Fig. 6. These graphs show that hydration of the original sample during sorption of water vapor (see Fig. 3, a) increased 6-fold its adsorptive activity at $p/p_s = 0.1$, while exposure to water produced an 8-fold increase. Comparison with the isotherm for adsorption of water vapor in silica gels (curve without points in Fig. 6 [11]) shows that adsorption of water vapor by a specimen of silica prepared by combustion of organosilicon compounds and hydrated by exposure to liquid water approaches the adsorption of water by silica gel. The absolute values of adsorption for the hydrated specimen are only 20% lower than for silica gel. As the result of prolonged action of liquid water, the surface state of this silica became similar to the state of the hydrated silica gel surface. The somewhat lower values for the adsorption are probably the consequence of a lower (by about 8%) hydroxyl content on the surface of this hydrated silica specimen (11 micromoles/ m^2) in comparison with the silica gel surface (~ 13 micromoles/ m^2).

Thus, the surface of silica obtained from organosilicon compounds is hydrated much less rapidly (some tens of times) in water vapor than silica gel or porous glass after dehydration by heat at temperatures up to 650° [12]; even prolonged exposure (more than half a year) of this silica to liquid water hydrates its surface less than the surface of silica gel.

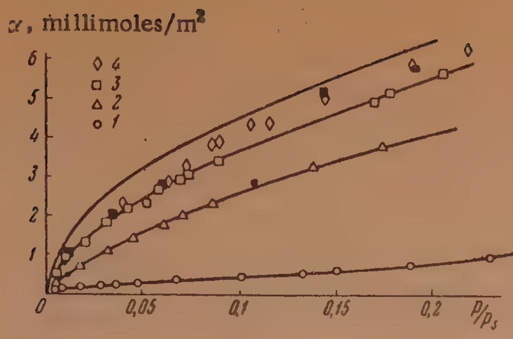

Fig. 6. Initial regions of isotherms for adsorption of water vapor (α-adsorption on 1 m²): 1) on original silica; 2) on silica hydrated in vapor; 3) on silica hydrated in water; 4) ditto, secondary adsorption. Curve without points represents the absolute reversible isotherm for adsorption of water vapor on silica gels [11].

Possible forms of hydration of the silica surface. Silica gels are formed by polymerization of orthosilicic acid in aqueous solution, and therefore they can have at least two different types of bonds with surface hydroxyls

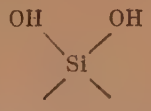

(I)

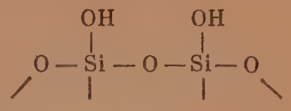

(II)

[8, 11, 12]. Such surface groups yield anhydride groups* on thermal dehydration of the silica gel, the anhydride groups also being of two different types** [5, 12]:

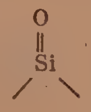

(III)

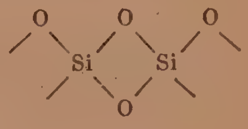

(IV)

Under the action of water vapor groups of Type (III) are probably hydrated more easily, becoming hydrate forms of type (I). It seems likely that hydration of anhydride groups of Type (IV) to give hydrate groups of Type (II) is slower, as this requires a greater activation energy. Thre presence of liquid water is probably necessary for this reaction to take place, i.e., this reaction occurs predominantly only in the capillary condensation region (at $p/p_s = 0.4$ and over). On thermal treatment of silica gels and silica, these reactions proceed in the reverse direction.

The relative content of Type (I) groups is probably higher in hydrated silica gels than in silica prepared from organosilicon compounds and then hydrated. Therefore the action of water vapor on silica gels thermally dehydrated at temperatures below 650° and on porous glasses [12] leads to hydration of a considerable number of Type (III) (siloxane) groups. These reactions take place on adsorption of water vapor even at relatively low p/p_s [5, 11].

Silica prepared by combustion of organosilicon compounds followed by heating to 1000° apparently has a predominance of Type (IV) anhydride groups on its surface. In particular, a recent investigation [31] indicates that the formation of these groups is probable. As this silica was not formed from the hydrate, as is the case with silica gel, the anhydride bonds are more stable than in dehydrated silica gel. Therefore the cleavage of such bonds in the silica used in our investigation occurs more slowly, i.e., requires a greater activation energy than in dehydrated silica gel.

Comparison of Silica Specimens and Silica Gel

Specimen	Treatment temperature, °C	Specific surface, m²/g	Water content, millimoles/g	OH group concentration α, micromoles/m²	$\omega_{OH} = \frac{1}{\alpha}$ in Å²
Original	200	195	0.3	3	50
Hydrated in vapor	25	185	0.75	8	21
Hydrated in water	115	135	0.75	11	16
Silica gel	20	320	1.7	12	14

---

[*] The hydrated forms are sometimes termed silanols, and the anhydrides, siloxanes [31].

[**] Type IV anhydride groups are formed in fibrous silica; see [32].

Thus, the sorption of water vapor by this silica at low relative pressures (up to $p/p_s = 0.4$) is mainly reversible adsorption, effected by ordinary van der Waals forces. In the case of thermally dehydrated silica gel, even at lower values of p/p_s, physical adsorption is followed by chemisorption and surface hydration [11].

At relative pressures above 0.4-0.6, vigorous chemical action occurs between liquid water and the surface of the original silica specimen, leading in all probability to formation of Type (II) hydrate forms. Increase of the temperature at which the water acts should correspondingly accelerate hydration, but in this case the changes in the geometrical structure of the silica: surface contraction, growth of the primary particles in the skeleton, and pore expansion [16, 17] are also accelerated. Thus, the course of the hydration of the silica surface varies according to its origin, both with regard to the kinetics and the concentration of water vapor required for hydration, and with regard to the maximum number of hydroxyl groups bound by the surface silicon atoms, although the latter differences are small.

The following tabulated values of the hydroxyl group contents retained on the surface after evacuation at 200°, compared with the values for silica gel, show that the differences between the final states are not large.

It was pointed out earlier (see Fig. 6) that the reversible absolute isotherm for adsorption of water vapor on a silica sample hydrated by exposure to liquid water does not lie, in its initial region, far below the curve for similarly treated silica gel. After reproducible adsorption-desorption cycles had been carried out, the mechanism of water vapor adsorption on hydrated silica and hydrated silica gel in all probability becomes the same, and the small difference between the absolute values of the adsorption is merely the consequence of somewhat different concentrations and forms of bonding of the hydroxyl groups on the silica and silica gel surfaces.

SUMMARY

1. The isotherms for the kinetics and equilibrium adsorption of water vapor on three specimens of silica prepared by combustion of organosilicon compounds have been studied: the original specimen, after hydration in water vapor, and after hydration in liquid water.

2. The adsorption isotherm for the original specimen is concave: in the region of low relative pressures the adsorption is small, and the interaction is predominatly physical in character. At higher pressures slow chemisorption also occurs, leading to hydration of the surface.

3. The isotherm for adsorption of water vapor on the specimen hydrated in liquid water is very similar to the isotherm for adsorption of water vapor on hydrated silica gel. The small differences are due to differences in concentration and types of hydrate forms on the surfaces of these adsorbents.

The authors express their gratitude to V. S. Bronshvager for his assistance in the construction of the vacuum balance used in this investiagion.

The M. V. Lomonosov State University, Moscow
Adsorption Laboratory

Received February 21, 1957

LITERATURE CITED

[1] A. V. Kiselev, in Symposium: "Surface Chemical Compounds and Their Role in Adsorption Phenomena" (Izd. MGU, 1957) p. 199.

[2] N. N. Avgul, O. M. Dzhigit, V. P. Dreving, M. V. Guryev, and O. A. Likhacheva, Proc. Acad. Sci. USSR, 77, 77 1951.

[3] N. N. Avgul, O.M. Dzhigit, A. A. Isirikyan, A. V. Kiselev, and K. D. Shcherbakova, Proc. Acad. Sci. USSR, 77, 625 1951.

[4] A. P. Karnaukhov, A. V. Kiselev, and E. V. Khrapova, Proc. Acad. Sci. USSR, 94, 915 1954.

[5] A. V. Kiselev, in Symposium: "Surface Chemical Compounds and Their Role in Adsorption Phenomena" (Izd. MGU, 1957) p. 90.

[6] A. V. Kiselev and Yu. A. Eltekov, J. Phys. Chem., 31, 250 1957.

[7] A. V. Kiselev, Progr. Chem., 25, 705 1956.

[8] A. V. Kiselev, Colloid J., 2, 17 1936.

[9] N. G. Yaroslavsky, J. Phys. Chem., 24, 68 1950.

[10] S. P. Zhdanov, Proc. Acad. Sci. USSR, 100, 1115 1955.

[11] L. D. Belyakova, O. M. Dzhigit, and A. V. Kiselev, J. Phys. Chem., 31, 1577 1957.

[12] S. P. Zhdanov and A. V. Kiselev, J. Phys. Chem., 31, No. 10 1957.

[13] A. V. Kiselev, Proc. Acad. Sci. USSR, 106, 1046 1956.

[14] A. N. Terenin, in Symposium: "Surface Chemical Compounds and Their Role in Adsorption Phenomena" (Izd. MGU, 1957) p. 206.

[15] V. A. Nikitin, A. N. Sidorov, and A. V. Karyakin, J. Phys. Chem., 30, 117 1956.

[16] A. V. Kiselev and E. V. Khrapova, Colloid J., 19, 572 1957.*

[17] A. V. Kiselev, E. A. Leontyev, V. M. Lukyanovich, and Yu. S. Nikitin, J. Phys. Chem., 30, 2149, 1956.

[18] H. Ries, in Catalysis. Catalysis for Organic Reactions (IL, 1955) p. 37.

[19] A. V. Kiselev and A. A. Isirikyan, Proc. Acad. Sci. USSR, 115, 244 1957.

[20] G. G. Muttik, J. Phys. Chem., 31, 263 1957.

[21] G. Rodin, in Catalysis. Investigations of Heterogeneous Processes (IL, 1956), p. 45.

[22] B. P. Bering and V. V. Serpinsky, Proc. Acad. Sci. USSR, 94, 497 1954.

[23] A. I. Sarakhov, Bull. Acad. Sci. USSR, Div. Chem. Sci., No. 1, 5 1956.

[24] S. J. Gregg, J. Chem. Soc., No. 5, 1438 1955.

[25] Steele, Grant, Proc. Roy. Soc. 82, 580 1909.

[26] A. V. Kiselev, V. F. Kiselev, N. N. Mikos, G. G. Muttik, A. D. Runov, and K. D. Shcherbakova, J. Phys. Chem., 23, 577 1949.

[27] G. G. Muttik, Factory Labs., 17, 1403 1951.

[28] F. Henning, Z. Instrumentenkunde 33, 33, 1913.

[29] K. V. Chmutov, Techniques of Physicochemical Research (Goskhimizdat 1954) p. 70.

[30] S. P. Zhdanov, Proc. Acad. Sci. USSR, 68, 99 1949.

[31] S. Brunauer, D. L. Kantro, C. H. Weise, Can. J. Chem. 34, 1438 1956.

[32] A. Weiss, Z. anorg. Chem. 276, 95 1954.

---

* Original Russian pagination. See C. B. translation.

INFLUENCE OF PORE SIZE AND SURFACE HYDRATION OF SILICA ON ADSORPTION OF NITROGEN VAPOR

A. V. Kiselev and E. V. Khrapova

It has been shown [1] that there are no significant differences between quartz and coarsely porous silica gels in absolute (i.e. calculated per unit surface) adsorption isotherms for nitrogen vapor. For adsorption on a finely porous silica gel specimen with effective pore diameter of ~ 25 A, the adsorption potential was found to be higher, and the isotherm was more convex. There were similar increases of the adsorption potential on silica gels of larger pore size for saturated hydrocarbons with large molecules, containing from 4 to 7 carbon atoms [2, 3], and for benzene [4-6]. The increased adsorption found for nitrogen and hydrocarbons [1] in fine silica gel pores is caused by an increase of the dispersional portion of the adsorption potential, which is additive. On the other hand, adsorption of nitrogen vapor depends on the nature of the adsorbent [7]. It has been shown [8-14] that the adsorptive properties of silica gels change, as the result of surface dehydration, esterification, and halogenation reactions, toward substances which are adsorbed not only by nonpolar van der Waals interaction, but are also capable of forming additional, closer bonds of the acid-base type with the acid hydroxyls of the silica gel surface [8, 15, 16]. This includes the adsorption of water vapor [17, 18], methanol [19, 20], and benzene [19, 21, 22]. The adsorption of saturated hydrocarbons, such as n-pentane [3] and n-hexane [22] is not very sensitive to dehydration of the silica surface. It was of interest to study the adsorption of nitrogen vapor in this respect. The nitrogen molecule has two free pairs of electrons [23] and therefore its adsorption should depend on the degree of hydration of acid adsorbents, including silica gels.

The adsorption of nitrogen vapor has usually been studied for determinations of specific surface by the BET (Brunauer, Emmett, and Teller) method, so that the measurements were carried out only in the region of high degrees of surface filling, $\theta > 1$. Therefore the question of the influence of the degree of surface hydration on the adsorption of nitrogen vapor remains unanswered. In the present investigation the effects of narrrowing of the pores in silica, and of the degree of surface hydration, were studied, starting with very low degrees of surface filling.

Specimens and Determinations

Adsorbents. The influence of silica structure on adsorption of nitrogen vapor was studied with silica gel No. 3 of the standard series [24] and two purified commercial specimens, KSK-2 and KSM-2, described previously [17]. The adsorption of nitrogen vapor on silica gels No.5 and No. 8 of the standard series and on a specimen of ground quartz was studied by us earlier [1]. It was therefore possible to evaluate the effects of constriction of pore dimensions (d) between approximately 100 and 25 A. Before the determinations all the specimens were evacuated at 280° down to a pressure $p < 10^{-5}$ mm Hg.

The following specimens were used for studying the effects of the degree of surface hydration of silica. The nonporous specimen used was quartz, hydrated by exposure to liquid water for one month; before the adsorption determinations this hydrated quartz specimen was dried at 100° and evacuated at 200° (a quartz specimen evacuated at 280° was used in the earlier investigation [1]). The next specimen was quartz evacuated for a long time at 430°. All these specimens were different fractions of the same portion of ground quartz. In addition, adsorption of nitrogen vapor was studied on an original and a hydrated specimen of silica prepared by G. V. Vinogradov by combustion of organosilicon compounds followed by heating of the fine powder at 800-1000°*. This method of preparation eliminated the possibility of formation of a dense layer of silicic acid hydroxyl groups on the surface (in contrast to silica gels made from hydrogels [8, 25]). The hydrated specimen was prepared by exposure of the original specimen to liquid water for six months, followed by drying at 120° [22, 26]. The effect of increasing the vacuum heating temperature from 280 to 400° was also studied for the finely porous silica gel specimen No. 28 [24]. The adsorption isotherms were determined with the use of a volumetric gas apparatus as previously [1, 27].

---

* The authors take this opportunity to thank G. V. Vinogradov for supplying this silica.

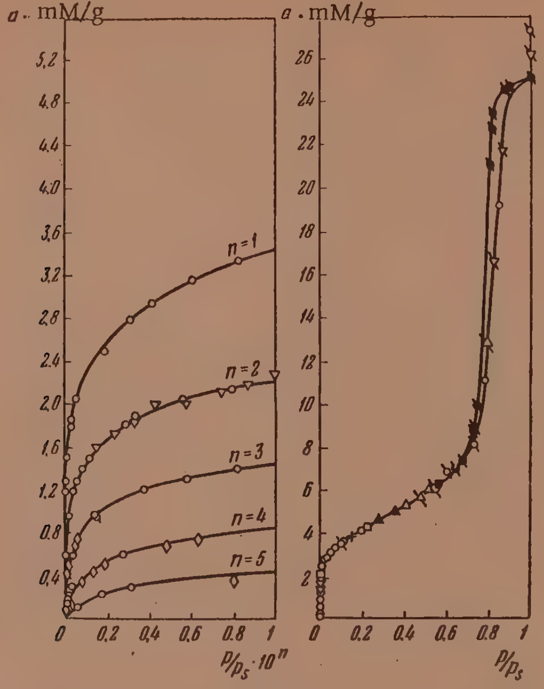

Fig. 1. Isotherm for the adsorption of nitrogen vapor on silica gel KSK-2. Here and subsequently different signs represent points obtained in different series of determinations; black points correspond to desorption.

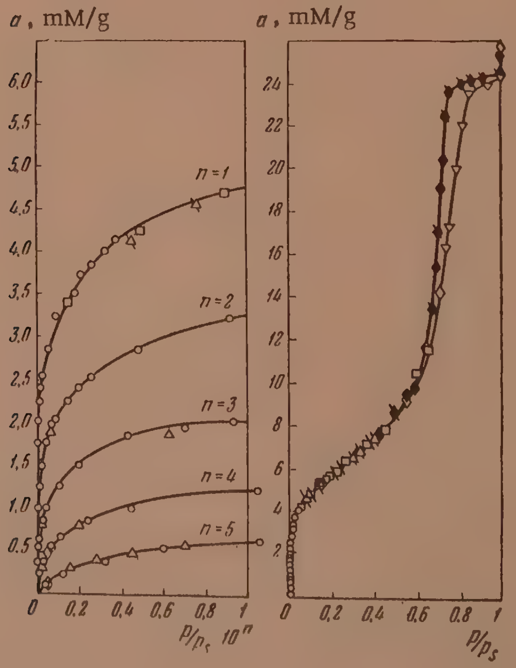

Fig. 2. Isotherm for adsorption of nitrogen vapor on silica gel No. 3 of the standard series.

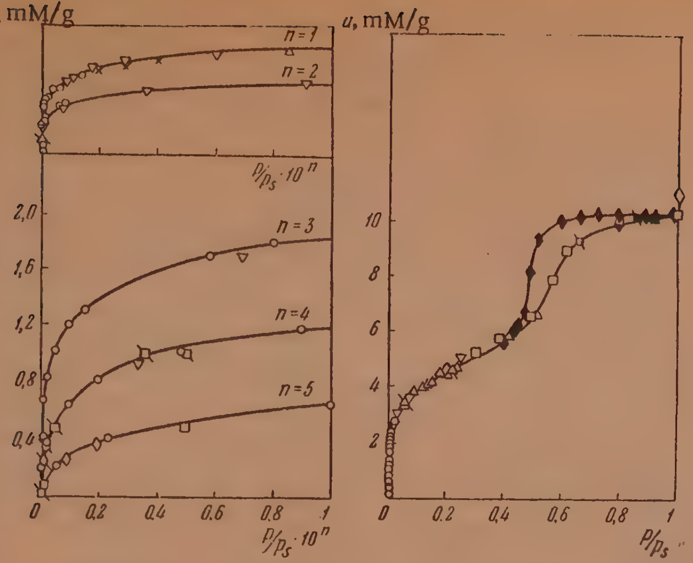

Fig. 3. Adsorption isotherm for nitrogen vapor on silica gel KSM-2. The scale along the ordinate axis is 5 times greater for the curves n = 1 and n = 2 than for the curves n = 3, n = 4, and n = 5.

Effect of Pore Size

Relative values of adsorption (per gram of adsorbent). Figs. 1-3 show isotherms for the adsorption of nitrogen vapor on silica gels KSK-2, No. 3, and KSM-2. The adsorption isotherms for silica gels No. 5 and No. 8 and for quartz heated at 280° are given in an earlier paper [1], and are used here for comparison only.

TABLE 1

Structural Characteristics of Silica Specimens Used for Studying the Effect of Pore construction on Adsorption of Nitrogen Vapor

Specimen	Total pore volume V_s in cm²/g	Pore neck diameter * $d_T + 2\tau$	Specific surface s in cm²/g	
			for nitrogen	for water[24]
Quartz	—	—	0.58	—
Silica gels:				
KSK-2	0.870	110	330	340
No. 3	0.843	70	460	430
No. 5	0.495	38	600	566
SKM-2	0.356	38	360	≈500
No. 8	0.262	24 **	510	800

---

* With a correction for the thickness of the adsorption film formed by the start of hysteresis.

** From water vapor adsorption data.

The adsorption isotherms for nitrogen vapor were used to calculate the specific surface s by the BET equation for the range of relative vapor pressures p/p_s from 0.01-0.2 to 0.30-0.35. The same isotherms were use to determine the effective pore neck diameters [8] (in the same way as in [24]). The data so found for the silica samples are given in Table 1, and curves for the distribution of pore volumes by their neck diameters [8] are given in Fig. 4.

Absolute and reduced adsorption isotherms. For comparison of the isotherms for adsorption of nitrogen vapor on specimens of different porosity, the adsorption values were recalculated per unit surface, determined by the BET method from these isotherms. This comparison is made in Fig. 5, which shows adsorption isotherms for five silica gels and for quartz, starting from $\theta = 0.01-0.03$, over a range of p/p_s values covering 5 tenth-

-powers. The absolute adsorption isotherms for nitrogen vapor in quartz and on silica gels No. 3, No. 5, and KSK-2 are similar, as these silica gels have fairly wide pores with respect to adsorption of nitrogen molecules. For the adsorption of nitrogen vapor on silica gel No. 8 ($d \approx 25$A) the isotherm is obviously distorted owing to the increase of the adsorption potential in these very fine pores, even for the small molecules of nitrogen. This makes the adsorption isotherm steeper [1]. A small increase of adsorption at low values of θ is also found with silica gel KSM-2. This increase is the consequence of the presence of fairly fine pores in KSM-2, as shown by the more diffuse character of the curve for the distribution of pore volumes by d, and by the lower value for the specific as determined by the adsorption of nitrogen vapor by the BET method in comparison with the value found from the adsorption of water vapor [17]. Thus the higher value of the adsorption potential for nitrogen, found previously [1] for silica gels with small pore diameters, conforms to theory*.

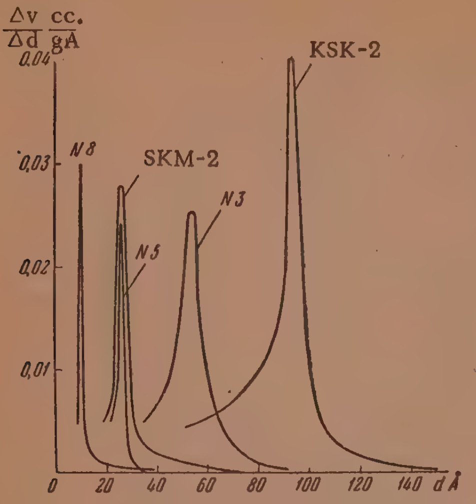

Fig. 4. Curves for pore volume distribution by pore neck diameters for silica gels: KSK-2, KSM-2, No. 3, No. 5, and No. 8 of the standard series.

Distortion of the shape of the isotherms for adsorption of nitrogen vapor on finely porous silica gels suggests that values found for their surface from these isotherms by the BET method should be regarded with caution. Indeed, in this case deviations from a layer covering of the surface in accordance with the usual BET scheme may become very prominent in the pore constrictions (gaps between the globular particles forming the silica gel skeleton) even for these small molecules. The BET equation in this case may be satisfied, but its constant a_m will not have the value of the capacity of a dense monolayer. For silica gel No. 8 the value of a_m determined by the BET method is 70% of the limiting value $a_s = 7.55$ millimoles/g at $p/p_s = 1$, i.e., of the total filling of all the pores of this silica gel. It has been reported [5, 21] that adsorption of hexane, heptane, and benzene vapors by this silica gel formally obeys the BET equation, but the value of a_m given by the BET equation is even greater than a_s.

Therefore, in the case of adsorption of nitrogen vapor on finely porous silica gels, as on carbons [27], the influence of pore constriction should be determined by reduction of the adsorption isotherms to the absolute isotherm, derived by us for quartz and coarsely porous silica gels.

For quartz and for silica gels with fairly large pores ($d > 40$ A) the isotherms for nitrogen vapor adsorption are not distorted and the absolute isotherms are satisfactorily reproduced by an interpolation curve. An interpolated absolute isotherm of this type, together with an isotherm based on the BET equation, is shown in Fig. 6. The BET isotherm in the p/p_s range between 10^{-6} and $1 \cdot 10^{-3}$, i.e., in the monomolecular region, in contrast to the isotherm for adsorption of nitrogen vapor on graphitized carbon blacks with nonporous homogeneous surfaces [27] at low pressures, deviates considerably from the experimental isotherm; it lies considerably lower and is more linear. The isotherm calculated by the BET equation coincides with the experimental curve only in the p/p_s range between 0.1 and 0.3, and then, as usual, it deviates upward from it. The higher adsorption of nitrogen than that given by the BET equation in the initial region is probably caused by chemical heterogeneity of the surface of the hydrated silica. The deviation of the isotherm calculated by the BET equation from the experimental curve at high p/p_s is the consequence of the considerable influence of small differences in the energies of adsorption in the second and subsequent layers, which is not taken into account in the BET theory [31].

---

* These results are in agreement with earlier data [28, 29] for a finely porous silica gel (Specimen A). In these papers [28, 29] the pore diameter of this specimen (20 A), as was pointed out in [30], was given without a correction for the thickness of the adsorbed film. Introduction of the appropriate correction increases the pore diameter to about 28 A. In one of these investigations [29] this silica gel specimen was also found to have a higher adsorption potential for nitrogen. This effect was distinctly observed at $p/p_s < 5 \cdot 10^{-3}$.

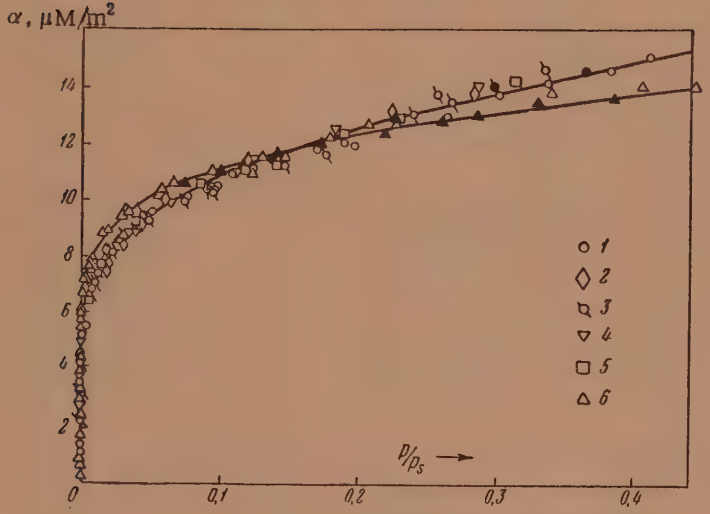

Fig. 5.
Absolute isotherms for adsorption of nitrogen vapor on quartz (1) and on silica gels: KSK-2 (2), No. 3 (3), No. 5 (4), KSM-2 (5), and No. 8 (6).

Effect of the nature of the surface.

As has already been stated, we studied the adsorption of nitrogen vapor on silica specimens of different degrees of hydration. The characteristics of the specimens used are given in Table 2. The specific surfaces were determined by the BET method from the experimental isotherms.

Fig. 7. shows the absolute isotherms for adsorption of nitrogen vapor on three quartz specimens, exposed to liquid water and evacuated at 200, 280 and 430°. In the monomolecular region ($p/p_s < 0.1$) the adsorption of nitrogen vapor on these quartz specimens decreases with increasing evacuation temperature. As θ increases, the difference decreases, and in the $p/p_s > 0.1$ range, i.e., in the multimolecular region, all three isotherms coincide.

The difference between the adsorptions of nitrogen vapor on the original and hydrated silica prepared from organosilicon compounds is particularly large. In Fig. 8 these isotherms are compared with the absolute isotherm for hydrated quartz. In the initial p/p_s region (Fig. 8, a, b) the adsorption on the original, low-

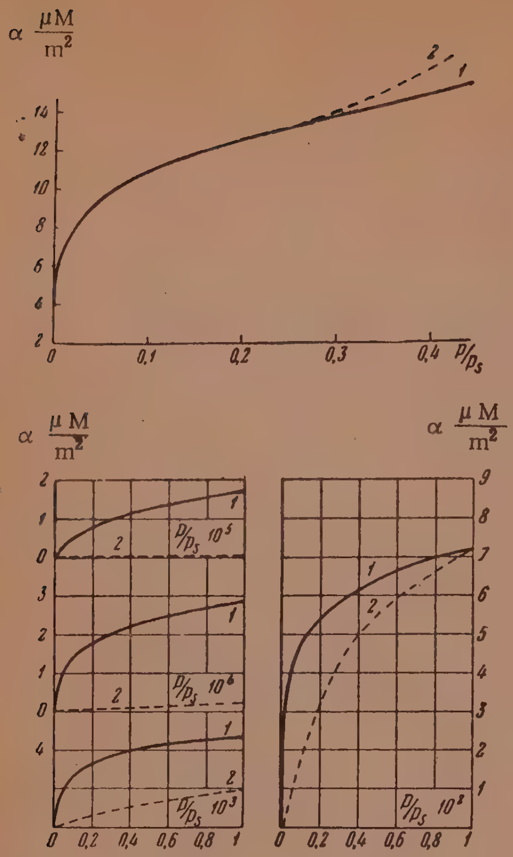

Fig. 6. Interpolated absolute isotherm for adsorption of nitrogen vapor on quartz and on coarsely porous silica gels with hydrated surface (1), and isotherm calculated by the BET equation (2).

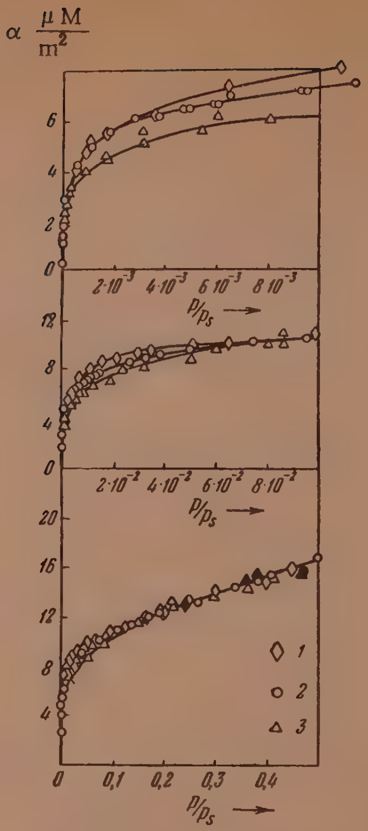

Fig. 7. Absolute isotherms for adsorption of nitrogen vapor on hydrated quartz, evacuated at 200° (1), 280° (2), and 430° (3).

TABLE 2

Structural Characteristics of Silica Specimens Used for Studying the Effects of Degree of Surface Hydration on the Adsorption of Nitrogen Vapor

Specimen	Evacuation temperature before adsorption determinations, °C	Specific surface s, m²/g	Contents of "structural" water, %	Surface concentration of hydroxyl groups, micromoles/m²
Silica gel KSK-2	280	330	3.0	12.0
Quartz, Fraction I	200	0.45	—	—
Quartz, Fraction III	280	5.8	—	—
Quartz, Fraction II	430	0.48	—	—
Silica from organosilicon compounds				
Silica hydrate in liquid water	200	135	1.32[22.26]	11
Silica hydrated in vapor and evacuated at 450°	200	145	0.66	5.0
Original silica	200	185	0.6[22.26]	3.0
Silica gel No. 8	280	510	4.6	(10.0)
Silica gel No. 8	400	495	3.3	(7.5)

-hydrated silica is less than half that on the hydrated silica. The absolute isotherm for quartz with hydrated surface lies even higher. This is in accordance with the fact that hydration of silica from organosilicon compounds had not yet reached the limit after prolonged exposure to water (see Table 2 and [26]). The difference between

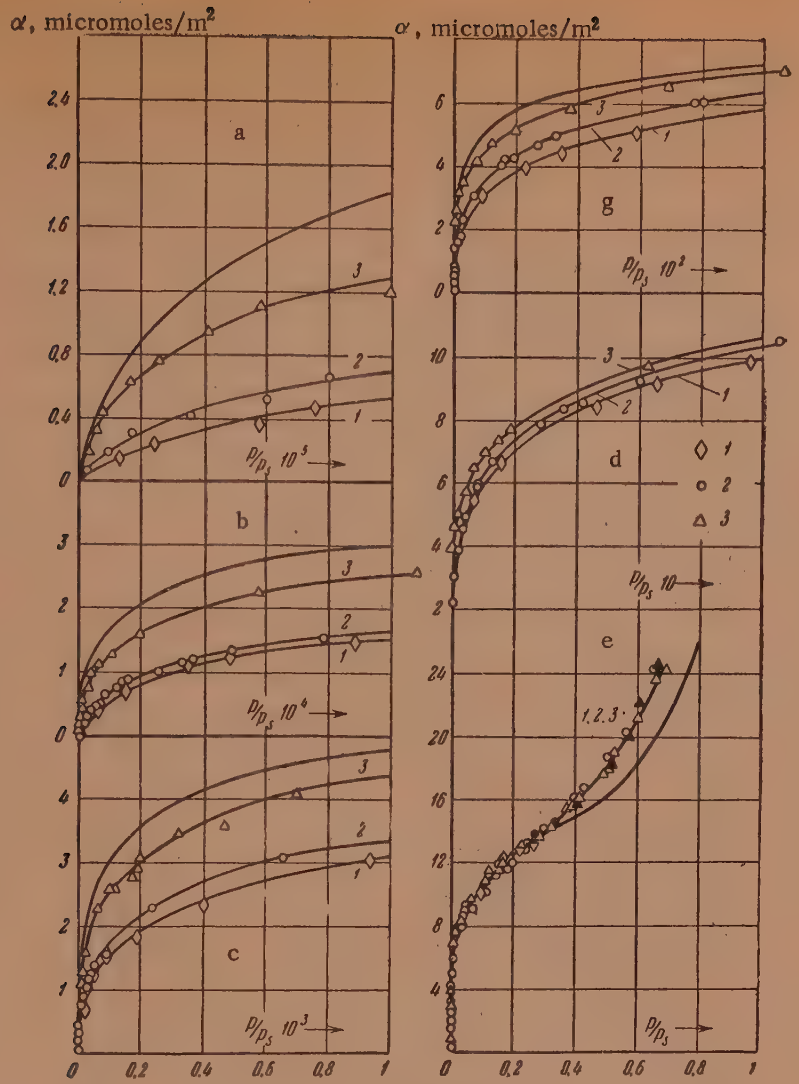

Fig. 8. Absolute isotherms for the adsorption of nitrogen vapor on silica specimens prepared from organosilicon compounds: original (1), evacuated at 450° after hydration of the original specimen in vapor (2), and hydrated in liquid water (3). Curve without points is the isotherm for adsorption on coarsely porous silica gels and on quartz (see Fig. 6, Curve 1).

the absolute isotherms for adsorption on silica hydrated in water vapor and then evacuated at 450°, and on the original silica is not large, in accordance with the similar values for the concentrations of surface hydroxyl groups, which are 3 and 5 micromoles/m² respectively. With increasing p/p_s the isotherms for adsorption of nitrogen vapor on all these specimens come closer together, and practically coincide in the p/p_s range between 0.1 and 0.25. In the region of higher p/p_s the isotherms for adsorption of nitrogen vapor on silica specimens made from organosilicon compounds deviate upward owing to the start of capillary condensation (it has been shown [22] that these specimens are not homogeneously porous).

Fig. 9 shows the reduced isotherms, at $p/p_s = 1$, for adsorption of nitrogen vapor on finely porous silica gel No. 8, evacuated at 280 and 400°. In the $p/p_s < 1 \times 10^{-4}$ and $\theta < 0.5$ range the isotherm for the dehydrated specimen lies below the other. As p/p_s increases the isotherms come closer together, and coincide in the p/p_s range between $1 \cdot 10^{-4}$ and 1*.

---

*It has been shown [32] that the absolute isotherms for adsorption of nitrogen vapor at high p/p_s (from 0.05 to 0.2) on silica gels dehydrated at higher temperatures (above 400°) also coincide. However, the authors of the paper [32] did not investigate the monomolecular filling region and therefore did not observe the influence of dehydration on the adsorption of nitrogen vapor.

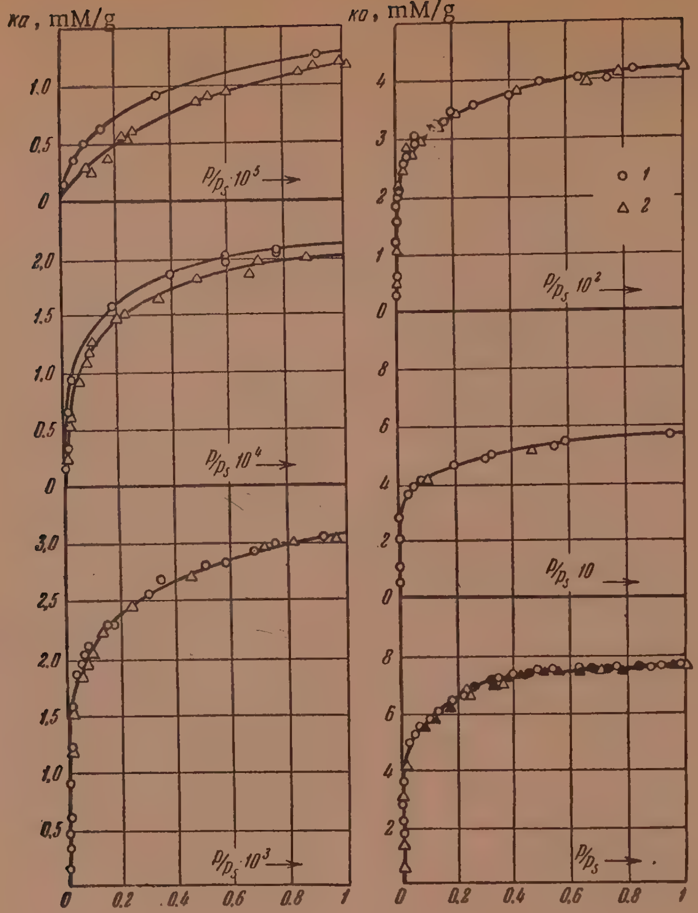

Fig. 9. Reduced isotherms for adsorption of nitrogen vapor on finely porous silica gel No. 8, evacuated at 280° (1) and 400° (2).

Therefore dehydration of the silica surface results in a quite distinct decrease of adsorption of nitrogen vapor in the monomolecular region. Whereas the increase of adsorption with constriction of the pores to $d < 38$ A indicates the important role of additive dispersional interaction of nitrogen molecules with silica, the decrease of adsorption on hydration also indicates the considerable contribution of interactions with acid hydroxyl groups. These interactions are probably effected by donor-acceptor bonding between the free electron pairs of the nitrogen molecules and the partially protonized hydrogen of the acid hydroxyl groups of silicic acid [15, 16]. The quadrupole moment of the nitrogen molecules may also have an influence.

It is also of interest to compare the absolute isotherms for adsorption of nitrogen vapor on silica with isotherms for adsorbents the whole skeleton of which has a different chemical nature. Fig. 10 shows absolute isotherms for adsorption of nitrogen vapor on barium sulfate [7], hydrated quartz [1], carbon black P-33 graphitized at 1700° [27], and metallic tungsten. Over the p/p_s range between 10^{-5} and $1 \cdot 10^{-4}$ the isotherm for adsorption on the homogeneous graphitized carbon black surface lies below the isotherm for the less homogeneous quartz surface covered with hydroxyl groups, and subsequently the increase of adsorption on quartz with increase of p/p_s is retarded and with further increase of p/p_s the isotherm for adsorption on quartz lies below that for carbon black. The isotherms for tungsten and barium sulfate occupy an intermediate position in the initial region. In the multimolecular adsorption region the difference between the absolute values of adsorption of nitrogen vapor on different adsorbents diminishes, and the isotherms come closer together. Thus, in the region of monolayer filling, the differences between the absolute isotherms for adsorbents of different chemical nature are large, especially at low θ. These differences diminish only in the transition to adsorption in the multimolecular region;

this is in agreement with earlier findings [7, 33]. It may be noted that near $\theta = 1$ the absolute values for the adsorption of nitrogen vapor probably differ somewhat for different adsorbents because of the influence of the energy of adsorption on the area ω_0 occupied by molecules of a given adsorbate in a dense monolayer. In our specific surface determinations, however, we assumed the same value $\omega_0 = 16.2$ A^2 per molecule of nitrogen for all the specimens* .

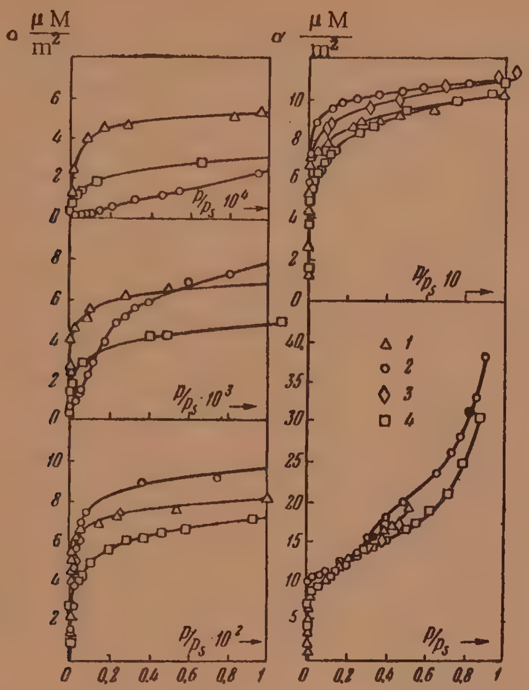

Fig. 10. Absolute isotherms for adsorption of nitrogen vapor on barium sulfate (1), graphitized carbon black (2), metallic tungsten (3), and hydrated quartz (4).

The difference between the absolute isotherms for adsorption of nitrogen vapor on barium sulfate, silica gel, and carbon black has already been demonstrated [7, 38]. The similarity which has been reported [7] between the absolute isotherms for adsorption of nitrogen vapor on hydrated surfaces of silica gel and aluminosilica gel with a low alumina content can be explained by the similarity of the chemical structure of surfaces of these xerogels, and is in accordance with the similarity of their adsorptional properties toward other adsorbates [39, 40].

---

* The authors of [32] consider that adsorption of nitrogen vapor is not sensitive to the degree of hydration of silica gels and even to the chemical nature of the absorbent surface in general; however, this is not supported by theory, as calculation of the energy of adsorption includes specific constants not only for the adsorbate but also for the adsorbent (its electrical, magnetic, and structural properties). In support of their views these authors refer to papers [34, 35] on heats of wetting by liquid nitrogen. However, the heat of wetting is only a very rough integral characteristic of the energy of adsorption of a liquid, and similar values for it cannot be used as an indication of the sensitivity or insensitivity of the energy of adsorption of a vapor to the chemical state of the surface. For example, the heats of wetting of original and graphitized channel blacks by nitrogen [34], hexane [31], and benzene [36] are similar, whereas the differential heats of adsorption of these vapors in the region of monolayer filling differ very much [37, 31, 36]. The reason is that the authors of the paper [32] measured the adsorption of nitrogen vapor largely in the multimolecular region (in the p/p_s range between 0.05 and 0.2), when the adsorbent surface is shielded by a layer of previously adsorbed nitrogen molecules.

SUMMARY

1. The isotherms for adsorption of nitrogen vapor on a number of silica specimens of different pore size and with different degrees of surface hydration have been studied.

2. The isotherms for nitrogen vapor adsorption on silica gels with effective pore diameters greater than ~ 40 A coincide, while in presence of smaller pores the adsorption potential for nitrogen increases.

3. Dehydration of the silica surface decreases the adsorption of nitrogen vapor at low degrees of filling.

4. For adsorbents of different chemical nature, the differences between the absolute values for the adsorption of nitrogen vapor at low degrees of surface filling are very large.

The M. V. Lomonosov State University, Moscow

Received March 21, 1957

LITERATURE CITED

[1] A. V. Kiselev, A. P. Karnaukhova, E. V. Khrapova, Proc. Acad. Sci. USSR, 94, 915 1954.

[2] A. V. Kiselev and Yu. A. Eltekov, J. Phys. Chem., 29, 904 1955.

[3] A. V. Kiselev and Yu. A. Eltekov, J. Phys. Chem., 31, 250 1957.

[4] A. V. Kiselev and Yu. A. Eltekov, Proc. Acad. Sci. USSR, 100, 107 1955.

[5] A. A. Isirikyan and A. V. Kiselev, J. Phys. Chem., 31, No. 9 1957.

[6] A. V. Kiselev, Trans. Commission Anal. Chem., 6 (9), (Izd. AN SSSR, 1955) p. 46.

[7] V. P. Dreving, A. V. Kiselev, and O. A. Likhacheva, Proc. Acad. Sci. USSR, 82, 277 1952.

[8] A. V. Kiselev, in Symposium: "Surface Chemical Compounds and Their Role in Adsorption Phenomena" (Izd. MGU, 1957) pp. 90 and 199.

[9] S. P. Zhdanov, Proc. Acad. Sci. USSR, 68, 99 1949.

[10] O. M. Dhzigit, A. V. Kiselev, N. N. Mikos-Avgul, and K. D. Shcherbakova, Proc. Acad. Sci. USSR, 70, 441 1950.

[11] A. V. Topchieva and A. P. Ballod, Proc. Acad. Sci. USSR, 75, 247 1950.

[12] A. P. Ballod and A. V. Topchieva, in Symposium "Surface Chemical Compounds and Their Role in Adsorption Phenomena Izd. MGU, 1957) p. 146.

[13] I. E. Neimark, R. Yu. Sheinfain, and L. G. Svintsova, Proc. Acad. Sci. USSR, 108, 871 1956.

[14] K. D. Shcherbakova and K. I. Slovetskaya, Proc. Acad. Sci. USSR, 111, 855 1956.

[15] A. V. Kiselev, Proc. Acad. Sci. USSR, 106, 1046 1956.

[16] A. V. Kiselev, Progr. Chem., 25, 705 1956.

[17] L. D. Belyakova, O. M. Dzhigit, and A. V. Kiselev, J. Phys. Chem., 31, 1577 1957.

[18] S. P. Zhdanov and A. V. Kiselev, J. Phys. Chem., 31 1957.

[19] A. V. Kiselev, K. G. Krasilnikov, and L. N. Soboleva, Proc. Acad. Sci. USSR, 94, 25 1954.

[20] L.N. Soboleva and A. V. Kiselev, J. Phys. Chem., 31 1957.

[21] A. A. Isirikyan and A. V. Kiselev, J. Phys. Chem., 31 1957.

[22] A. A. Isirikyan and A. V. Kiselev, Proc. Acad. Sci. USSR, 115, 244 1957.

[23] J. Lennard-Jones, J.A. Pople, Proc. Roy. Soc., 205, 155 1951.

[24] O. M. Dzhigit, A. V. Kiselev, and I. E. Neimark, J. Phys. Chem., 28, 1804 1954.

[25] A. V. Kiselev, Colloid J., 2, 17 1936.

[26] A. V. Kiselev and G. G. Muttik, Colloid J., 19, 562 1957.*

[27] A. V. Kiselev and E. V. Khrapova, Bull. Acad. Sci. USSR, Div. Chem. Sci. 1957.

[28] N. N. Avgul, O. M. Dzhigit, V. P. Dreving, M. V. Guryev, A. V. Kiselev, and O. A. Likhacheva, Proc. Acad. Sci. USSR, 77, 77 1951.

[29] O. A. Likhacheva, Dissertation (Moscow State Univ. 1952).

[30] A. V. Kiselev, in Symposium: "Methods for Studying the Structure of Highly Disperse and Porous Bodies (Izd. AN SSSR, Div. Chem. Sci., 1953) p. 86.

[31] N. N. Avgul, G. I. Berezin, A. V. Kiselev, and I. A. Lygina, J. Phys. Chem., 30, 2106 1956.

[32] G. I. Aleksandrova, V. F. Kiselev, K. G. Krasilshchikov, V. V. Murina, E. A. Sysoev (Proc. Acad. Sci. USSR, 108, 283 1956.

[33] C. Shuell, J. Am. Chem. Soc., 70, 1405 1948.

[34] J. J. Chessick, G. J. Joung, A. C. Zettlemoyer, Trans. Farad. Soc., 50, 587 1954.

[35] G. Kraus, J. Phys. Chem. 59, 343 1955.

[36] N. N. Avgul, G. I. Berezin, A. V. Kiselev, and I. A. Lygina, Bull. Acad. Sci. USSR, Div. Chem. Chem. Sci., 1304 1956.

[37] R. A. Beebe, J. Biscoe, W. R. Smith, C. B. Wendell, J. Am. Chem. Soc., 69, 95 1947.

[38] A. P. Karnaukhov, A. V. Kiselev, and E. V. Khrapova, Proc. Acad. Sci. USSR, 92, 361 1953.

[39] M. A. Romanchuk, Dissertation (Moscow State Univ., 1946).

[40] A. V. Kiselev and N. M. Kamakin, Proc. Acad. Sci. USSR, 80, 393 1951.

---

* This issue, p. 563.

THE SPECIFIC HEAT OF BOUND WATER

O.D. Kurilenko

The data available in the literature on the specific heat of bound water are highly contradictory [1]. Some authors found that the specific heat of bound water is less than unity. For example, values of less than unity for the specific heat of bound water were found by Andrianov, Kotukov, and Smolina [2]. At the same time there are convincing data indicating that the specific heat of water is unchanged by binding. For example, Dumansky and Ponomarev, with Skuratov's assistance [1] obtained a value near to unity for the specific heat of water bound by starch. A similar result was obtained by Porter and Swain [3] in a study of the adsorption of water on carbon.

Finally, careful experiments led Skuratov [4] to the conclusion that the specific heat of water is not changed by binding.

It must be remembered, however, that, as Dumansky [1] points out, only the experimentally determined specific heat of the whole system is unquestionable. The specific heats of the components are determined by the additivity rule. Dumansky states that the calculation of the specific heat of bound water will be correct if the specific heat of the other component is known. If during the wetting process the specific heat of the wetted object changes, then calculations based on the additivity rule cannot be correct. This can be convincingly demonstrated as follows.

As is known, the heat of wetting of hydrophilic substances is practically independent of the temperature, so that

$$\frac{dQ}{dT} = 0. \tag{1}$$

where Q is the heat of wetting of 1 g of the hydrophilic substance. By Kirchhoff's law

$$\frac{dQ}{dT} = \Sigma C. \tag{2}$$

Here ΣC is the algebraic sum of the specific heats of all the substances taking part in a reaction.

From Equations (1) and (2) it follows that

$$\Sigma C = 0 \quad \text{or} \quad C_k + G'_b C_w - C'_k - G_b C_b = 0, \tag{3}$$

where C_k and C'_k are the specific heats of the hydrophilic substance before and after wetting, C_w and C_b are the specific heats of water before and after wetting (C_b is the specific heat of bound water). G_b is the amount of water bound by 1 g of the substance in question.

It follows directly from Equation (3) that if C_k is equal to C'_k, C_w must be equal to C_b. Thus the heat of wetting – temperature relationship leads to the conclusion reached by Skuratov. This conclusion will be incorrect if the specific heat of the substance changes during wetting. It is then possible, for example, that $C_k < C'_k$ and $C_w > C_b$ or vice versa. There are reasons for believing that the specific heat of a wetted substance remains practically constant during wetting. Experiments show that the heats of wetting are independent of the temperature for substances of the most diverse origins; this is found to be the case for starch, silica gel, carbon, bentonite, and other substances; if their specific heats changed during wetting, the changes could not be equal. Consequently, the heat of wetting – temperature relationship for different substances could not remain equally constant. The more likely conclusion is that $C_k = C'_k$ and $C_w = C_b$, i.e., that the specific heat of bound water is equal to the specific heat of ordinary water. This same conclusion is reached both from Skuratov's data and from an analysis of values for the heats of wetting. Nevertheless, it is difficult to agree with the view that the specific heat of water does not change during binding.

When water passes from the free into the bound state, there are abrupt changes in its thermodynamic properties such as enthalpy, entropy, density etc. In other words, transition of water into the bound state is formally analogous to phase transation: the specific heat cannot then remain constant. This apparent contradiction is easily resolved as follows. A state of equilibrium exists between bound and ordinary water. When the system is heated, this equilibrium is displaced in the direction of desorption of water. In other words, the amount of bound water decreases with increase of temperature. This follows from the Le Chatelier principle. There is also direct experimental evidence for this [5]. In experimental determinations of specific heat, the added heat is used not only to heat the system, but also to displace the equilibrium in it. In such cases Equation (3) cannot be used for calculations. It is necessary to take into account the heat which is expended in displacement of the equilibrium in addition to the heat required to heat the system. Simple thermodynamic calculations show [6] that if it is assumed that $C_k = C'_k$, Equation (3) becomes:

$$C_b = C_w - \frac{Q}{T}, \tag{4}$$

where Q is the heat of addition (binding) of one gram of water; T is the absolute temperature.

By Dumansky's data, the heat of wetting per 1 g of bound water is approximately 80 calories for many hydrophilic substances. Then for experiments at room temperature we have:

$$C_b = 1 - \frac{80}{293} = 0.73.$$

It is known that the addition of the earliest portions of water is accompanied by a larger heat effect. This means that the specific heat of bound water will be less if the wetted substance is not completely saturated with water.

SUMMARY

1. Calculations of the specific heat of bound water by the additivity rule give a high value.
2. The specific heat of bound water is less than unity.

The Kiev Technological Institute for the
Food Industry

Received March 12, 1957

LITERATURE CITED

[1] A. V. Dumansky, Colloid J., 8, 133 1946.

[2] P. I. Andrianov, Koll. -Z., 107 1937; A. Z. Kotikov, Colloid J., 2, 293 1936; L. B. Smolina, Colloid J., 7, 459 1941.

[3] J. Porter, R.C. Swain, J. Am. Chem. Soc. 55, 2792 1933.

[4] S. M. Skuratov, Colloid J., 9, 133 1947.

[5] T. A. Granskaya and N. E. Sakun, Colloid J., 3, 117 1937.

[6] M. Kh. Karapetyants, Chemical Thermodynamics (Goskhimizdat, 1953) p. 212.

VARIATIONS OF THE SPECIFIC VOLUME OF RUBBER DURING STRETCHING

A.B. Kusov, V.I. Trofimova, and Yu. I. Nilova

Studies of volume changes during the stretching of rubber, apart from their practical significance, are of considerable theoretical interest. Experimental data obtained in such studies may be applied to considerations of the structural changes which occur during deformation, and of the nature of the forces involved in this process.

The first investigations of the volume changes in rubber were probably those of Joule [1] who found that when rubber is stretched 100-150% there is a density decrease of up to 0.2%. An increase of volume during stretching of rubber was also observed by Villari [2]; he found that the volume increase is retarded with increasing extension. In contrast to others, Thomas [3] did not observe an increase in the volume of rubber during stretching. As Whitby [3] points out, this is perhaps because Thomas used previously deformed specimens. Lundal [4] observed volume increases of up to 0.45% when rubber was stretched by 23%. Schippel [5], who studied the behavior of loaded mixtures, concluded that increase of volume on stretching greatly increases with increasing amounts of filler. The nature of the filler also influences the magnitude of the effect. Schippel was the first to advance the view that when rubber is stretched, vacuoles are formed near the filler particles in the direction of the extension, in consequence of detachment of rubber from the particles. Holt and MacPherson [6] studied loaded (with carbon black and chalk) and unloaded mixtures. With the exception of the mixture with chalk, which showed a volume increase on stretching, the volumes of the other mixtures remained unchanged up to 200 or 300% extensions. Above this limit, the volume decreased, the decrease being greater with greater extensions, lower temperatures, and longer times during which the rubber was kept in the stretched state. Increase of the degree of vulcanization in general decreases volume changes on stretching. The volume decrease in these experiments reached 2%.

Gee, Stern, and Treloar [7] studied volume changes during stretching of natural rubber vulcanizates entirely free of filler particles or of other particles not dissolved in the rubber; they found that the volume increases by 0.01-0.02% at extensions up to 100%. There is a correlation between volume (V) – extension (ϵ) and stress (σ) – extension (ϵ) curves. The authors attribute the volume increase to the hydrostatic pressure which arises in any isotropic body on stretching. If the compressibility of the material and the degree of elongation are known, the volume increase can be calculated. The authors carried out such calculations for their specimens and obtained values in close agreement with the experimental data.

The objects of the present investigation included: a) a study of volume changes during stretching of synthetic rubber vulcanizates, which have not been studied previously; b) experiments at large deformations; c) attempts to establish a correlation between volume changes during deformation and the stress.

The procedure used was based on a hydrostatic weighing method similar to that used by Gee, Stern, and Treloar [7].

Rings of 25 mm internal and 28 mm external diameter were cut by a special knife from vulcanized rubber plates. A special steel plate was drilled with holes into which steel rods could be inserted at various distances apart. The rubber rings were stretched on the steel rods on both sides of the plate. In this way extensions from 0 to 700% or over, with 50% intervals, could be produced. This device with the specimens was weighed on an analytical balance in air and in distilled water at various extensions, starting from zero. The data were used to calculate volume changes. All the necessary precautions were taken to maintain a constant temperature and to obtain reproducible results. For better wetting of the rubber and avoidance of air bubbles, several drops of ethyl alcohol were added to the water. The experiments were carried out with vulcanizates based on natural, sodium–butadiene, butadiene–styrene, nitrile, chloroprene, and butyl rubbers. Both unloaded mixtures and mixtures containing carbon black, with different degrees of loading and vulcanization, were studied. Extension–load curves were also plotted for all the rubbers, with the use of spade-shaped specimens cut from the plates which were used for the volume determinations. The formulations of the mixes were similar to the standard, and are therefore not given. Only the degree of loading is given in the graphs.

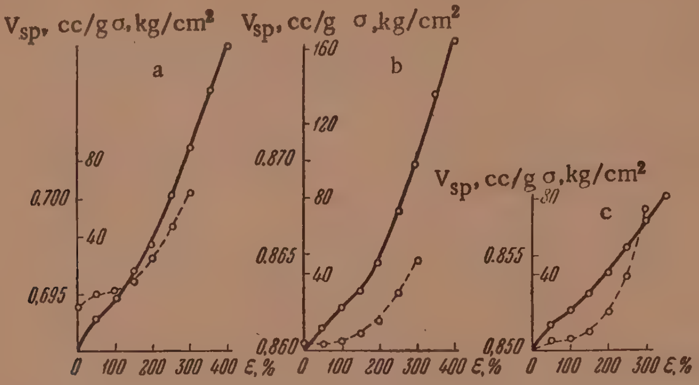

Fig. 1. Variations of stress and specific volume with extension for vulcanizates based on a) chloroprene; b) butadiene–styrene (SKS-30); c) sodium–butadiene rubbers; —) stress; – – –) specific volume.

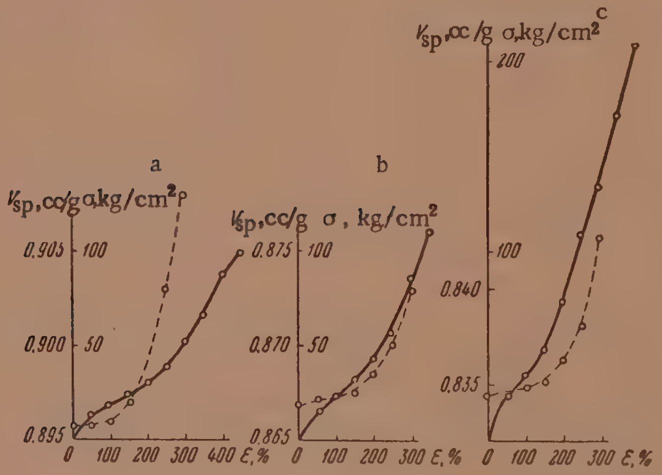

Fig. 2. Variations of stress and specific volume with extension for SKS-30 vulcanizates containing: a) 30; b) 45; c) 60 parts of carbon black; —) stress; – – –) specific volume.

The experiments showed that extension of the various rubbers is accompanied by volume increase, reaching 1.7-1.8% at maximum extension in some cases. The specific volume – extension curve is in general S-shaped; at first the volume increase per unit extension decreases, and then (after the point of inflection on the curve has been reached) the volume begins to increase strongly with extension (see Figs. 1 and 2). In some cases the S-shaped is weak or absent, but in the majority of cases it is pronounced. This is found for all vulcanizates except natural rubber; for the latter, at a certain extension, which is higher at higher degrees of vulcanization, the volume increase is replaced by a decrease, slight at first and then very rapid. Fig. 3 gives specific volume – extension curves for natural rubber vulcanizates based on the same formulation but with different vulcanization times. It is seen that these curves also have inflection points at extensions of ~ 100%, but these are followed by breaks indicating the start of an increase in density (decrease of volume). Fig. 4 shows the

the degree of vulcanization of the specimens, represented by the vulcanization time, plotted against the extension at which the volume increase is replaced by a decrease (the inversion point). This graph shows that at a certain degree of vulcanization, in our case for 15 minutes of vulcanization, the maximum extension corresponding to the inversion point is reached. Fig. 5 shows the critical extension (when the density of the rubber begins to increase) plotted against the bound sulfur content. The latter was determined from the difference between total and free sulfur.

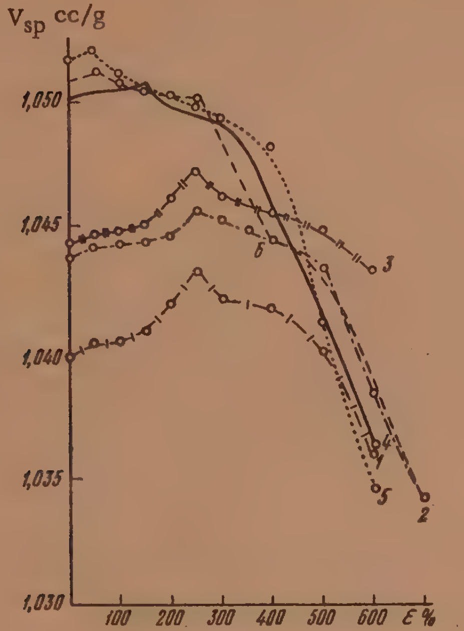

Fig. 3. Specific volume – extension curves for natural rubber vulcanized for : 1) 15; 2) 30; 3) 90; 4) 10; 5) 7.5 and 6) 6 minutes.

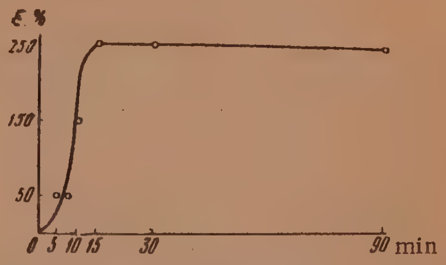

Fig. 4. Extension corresponding to the start of density increase in natural rubber vulcanizates, as a function of the vulcanization time.

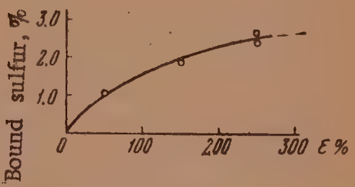

Fig. 5. Extension corresponding to the start of density increase in natural rubber vulcanizates, as a function of the bound sulfur content.

In Figs. 1 and 2, load-extension curves are given together with the specific volume – extension curves. A correlation between the two relationships is clearly seen. The inflections in the curves are found at the same extensions (from 75 to 150%). These plots are typical for most rubber mixes. The different relationships found for natural rubber mixes can probably be ascribed to crystallization. An attempt was made to find a volume decrease in chloroprene and butyl rubber mixes, which can also crystallize on stretching. A volume decrease was observed only after the specimens had been kept for a long time (for 7 days) in the stretched state. The volume of the chloroprene rubber decreased by 0.66% at 300 extension, and that of the butyl rubber by only 0.09% at 250 % extension. Greater extensions could not be reached in these periods.

The specimens used in these experiments had not been fatigued. It was of interest to study the behavior of rubber after repeated deformations. For this, ring-shaped specimens cut from the plates were stretched to 300% several times and then tested at several extensions as previously. Preliminary tenfold extension nearly always resulted in practically the limiting value of volume change.

These experiments showed that the nature of the volume-extension curves of such fatigued rubbers remains the same as before, and only the volume increase changes. Thus, in rubbers based on SKB, tenfold stretching increased the volume in the extension range up to 300% from 0.04 to 0.15% in comparison with unstretched specimens. SKN-26 mixtures showed somewhat larger changes in this extension range from 0.4 to 0.7%).

It is interesting to note that in a relatively few cases the volume-extension curves had a second inflection point in the region close to breaking extensions, indicating a gradual cessation of the volume increase. A similar inflection point can sometimes be seen in stress— extension curves in the higher extension region, predominantly in strongly loaded mixtures.

These results leave no doubt that an increase of volume during extension, up to failure of the specimen, is a common property of vulcanizates. The decrease of volume observed in natural rubber after a definite extension is in all probability the result of crystallization superposed on the primary effect. The magnitude of the observed volume increase indicates that it cannot be caused by the hydrostatic component of the stress only. It is highly probable that deformation results in destruction of the material at the inner surfaces of the rubber itself and at the rubber – added particle interfaces. The possibility of destruction of the added particles, i.e., loosening with formation of vacuoles within them, is also not excluded. Not all these effects are equally probable, but because of the lack of exact information we can only speak of the combined effects of different factors.

However, there is one striking fact – the existence of an inflection point on the specific volume – extension curve, its S-shape. The increase of volume might be expected to vary steadily with extension. The fact that the inflection points on the volume-extension and the stress-extension curves coincide is very interesting.

It might be possible to explain this fact on the assumption that the rubber contains some kind of an unstable spatial network, formed by different types of secondary bonds, which can be broken by deformation. Destruction of the network will be accompanied by a decrease of the modulus and an increase of volume owing to increased chain vibration and decreased steric hindrance. However, as the number of cross links capable of being broken decreases (the chains being already oriented), the rate of volume increase should fall to a minimum, corresponding to the inflection point on the curve. This also corresponds to the maximum decrease of the extensibility modulus. The subsequent volume increase may be caused by a different mechanism, or more accurately by the predominance of another component of the total volume increase, possibly by vacuole formation. Incidentally, this deformation stage is usually characterized by a sharp increase of hysteresis loss, indicating considerable structural breakdown.

The behavior of natural rubber definitely points to crystallization during extension. In this case the volume decrease reaches 1.5-1.7%. It is significant that increase of the degree of vulcanization, which decreases the distances between the points of cross linking, does not alter the extension, beyond a certain value, at which crystallization begins. The crystallization occurs more easily with greater "freedom" of the molecular chains (at lower degrees of vulcanization).

SUMMARY

1. It is shown that volume increases during extension occur both in loaded and unloaded vulcanizates of different rubbers, reaching 2% at maximum extension.

2. The specific volume – extension curves are in general S-shaped, and the inflection points on these curves correspond to the same extensions as the inflection points on stress-extension curves.

3. Vulcanizates based on natural rubber show volume decreases, caused by crystallization of the rubber, at a certain degree of extension, which is higher for higher degrees of vulcanization.

The Lensoviet Technological Institute Leningrad
Chair of Rubber Technology

Received November 3, 1956.

LITERATURE CITED

[1] J. P. Joule, Phil. Trans. 149, 104, 1859 (see [3], p. 490).

[2] E. Villari, Ann. Physik 143, 88, 290 1871.

[3] G. S. Whitby, Plantation rubber and the testing of Rubber, London 1920.

[4] A. E. Lundal, Ann. Physik 66, 741 1898.

[5] H. F. Schippel, Ind. Eng. Chem. 12, 33 1920.

[6] W. L. Holt, A. T. MacPherson, J. Res. Nat. Bur. Stand. 17, 657 1936.

[7] G. Gee, H.J. Stern, L. Treloar, Trans. Faraday Soc. 46, 1101 1950.

EFFECT OF THE NATURE OF THE EMULSIFIER ON THE THERMAL DECOMPOSITION OF CUMENE AND 1,1-DIPHENYLETHANE HYDROPEROXIDES IN ~~AN~~ AQUEOUS MEDIUM

R.V. Kucher and S.D. Kazmin

The influence of an emulsifier on reaction rates in emulsion systems is associated to a considerable extent with its effect on the rate of free radical formation during the thermal decomposition of hydroperoxide reaction initiators. Despite the fact that we have already carried out some investigations of this question [1, 2], the effects of emulsifiers on the thermal stability of hydroperoxides are not yet fully understood. The rate and mechanism of hydroperoxide decomposition in aqueous media primarily depend on the pH. In a strongly acid medium the decomposition of isopropylbenzene hydroperoxide proceeds at a very high rate with formation of phenol and acetone as the primary products. In an alkaline medium different decomposition products are formed (acetophenone, tertiary carbinol). However, the data on the influence of the emulsifier, and in particular of its colloidal nature, are very limited, and this question still remains obscure. Investigations of the influence of the nature of the emulsifier on the rate of thermal decomposition of hydroperoxides are of considerable interest in this connection. Studies of the thermal stability of tertiary hydroperoxides are also of interest, as these compounds can be prepared relatively easily by oxidation of the corresponding hydrocarbons. The stability of these hydroperoxides depends on the nature of the substituents at the third carbon atom [3]. This also influences the initiating activity of the hydroperoxides [4]. However, such data are at present lacking with regard to the aqueous phase.

The purpose of the present investigation was a study of the thermal decomposition of cumene and 1,1-diphenylethane hydroperoxides in an aqueous medium in presence of different types of emulsifiers. The effects of certain sulfonates and of a number of higher fatty acid salts on the thermal stability of these hydroperoxides were studied. This work is therefore a continuation of our earlier investigation [2].

EXPERIMENTAL

The thermal decomposition of cumene hydroperoxide (CHP, 100% pure) and 1,1-dipehnylethane hydroperoxide (DEH, 100% pure) was effected in sealed tubes in an atmosphere of pure nitrogen in a thermostat at 98.5 and 80°. The tubes were taken out of the thermostat at definite invervals, opened, and their contents analyzed for hydroperoxide. The analysis was carried out by the iodometric method [5].

The decomposition of CHP and DEH was studied in an aqueous medium at pH 9.9 in 0.1 N sodium carbonate solution, in presence of different types of emulsifiers. The emulsifiers used were Aerosols OT and IB (sodium salts of the dioctyl and dibutyl esters of sulfosuccinic acid), Alkanol S (imported sodium tetralinsulfonate [6]), sodium tetralinsulfonate synthesized by ourselves [7], Nekal, Leukanol [8], and sodium soaps of fatty acids – caproate, caprylate, and palmitate, free from unsaturated impurities; we also used a cation-active colloidal electrolyte, cetylpyridinium bromide, and Igepon T (a condensation product of oleyl chloride with methyltaurine [7]), containing a double bond in the molecule. The initial concentration of CHP was 1.4%, and of DEH, of the order of 10^{-3} mole/liter.

Data on the rate of the thermal decomposition of CHP in presence of a number of emulsifiers at 98.5° are shown in Fig. 1. It is seen that the rate of hydroperoxide decomposition decreases in presence of sulfonates. The small increase of the thermal stability of the hydroperoxide cannot, however, be attributed only to the "colloidality" (micelle size) of the emulsifier used, as with emulsifiers of the same type, one of which has a greater tendency to micelle formation in aqueous solutions (for example, Aerosols IB and OT, the micellar weight of the latter being considerably greater), the latter has the higher rate of thermal decomposition. Increase of micelle size of the emulsifier thus favors an increase in the rate of thermal decomposition of the hydroperoxide. The decrease of the rate of hydroperoxide decomposition in presence of sulfonates must be attributed to the specific action of these emulsifiers on the decomposition of CHP.

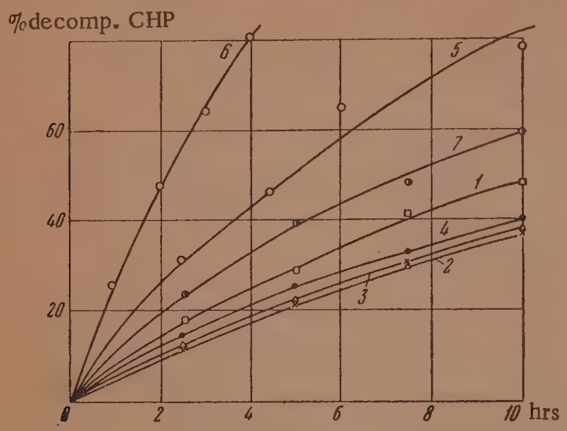

Fig. 1. Curves for the decomposition of CHP at 98.5° and pH 9.9 in presence of 2% of various emulsifiers: 1) Aerosol OT; 2) Aerosol IB; 3) sodium tetralinsulfonate; 4) Alkanol S; 5) Igepon T; 6) cetylpyridinium bromide; 7) without emulsifier.

As regards the action of Igepon T, the considerable increase of the rate of hydroperoxide decomposition in presence of this colloidal electrolyte can be attributed to partial interaction of the hydroperoxide with the emulsifier molecules at the double bond. A similar effect was observed in the influence of sodium oleate on the thermal stability of CHP [2].

It should also be noted that the thermal decomposition of CHP is accelerated considerably in presence of cation-active cetylpyridinium bromide. A curious feature is that in this case the rate of decomposition is much higher than in presence of other emulsifiers. When the temperature is decreased to 20° the decomposition of CHP still proceeds at an appreciable rate in presence of cetylpyridinium bromide, while in presence of the others emulsifiers no appreciable decomposition of CHP was observed during several days at room temperature. This effect of cetylpyridinium bromide must be attributed to its chemical nature and not to the colloidal nature (micelle formation) of this colloidal electrolyte. One probable explanation of the action of cetylpyridinium bromide is oxidation-reduction interaction between the hydroperoxide molecules and the nitrogen of the pyridine ring. Evidence for this interaction is provided by the behavior of this colloidal electrolyte in emulsion polymerization; experiments in our laboratory showed that this emulsifier acts in this case as an activator (reducing agent).

The influence of colloidal character on the decomposition rate of CHP is clearly seen in the results of experiments with sodium soaps of fatty acids. These results are given in Fig. 2. It is seen that the presence of fatty acid soaps in solution accelerates the thermal decomposition of CHP. In this case it proved possible to formulate a quantitative empirical relationship between the decomposition rate constant for CHP (calculated from a first-order equation) and the number of carbon atoms in the soap molecule. This relationship is presented graphically in Fig. 2, and is given by the equation:

$$k = 0{,}432\, n_c + 1{,}63 \cdot 10^{-3},$$

where k is the rate constant for hydroperoxide decomposition; n_c is the number of carbon atoms in the soap molecule. The size of the soap molecule may be a measure of the colloidal character of the solutions, as according to MacBain [9] the micelle size in soaps of the same nature is determined by the molecular weight of the soap.

The intercept cut off by the straight line along the ordinate axis corresponds to the rate constant for decomposition of CHP in absence of soap. It may be noted that the decomposition rate constant in absence of colloidal electrolytes fits exactly into this relationship.

As was noted in paper by Yurzhenko et al. [3], 1,1-diphenylethane hydroperoxide is less stable than isopropylbenzene hydroperoxide in a hydrocarbon medium. It was therefore interesting to investigate this relationship in an aqueous medium. Study of the decomposition of DEH in such conditions is difficult owing to the very low solubility of this compound in water ($3.75 \cdot 10^{-4}$ mole/liter at 20°). However, in presence of soaps the solubility of this hydroperoxide is increased considerably. Therefore in studies of the thermal decomposition of DEH in an aqueous medium the solutions were first saturated with the hydroperoxide.

The results of the study of the rate of thermal decomposition of DEH in an aqueous medium are given in Fig. 3. It follows from a comparison of the data in Fig. 1 and Fig. 3 that the thermal decomposition of DEH

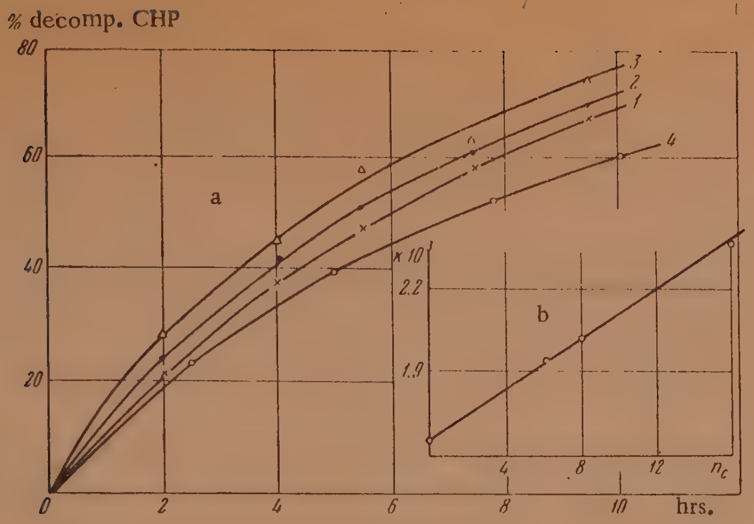

Fig. 2. Curves for the decomposition of CHP in presence of 2% of emulsifiers: (a): 1) Na caproate; 2) Na caprylate; 3) Na palmitate; 4) without emulsifier; decomposition rate constant for CHP as a function of the number of carbon atoms in the soap molecule (b).

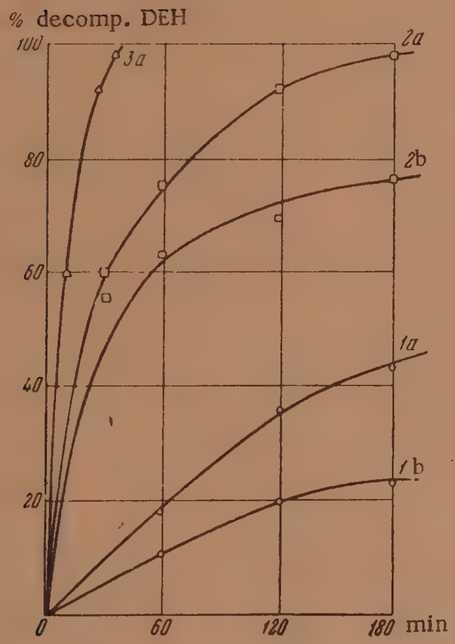

Fig. 3. Curves for the decomposition of DEH at 98.5° (a) and 80° (b) at pH 9.9 in presence of 2% of emulsifiers: 1) Nekal; 2) Na tetralinsulfonate; 3) Leukanol.

Rate Constants at 98.5 and 80°, and Activation Energies for the Decomposition of CHP and DEH in an Aqueous Medium

Emulsifier (c = 2%)	$k_{80°} \cdot 10^3$ min.$^{-1}$	$k_{98.5°} \cdot 10^3$ min.$^{-1}$	E (kcal./mole
CHP			
Soda without emulsifier	0.334	1.63	22.3
Aerosol IB	0.180	0.835	21.5
Aerosol OT	0.273	1.271	21.6
Alkanol S	0.187	0.842	21.1
Na caproate	0.366	1.927	23.3
Na palmitate	0.451	2.340	23.1
DEH			
Na tetralinsulfonate	11.2	23.3	10.3
Nekal	1.65	3.34	9.9

is considerably more rapid than that of CHP. This is in agreement with the data obtained by T.I. Yurzhenko et al. [3] for a hydrocarbon medium. The effects of the nature of the emulsifier on the decomposition of DEH in an aqueous medium are similar to those in the thermal decomposition of CHP.

From the results of experiments at 98.5 and 80° it was possible to calculate the activation energy of the thermal decomposition of the hydroperoxide by means of the Arrhenius equation. The rate constants were calculated for a reaction of the first order. The results of these calculations are given in the Table.

It should first be noted that the activation energy shows only small variations in presence of different emulsifiers for the same hydroperoxide (CHP). The data in the table also show that the activation energy of thermal decomposition is considerably lower for DEH than for CHP. However, the activation energy for the decomposition of DEH is approximately 10-12 kcal. less than for the first; this should lead to a $\sim 10^5$-fold increase of k. In fact the reaction rate is increased approximately 60-fold. This is to be explained by the considerable difference between the pre-exponential terms for the decomposition of these two hydroperoxides; these are respectively of the order of 10^{10} for the decomposition of CHP, and 10^4 for DEH. This, in turn, is determined by the structure of the hydroperoxide molecule (replacement of a methyl by a phenyl radical), resulting in a considerable change of the steric factor.

In summing up the foregoing, we may note that, in the initiation of liquid-phase reactions in emulsions by means of hydroperoxides, the colloidal nature of the emulsifier plays an important role, in addition to the nature of the hydroperoxide, and the thermal stability of the hydroperoxides in an aqueous medium decreases somewhat with increasing micelle size.

SUMMARY

1. The rate of thermal decomposition of cumene and 1,1-diphenylethane hydroperoxides in an aqueous medium in presence of various emulsifiers has been studied. Sulfonates decrease, while fatty acid soaps and cetylpyridinium bromide increase the decomposition rate of hydroperoxides.

2. Increase of the "colloidality" (micelle formation) of the emulsifier results in an increase in the rate of thermal decomposition of cumene hydroperoxide. In the case of fatty acid soaps this increase is a linear function of the number of carbon atoms in the colloidal electrolyte molecule.

3. The rate of thermal decomposition of 1,1-diphenylethane hydroperoxide in an aqueous medium is considerably higher than the rate of decomposition of isopropylbenzene (cumene) hydroperoxide, i.e., the relative stability of these hydroperoxides is the same as in a hydrocarbon medium.

The I. Franko State University, Lvov
Chair of Physical and Colloid Chemistry

Received September 14, 1956.

LITERATURE CITED

[1] A. I. Yurzhenko and F. I. Grobshtein, Ukrain. Chem. J., 20, 373 1954.

[2] R. V. Kucher and A. I. Yurzhenko, Colloid J., 18, 555 1956.*

[3] T. I. Yurzhenko, D. K. Tolopko, and V. A. Puchin, Proc. Acad. Sci. USSR, 74, 85 1950.

[4] T. I. Yurzhenko, V. A. Puchin, and K. S. Grigoryeva, Proc. Acad. Sci. USSR, 75, 547 1950.

[5] V. Kokatnur, M. Jelling, J. Am. Chem. Soc. 63, 1432 1941.

[6] A. Schwartz and J. Perry, Surface Active Agents (IL, Moscow 1953) p. 124.

[7] R. V. Kucher and S. D. Kazmin, Proc. and Comm. Lvov State Univ., No. 6, pt. 2, 140 1955.

[8] R. V. Kucher and M. A. Kovbuz, Colloid J., 18, 193 1956.*

[9] J. W. MacBain, J. Phys. Coll. Chem., 51, 286 1947.

---

* Original Russian pagination. See C. B. translation.

THE STRUCTURE OF THIN COPPER SULFIDE FILMS AT THE SOLUTION–GAS INTERFACE

S.G. Mokrushin, Yu. D. Tkachev, and O.K. Shabalina

Devaux [1] put forward the view that sulfide films formed on the surface of solution of the salts of copper and other metals by chemical reactions between the salts and hydrogen sulfide are, in the limit, monomolecular layers. The subsequent increase of the film thickness was regarded by Devaux as the result of stratification of a number of monomolecular layers. Similar views were advanced by Perrin [2] for explaining the structure of thin soap films, the thickness of which, according to Perrin, is a multiple of the thickness of a bimolecular film. These views were accepted by Mokrushin et al. [3], but subsequent experimental work [4] showed that Devaux's views on the monomolecular and polymolecular structure of metal sulfide films are not in agreement with the experimental data.

It was shown by Mokrushin et al. [5] that very thin films are capable of spontaneous contraction; this is seen especially clearly if the films are compressed in Marcelin's apparatus. These experimental results led to the adoption of another concept of film formation, according to which the sulfide films are not mono- or polymolecular, but are surface colloidal solutions, which coagulate into surface networks of varying degrees of porosity, depending on the concentration of the colloidal solution. It followed from these investigations that the films must be regarded as being mono- and polymicellar, i.e., the structural elements in them are colloidal particles and not molecules. A similar conclusion was reached by Demenev [6] from the results of microscopical and electron-microscopical studies of thin metal films formed on surfaces of solutions by the action of reducing gases. Although the formation of metallic films as the result of coagulation was proved experimentally by Demenev et al. [7], only indirect proof was available with regard to the formation of sulfide films. It should be noted that it has been shown by electron microscopy that copper hydroxide films formed on solution surfaces as the result of hydrolysis consist of colloidal hydroxide particles [8].

The films of copper sulfide, electron micrographs of which (magnification 12,000) are given below, were prepared by the action of hydrogen sulfide gas (0.05% by volume) on 0.2 and 2.0 N solutions of copper sulfate. The time of action of the hydrogen sulfide was between 15 and 600 seconds.

The micrographs of the films formed on 0.2 N copper sulfate solution by the action of hydrogen sulfide for 15 seconds (Photo 1, a) and 150 seconds (Photo 1, b) show that the sulfide particles are typical secondary colloidal particles formed by coagulation. As far as can be seen from the photographs, the primary sulfide particles are probably globular. As was shown by Kargin and Berestneva [9], this form is found in the formation of many kinds of colloidal particles. It must be pointed out that the colloidal particles formed during a brief action of the gas (Photo 1, a) are not interconnected and exhibit Brownian movement, whereas after 150 seconds of the action of hydrogen sulfide (Photo 1, b) the particles form a network with large gaps of free surface. The photographs also show that the secondary particles were formed by surface (two-dimensional) coagulation.

The colloidal particles were compressed by the Langmuir-Blodgett "oil piston" method [10]. However, a film compressed by castor oil is still very porous (see Photo 2).

Films formed by the action of hydrogen sulfide for 10 minutes (Photo 3) at first sight resemble films compressed by castor oil, but the former differ from the latter in that, in the gaps between the colloidal particles, thin dendritic formations can be seen along the particle boundaries; these are oriented microcrystalline products of the crystallization or recrystallization of the copper sulfide particles. By addition of gelatin to the copper sulfate solution it is possible to prevent completely the formation of secondary colloidal particles, so that the film consists of primary globular colloidal particles. An example of such a film is shown in Photo 4. The film was prepared from a solution of copper sulfate to which 0.2% gelatin had been added.

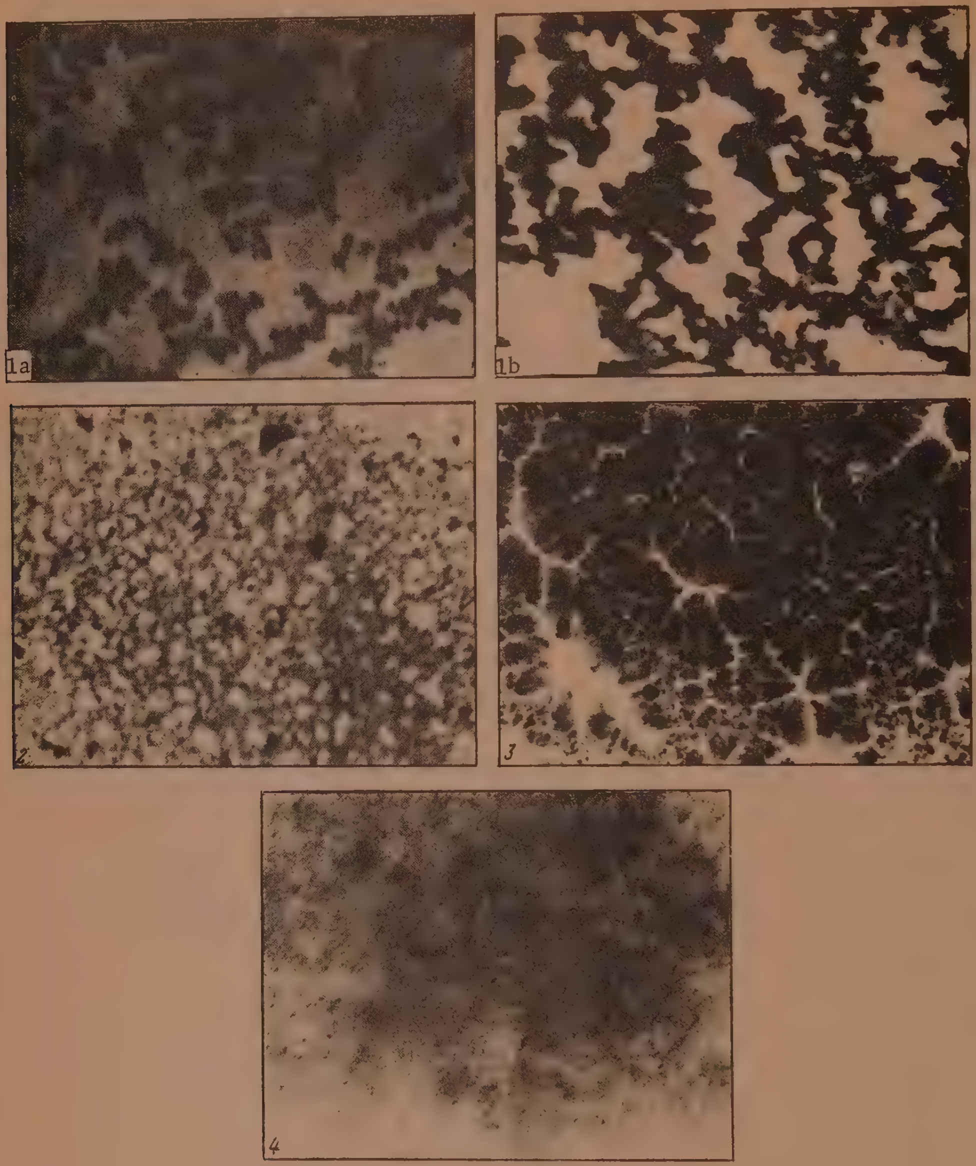

Electron micrographs of films on 0.2 N copper sulfate solution (magnification x 12,000) formed: 1) by action of H_2S for 15 seconds; 1,b) ditto, 150 seconds; 3) ditto, 10 minutes; 2) film compressed by castor oil; 4) with addition of 0.2% gelatin.

SUMMARY

Films of copper sulfide, and probably of other sulfides, like metallic and hydroxide films, consist of secondary colloidal particles formed by coagulation of primary sulfide particles and attached, owing to their hydrophobic nature, at the solution–gas interface.

The S. M. Kirov Polytechnic Institute, Urals
Sverdlovsk

Received April 28, 1956.

LITERATURE CITED

[1] H. Devaux, Koll.-Z 58, 129 1932.

[2] J. Perrin, Koll.-Z. 51, 5 1930.

[3] S. G. Mokrushin and A. M. Demyanova, J. Phys. Chem., 5, 1092 1934.

[4] S. G. Mokrushin and R. B. Ginzburg, Colloid J., 5, 5, 818 1939.

[5] S. G. Mokrushin, V. A. Kozheurov, and I. A. Blum, Colloid J., 6, 119 1940.

[6] N. V. Demenev, Trans. Inst. Chemistry and Metallurgy, Urals Branch, Acad. Sci. USSR, No. 1, 10 1948.

[7] N. V. Demenov, N. N. Buinov, and M. I. Milyutina, Colloid J., 12, 252 1950.

[8] S. G. Mokrushin, G. A. Kitaev, and O. K. Shabalina, Proc. Acad. Sci. USSR, 94, 1109 1954.

[9] Z. Ya. Berestneva, T. A. Koretskaya, and V. A. Kargin, Colloid J., 13, 323 1951.

[10] I. Langmuir, Progr. Chem., 8, 1195 1939; I.Langmuir and V. Schaefer, Colloid J., 8, 1231 1939.

THE EFFECT OF STRUCTURE ON THE VISCOSITY OF BUTADIENE —STYRENE RUBBERS

A.S. Novikov and F.S. Tolstukhina

Relative few investigations have dealt with the influence of molecular structure on the viscous flow of polymers. These studies have been carried out with polymers with molecules of simple linear structure, resistant to oxidation. In an investigation of the viscosity of polyester melts, a linear relationship was found between the logarithm of the viscosity and the square root of the molecular weight [1]:

$$\log \eta = A + CM^{1/2}.$$

Similar relationships have been found for butyl rubber [2] and polyethylene [3]. Recently the following equation was derived for a number of polymers with long flexible molecular chains:

$$\log \eta = A \log z + B,$$

where z is the number of atoms in the chain; A and B are constants. This empirical law of flow proved to be valid for polyisobutylene and polystyrene [4], polymethyl methacrylate [5], and butadiene-styrene polymers [6].

The viscosity of butadiene-styrene copolymers has been studied as a function of the molecular structure in the present investigation. It was desired to correlate the structure of the polymer with its viscous properties in solution and in bulk under steady flow conditions. The copolymers taken for the work were SKS-30 and SKS-30A, polymerized at +50 and +5° respectively. The structure of the copolymer fractions was characterized by the molecular weight, intrinsic viscosity, and the Huggins constant K'. The viscosity of the polymers was measured by means of Tolstoi's plastoelastometer [7] in shearing deformation conditions.

Fractionation. Specimens of the rubbers with different molecular weights were obtained by fractionation. The rubber was extracted with acetone in a nitrogen atmosphere before fractionation, at room temperature in darkness, over a period of two days. After extraction the rubber was dissolved in benzene (thiophene-free), with the addition of 3 parts by weight of recrystallized phenyl-β-naphthylamine (P-β-NA) per 100 parts of rubber. The solutions were filtered twice through a double layer of silk.

The fractionation was effected from 1.6% solutions by decrease of temperature. Methyl alcohol was used as precipitant. The fractions were dissolved, without drying, in benzene with P-β-NA (2 parts by weight per 100 parts of rubber) and kept under nitrogen in the dark. SKS-30A was separated into 7 fractions, the first of which was insoluble after the separation. SKS-30 was separated into fractions, of which the first and second were insoluble after the separation. The insoluble gel fractions were not studied.

For characterization of the molecular structure of the soluble sol fractions, a part of the solution was taken, and methyl alcohol was distilled off under vacuum at room temperature. The distillation was stopped when the refractive index of the distillate coincided with that of pure benzene. The molecular weights of the SKS-30A fractions were found from the intrinsic viscosity of solutions in benzene, determined at 25°.

The calculations were based on the equation

The molecular weights of the SKS-30 fractions were determined by the osmotic method by means of Digadkin's osmometers [8]. The degree of molecular chain branching was characterized by the Huggins constant K', which was determined for each fraction from the corresponding reduced specific viscosity – concentration relationship (Table 1, Figs. 1 and 2.) The values of K' for the fractions of low molecular weight are not given, as the slope of the reduced specific viscosity – concentration lines was very small and the accuracy of K' determined in this way was doubtful.

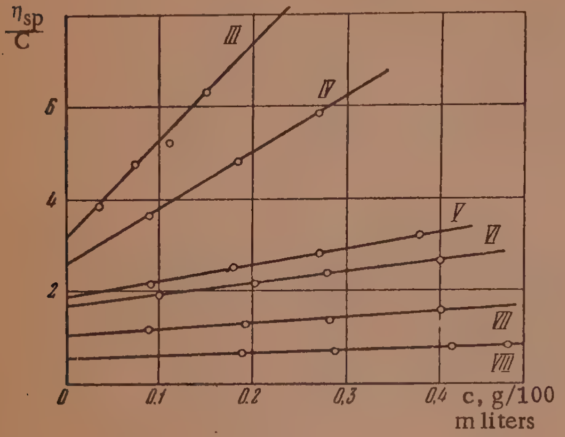

Fig. 1. Reduced specific viscosity – concentration relationships for solutions of SKS-30A fractions.

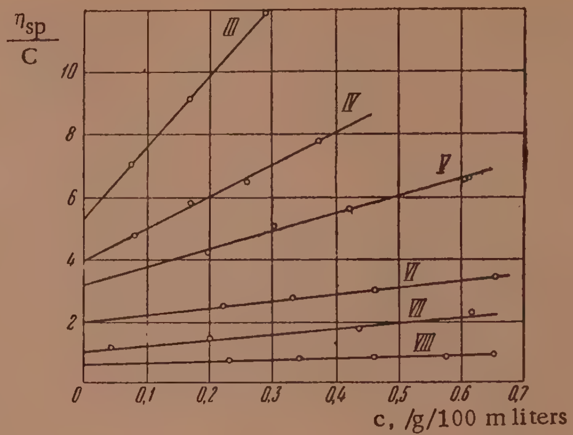

Fig. 2. Reduced specific viscosity – concentration relationships for solution of SKS-30 fractions.

Increase of the constant K' indicates increased molecular chain branching. It is seen from the data in Table 1 that the degree of branching increases with molecular weight for both rubbers. The SKS-30 fractions have lower intrinsic viscosities in solution and a more branched molecular structure than the SKS-30A fractions. For example, for the SKS-30 fraction of molecular weight 900,000, $[\eta] = 2.6$; $K' = 1.80$, and for the SKS-30A fraction of molecular weight 775,000, $[\eta] = 5.24$; $K' = 0.845$.

Preparation of the specimens. The specimens were prepared in the form of plates 1.5-1.7 mm thick by consecutive pouring of small amounts of solutions of the fractions into chrome plated molds. The benzene solvent was evaporated at 30°; the plates were then taken to constant weight under a residual pressure of 10^{-3} mm Hg at room temperature.

TABLE 1

Principal Molecular Characteristics of the Butadiene – Styrene Rubber Fractions

Fractions	SKS-30A			SKS-30		
	Molecular wt. of fraction	K'	$[\eta]$	Molecular wt. of fraction	K'	$[\eta]$
I	Insoluble gel fraction			Insoluble gel fraction		
II	775 000	0.845	5.24	»		»
III	515 000	0.725	3.92	1 000 000	2.38	3.2
IV	377 000	0.589	3.14	901 000	1.80	2.6
V	199 500	0.535	2.00	257 000	0.92	1.92
VI	75 200	—	1.00	180 300	0.70	1.76
VII	40 100	—	0.64	97 400	—	1.12
VIII	—	—	—	48 000	—	0.60

Determination of the viscosity of polymer fraction melts. The Tolstoi plastoelastometer was used to determine, at constant stress, the shear deformation kinetics of the polymer placed between two plane parallel plates. The apparatus is shown diagrammatically in Fig. 3.

The essential parts of the apparatus are two metal plates with straight grooves on their inner sides, cut in at right angles to the displacement of the plates. The grooves provide a better grip between the rubber and

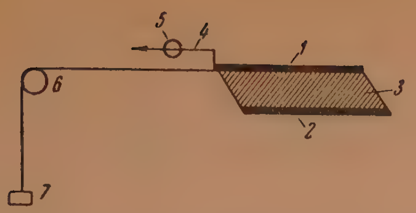

Fig. 3. Diagram of apparatus for measurement of shearing deformation in a polymer layer between two plane parallel plates: 1,2) steel plates; 3) polymer; 4) microphotographic scale; 5) cathetometer; 6) pulley; 7) load.

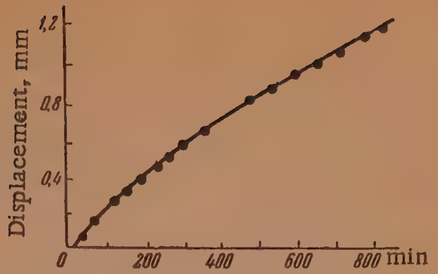

Fig. 4. Variation of shearing deformation with time for butadiene – styrene rubber.

the metal plates and eliminate the risk of slippage. The bottom plate is fixed, while the top plate is displaced by means of a load attached to a thread passing over a pulley resting on needle bearings. The action of an applied load causes horizontal displacement of the top plate and of the microphotographic scale fixed rigidly to it. The displacements were measured to an accuracy of 0.00025 cm by means of a cathetometer. The apparatus was placed in an air thermostat, the temperature in which was kept constant by means of an ultrathermostat. The test specimen, in the form of a plate, was clamped between the plane parallel plates in a press. The rubber filled the grooves under pressure; after subsequent relaxation of internal stresses it acquired residual deformation. The press was placed in a thermostat at 70°. The time required for stress relaxation varied with the molecular weight. The correct choice of the relaxation time was confirmed by the kinetics of the developing deformation, and also by absence of changes in the height of the specimen during the relaxation process.

A typical deformation-time curve is shown in Fig. 4. At the start of the process the deformation rate decreases at constant temperature and constant stress, gradually approaching a certain constant value. The curve then passes into a straight line. The slope of this linear region represents the rate of increase of irreversible deformation. When steady flow occurs under constant stress, the viscosity can be calculated by the simple formula

where η is the viscosity in poises; σ is the stress in dynes/cm^2; $\underline{h}$ is the thickness of the specimen in cm; ϵ is the displacement in cm; $\underline{t}$ is the time in seconds.

TABLE 2
Determinations of the Viscosity of Butadiene–Styrene Polymer Fractions in the Solid Phase at 82°

Fraction	Stress in dynes/cm^2	Layer thickness, cm	Velocity gradient in sec.$^{-1}$	Viscosity in poises
		SKS-30A		
III	67 590	0.1583	$3.67 \cdot 10^{-7}$	$1,85 \cdot 10^{11}$
IV	67 590	0.1377	$5.76 \cdot 10^{-7}$	$1.17 \cdot 10^{11}$
V	67 590	0.1814	$8,82 \cdot 10^{-6}$	$7.66 \cdot 10^{10}$
VI	23 838	0.1362	$4,71 \cdot 10^{-6}$	$5,08 \cdot 10^{9}$
VII	23 838	0.1229	$1,88 \cdot 10^{-3}$	$1,26 \cdot 10^{7}$
VIII	4905	0.1125	$1,72 \cdot 10^{-2}$	$2.84 \cdot 10^{5}$
		SKS-30		
IV	67 590	0.1400	$3,62 \cdot 10^{-6}$	$1,86 \cdot 10^{10}$
V	23 838	0.1158	$2,61 \cdot 10^{-4}$	$9.11 \cdot 10^{7}$
VI	23 838	0.1071	$2.98 \cdot 10^{-3}$	$7.50 \cdot 10^{6}$
VII	4905	0.0975	$2,10 \cdot 10^{-2}$	$2.33 \cdot 10^{5}$

In determinations of polymer viscosity, the question arises as to what is to be regarded as viscosity; the ratio of the total tangential stress to the velocity gradient, or the ratio of only the viscosity component of the stress to the velocity gradient. Here it is necessary to examine the molecular mechanism of polymer deformation, the physical origin of different forms of resistance to shear in the deformed system. Plastic and elastic deformations develop simultaneously under the action of an applied stress. At the start of the process the rate of plastic deformation changes owing to changes in the configuration of the molecular chains [9]. Then, after some time, the molecular chain configuration reaches a state of equilibrium for the given stress and temperature, and the subsequent deformation proceeds at a constant rate. Under the action of a constant stress the fully developed elastic deformation is maintained and plastic flow occurs. Thus, these two processes are inseparable, one accompanies the other, and therefore it is more correct to use the total tangential stress for viscosity calculations.

Variation of viscosity of the fractions with molecular weight. The viscosities of SKS-30 and SKS-30A fractions were measured at 82° in the stress region of 10^3 - 10^4 dynes/cm^2 (Table 2), where the flow remains practically Newtonian* [4,10]. Constancy of the molecular structure of the fractions in the course of the experiments was checked by determinations of solubility and intrinsic viscosity. These determinations showed that 2% (calculated on the rubber) of P-β-NA ensures stability of SKS-30 and SKS-30A rubbers under the experimental conditions (up to 5 days at 82°). However, the fractions of high molecular weight, which were soluble immediately after fractionation, partially lost solubility after preparation of the films. This was found for Fractions III and IV of SKS-30A and Fraction III of SKS-30.

It is seen in Table 2 that the viscosity varies over a range of 5-6 tenth-powers with molecular weight. With a variation of the molecular weight of SKS-30A from 40,000 to 800,000, the viscosity increased from $2.84 \cdot 10^5$ to $1.85 \cdot 10^{11}$ poises, and for SKS-30, as the molecular weight varied form 48,000 to 900,000 the viscosity varied from $2.33 \cdot 10^3$ to $1.86 \cdot 10^{10}$ poises. This viscosity variation resulted in a change in the duration of the experiments from a few seconds for the low molecular weight fractions to several days for the high fractions.

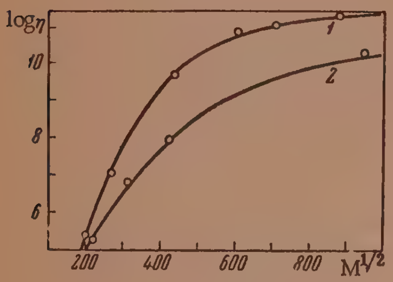

Fig. 5. Variation of the viscosity of fraction melts with the molecular weight: 1) SKS-30A; 2) SKS-30.

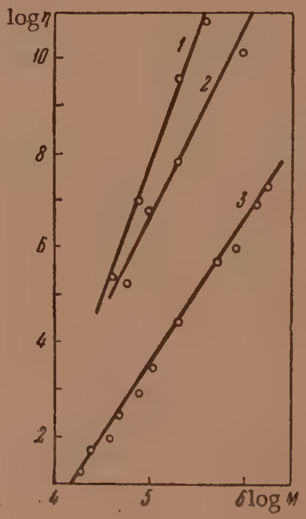

Fig. 6. Variation of log η with log M: 1) SKS-30A; 2) SKS-30; 3) polyisobutylene from the data of Fox and Flory.

Fig. 5 shows the viscosities of the fractions plotted against the square root of the molecular weight. SKS-30 fractions, which have greater chain branching and lower intrinsic viscosities in solution than SKS-30A fractions, also have lower viscosities in the solid phase in steady flow

---

* We showed for polyisobutylene that with a 30-fold change of stress from $5 \cdot 10^3$ to $1.5 \cdot 10^5$ dynes/cm^2 the viscosity decreased by 12%. The fact that at 82° the viscosity is independent of the stress in the low stress region for butadiene-styrene copolymer is seen from the following table:

Stress, dynes/cm^2	Layer thickness, cm	Displacement rate	Viscosity, poises
45 710	0.1304	$1.07 \cdot 10^{-6}$	$5.57 \cdot 10^{9}$
23 840	0.1414	$6.07 \cdot 10^{-7}$	$5.55 \cdot 10^{9}$

conditions. The difference between the viscosities of SKS-30 and SKS-30A melts diminishes with decreasing molecular weight; this is consistent with the simultaneous equalization of the constants K'. Thus, both in solutions and in melts under steady flow conditions the viscosity decreases with increasing degree of branching, which is probably the consequence of higher packing density for the branched polymer chains. This is based on the known fact that branched structure in a molecular chain decreases its geometrical dimensions [11, 12].

It follows from the data in Fig. 6 for fractions the molecular structure of which did not change during the experiments that a linear relationship between log η and log M holds for butadiene-styrene polymers over a wide molecular weight range.

For comparison, the results obtained by Fox and Flory [4] for polyisobutylene are also shown in Fig. 6. The linear relationships give the following expressions:

For SKS-30. . . . . $\log \eta = 4 \log M - 13.2$
For SKS-30A . . . . $\log \eta = 6.94 \log M - 26.7$
For polyisobutylene . . $\log \eta = 3.17 \log M - 12.37$

TABLE 3

Effect of Temperature on the Viscosity of Butadiene-Styrene Polymers

Temperature, °C	Stress, dynes/cm²	Displacement rate, cm/sec.	Thickness of plate, cm	Velocity gradient, sec.$^{-1}$	Viscosity, poises
SKS-30 [η] = 1.12; mol. wt. 97,400					
24	23 838	$2.31 \cdot 10^{-5}$	0.1084	$0.213 \cdot 10^{-3}$	$1.11 \cdot 10^{8}$
40	23 838	$5.70 \cdot 10^{-5}$	0.1085	$0.543 \cdot 10^{-3}$	$4.53 \cdot 10^{7}$
60	23 838	$1.29 \cdot 10^{-4}$	0.1092	$1,18 \cdot 10^{-3}$	$2.01 \cdot 10^{7}$
82	23 838	$2.666 \cdot 10^{-4}$	0.1086	$2,45 \cdot 10^{-3}$	$9.73 \cdot 10^{6}$
SKS-30A [η] = 1.00; mol. wt. 75,000					
24.5	23 838	$1.08 \cdot 10^{-5}$	0.1162	$0.93 \cdot 10^{-4}$	$2.56 \cdot 10^{8}$
45	23 838	$2.11 \cdot 10^{-5}$	0.1169	$1.80 \cdot 10^{-4}$	$1.32 \cdot 10^{8}$
60	23 838	$7.60 \cdot 10^{-5}$	0.1172	$6,49 \cdot 10^{-4}$	$3.63 \cdot 10^{7}$
82	23 838	$3.32 \cdot 10^{-4}$	0.1229	$1.886 \cdot 10^{-3}$	$1.261 \cdot 10^{7}$
SKS-30A; mol. wt. 199,500					
41.5	67 590	$2.59 \cdot 10^{-7}$	0.1104	$2,34 \cdot 10^{-6}$	$2.88 \cdot 10^{10}$
60	67 590	$1.09 \cdot 10^{-6}$	0.1263	$8.59 \cdot 10^{-6}$	$7.00 \cdot 10^{9}$
70	67 590	$1.38 \cdot 10^{-6}$	0.1230	$1.12 \cdot 10^{-5}$	$6.02 \cdot 10^{9}$
82	23 838	$6.41 \cdot 10^{-7}$	0.1362	$4.70 \cdot 10^{-6}$	$5.06 \cdot 10^{9}$

The variations of viscosity with molecular weight for these butadiene-styrene polyemers are analogous to those for polyisobutylene and polystyrene [4]. The viscosity first rises sharply with molecular weight, and then from molecular weights of 300,000-400,000 onward, the viscosity increases much more slowly. It is probable that in the molecular weight range studied this relationship applies to all polymers. An analogous relationship between the mechanical properties of vulcanizates and the molecular weight of butadiene-styrene rubber was discovered earlier [13]. It is significant that the limiting molecular weight at which the change in the property in question begins to occur at a lower rate is the same for vulcanizates and raw rubbers. This type of variation of polymer properties with molecular weight can probably be atributed to tangling of molecular chains with formation of knots and loops, which behave similarly to chemical cross links, from the mechanical aspect, under the action of external stresses.

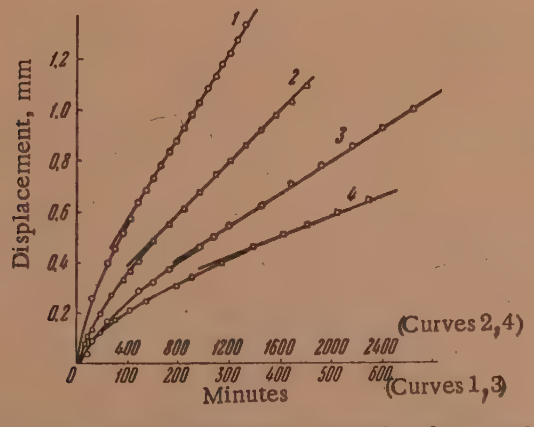

Fig. 7. Deformation–time relationship for SKS-30 of molecular weight 97,400 at various temperatures: 1) 82°; 2) 40°; 3) 60°; 4) 24°

Effect of temperature on the viscosity of butadiene-styrene rubbers. The viscosity of fractionated specimens of SKS-30 and SKS-30A was measured at four temperatures between 24 and 82°. The determinations were carried out under equal stresses (Table 3).

Deformation–time curves for different temperatures are shown in Fig. 7. It follows from Fig. 7 and Table 3 that increase of temperature results in earlier completion of high-elastic deformation, when the linear portion of the curve is reached, and in increase of the rate of plastic deformation. As the temperature increases from 24 to 82°, the viscosity decreases more than tenfold: from $1.11 \cdot 10^8$ to $9.73 \cdot 10^6$ poises for SKS-30 and from $2.56 \cdot 10^8$ to $1.26 \cdot 10^7$ poises for SKS-30A.

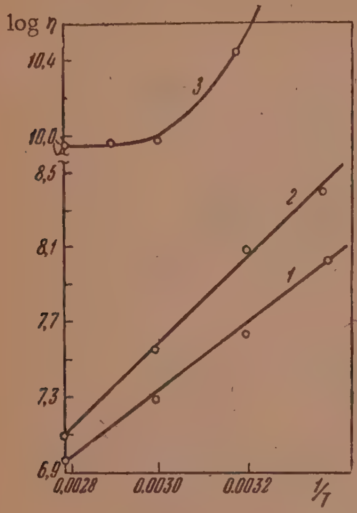

Fig. 8. Log η – 1/T relationship for: 1) SKS-30, mol. wt. 7.400; 2) SKS-30A, mol. wt. 75,200; 3) SKS-30A, mol. wt. 199,500.

The data of Table 3 are plotted in log η – 1/T coordinates in Fig. 8. The log η – 1/T relationship for fractions of low molecular weight (Curves 1 and 2) is linear, i.e., the activation energy does not change with temperature in the 24-82° range. The corresponding values of the activation energy E are 10.8 kcal./mole for SKS-30A and 7.8 kcal./mole for SKS-30. The reason why the branched polymer gave a lower value of E is probably that the segments near the chain ends are capable of moving more freely than segments far from the chain ends, and the number of free ends is greater in branched polymers.

The equation

$$\eta = Ae^{E/RT}$$

is not applicable to fractions of higher molecular weight (Curve 3), as the log η – 1/T relationship is nonlinear. The variation of the activation energy with temperature for a specimen of high molecular weight can probably be attributed to changes of the degree of the nearest order and of the intermolecular forces. The constancy of the activation energy for fractions of low molecular weight can be explained by the looseness of the structure.

SUMMARY

1. The viscosities of melts of fractions of butadiene-styrene rubbers SKS-30 and SKS-30A have been measured.

2. The degree of molecular chain branching in SKS-30 and SKS-30A fractions has been estimated by the Huggins constant K', and it is shown that the degree of branching increases with molecular weight for both rubbers. The molecules of SKS-30 fractions have a more branched structure than the molecules of SKS-30A fractions of the same molecular weight.

3. SKS-30 and SKS-30A rubbers conform to the flow law $\log \eta = A \log M + B$, over a wide range of molecular weights.

4. The degree of molecular chain branching influences the viscosity of polymers in solutions and melts. SKS-30 fractions, with a more branched molecular structure, have lower intrinsic viscosities in solution and, under steady flow conditions, lower melt viscosities.

5. The activation energy of viscous flow E has been determined for the low molecular weight fractions of SKS-30 and SKS-30A in the 24-82° range; the values were 7.8 kcal./mole for SKS-30 and 10.8 kcal./mole for SKS-30A. The activation energy for the fraction of high molecular weight depends on the temperature in this temperature range.

Scientific Research Institute for the Rubber Industry.
Moscow

Received November 23, 1956.

LITERATURE CITED

[1] Flory P., J. Am. chem. Soc. 62, 1057, 1940.

[2] Zapp, Baldwin, High Polymers, No. 8, (Goskhimizdat 1949).

[3] G. Diens, H. Klemm, J. Appl. Phys. 17, 458 1946.

[4] T. Fox, P. Flory, J. Am. chem. Soc. 70, 2384, 1948.

[5] F. Bueche, J. Appl. Phys. 26, 738 1955.

[6] A. S. Novikov and F. S. Tolstukhina, Proc. Acad. Sci. USSR, 109, 576 1956.

[7] D. M. Tolstoi, Colloid J., 10, 133 1948.

[8] B. Dogadkin, I.Soboleva and M. Arkhangelskaya, Investigations in the Field of High Polymers (Izd. AN SSSR, 1949) p. 253.

[9] G. M. Bartenev, J. Phys. Chem., 24, 10, 1210 1950.

[10] K. Van Holde, J.W. Williams, J. Pol. Sci. 11, 243 1953.

[11] V. N. Tsvetkov, Proc. Acad. Sci. USSR, 78, 1123 1951.

[12] I. G. Soboleva, N. V. Makletsova, A. V. Matveeva, and S. S. Medvedev, Colloid J., 18, 344 1956.*

[13] A. S. Novikov, M. B. Khaikina, and T. V. Dorokhina, Colloid J., 15, 1, 51 1953. *

---

* Original Russian pagination. See C. B. translation.

DEPENDENCE OF THE ELASTIC CONSTANT OF A VULCANIZATE ON THE MOLECULAR WEIGHT OF THE ORIGINAL RUBBER

L.S. Priss

By the kinetic theory of high elasticity, the equilibrium stress in a deformed vulcanizate without filler is

$$\sigma = C(\lambda^2 - 1/\lambda), \tag{1}$$

where $\lambda = l/l_0$ is the relative elongation, and

$$C = 2\nu_0 kT^*, \tag{2}$$

where ν_0 is the number of linkage points per unit volume of the material; T is the absolute temperature; k is the Boltzmann constant.

The latter expression is valid only if the average number of cross links per molecule of the original rubber is fairly large. We shall denote this number by γ. For sparse networks, when γ is a few units, Equation (2) requires modification. An approximate calculation for networks based on monodisperse linear polymers was made by Flory [1]; his result

$$C = 2\nu kT = 2\nu_0(1 - 2M_c/M) = n\gamma(1 - 2/\gamma) \tag{3}$$

(here ν and n are the numbers of "effective" network-forming cross links and original molecules per unit volume respectively; M_c and M are the molecular weights of the chain and the original rubber) should, according to Flory, be valid from $\gamma \approx 3$.

Since Equation (3) is sometimes very useful in certain physicochemical investigations of vulcanizates [4, 5], we decided to derive a more strict relationship between C and γ for networks formed from a monodisperse original rubber, and a rubber with a molecular weight distribution conforming to Poisson's law.

Considerable deviations from Equation (3) were found even at high values of γ. It was found that Flory's derivation contains an error, elimination of which leads to the expression

$$C = kT(2\nu_0 - n) = n\gamma kT(1 - 1/\gamma) = NkT \tag{4}$$

in agreement with the results (for large values of γ) of the calculations given below.

The following gives (4). Eq. (2) is valid for a network formed by cross linking of an infinitely long molecule. If n chains are broken in 1 cc of such a network, it will be equivalent to a network formed from a rubber containing $n + 1 \approx n$ molecules in 1 cc. The remaining chains number $2\nu_0 - n$, which leads to (4).

Flory's error is that he assumes the effective number of chains in 1 cc, N, to be twice the number of network-forming cross linkage points ν, defined as the difference $\nu_0 - n$. However, comparison of the number of cross linkage points per given molecule with the number of chains which results easily shows that $N = 2\nu + n$, and this leads to Equation (4).

Before we pass to a more rigid calculation, we shall consider the general structure of the network and introduce certain assumptions.

---

* Generally speaking, this relationship between C and ν_0 is not confirmed by experiment [2,3]. The reasons for this deviation will be discussed elswhere. Here we consider only the question of the dependence of C on the molecular weight of the original rubber.

Network structure. If the molecular weight of the original rubber has a finite value, then not all the molecules are incorporated in the network, and some of them form the soluble part of the vulcanizate, the sol fraction. The ratio between the soluble and insoluble (gel fraction) parts of vulcanizates has been calculated for different types of molecular weight distribution in the original rubber [6-8].

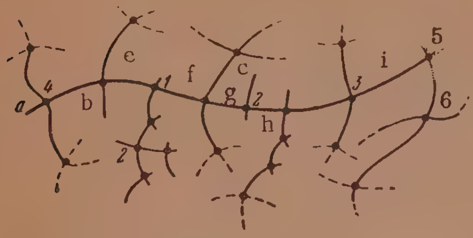

Fig. 1

The gel fraction can be mathematically defined as an entity of interconnected molecules of infinitely large molecular weight. Fig. 1 diagrammatically shows one of the original molecules contained in the gel fraction, and different types of attachment of other molecules to it. Chains which continue indefinitely are shown by broken lines.

As is seen from the diagram, in addition to the chains the network contains free ends of molecules of type a and b, and attachments, molecules c or groups of molecules d, attached to the network at single points. Points of type 1 and 2, to which groups of molecules of finite molecular weight are attached, will be regarded as inactive, and the chains e and f will be considered as a single chain; the same applies to chains g and h.

The network-forming points do not all lead to the formation of the same numbers of chains. For example, there are two chains corresponding to each point of type 3, which is a middle point for both the molecules joined there; for each point of type 4, which is a middle point for one molecule and an end point for another, there are 1.5 chains; while a junction of type 5, an end point for both molecules, does not lead to formation of new chains – the chains i and j constitute a single chain joining points 3 and 6. Thus, the total number of active chains in 1 cc of the network is

$$N = 2\nu_{mm} + 1,5\,\nu_{me} \tag{5}$$

where ν_{mm} and ν_{me} are the numbers of network-forming points of types 3 and 4 respectively (Fig. 1).

Apart from the above types of linkage, cross links can also be formed between two segments of the same molecule. If there are no other cross links between these segments, a point of this type, although it is network-forming and belongs to type 3 or 4 (Fig. 1) does not lead to chain formation. The probability of linkages of this type in not very dense networks is small and they will not be considered in the calculations below.

Network of molecules of equal length. Let us assume that 1 cc of the original rubber contains n molecules, each consisting of u units. Let q be the probability of the inclusion of a given unit in a cross link, i. e., double the ratio of the number of network points in 1 cc to the total number of reactive bonds nu (it is assumed that each monomer unit contains one reactive bond). Then the number of original molecules containing c monomer units entering the network points is

$$n(c) = nq^c(1-q)^{u-c}\frac{u!}{(u-c)!\,c!}, \tag{6}$$

and the ratio of the number of units entering the network points in these molecules to the total number of these units is

$$t(c) = \frac{cn(c)}{nuq} = \frac{c}{uq}\left(\frac{q}{1-q}\right)^c(1-q)^u\frac{u!}{(u-c)!\,c!}. \tag{7}$$

It is evident that t (c) will determine the probability that a molecule B, attached to a molecule A, will have c – 1 more cross links, which can continue the network. Thus, t (1) is the probability of the addition of a molecule containing no more cross links, t (2) is the probability of the addition of a molecule containing one cross link, etc.

If a molecule B, joined at some point to a molecule A, has limited continuation, such a point is conventionally taken to be non-network forming. Let the corresponding probability be represented by s. It is easily seen that

$$s = t(1) + t(2)s + t(3)s^2 + \ldots = \sum_{c=1}^{u} t(c)s^{c-1} = \frac{(1-q)}{suq}\sum_{c=1}^{u} c\left(\frac{qs}{1-q}\right)\frac{u!}{(u-c)!\,c!} =$$

$$= (1-q+qs)^{u-1} \approx e^{-\gamma(1-s)}, \tag{8}$$

where $\gamma = uq$. The last equality in Equation (8) is valid only at high values of u, as is almost always the case.

It can be shown that s is equal to the relative content of the soluble fraction in the vulcanizate, and that the equation

$$s = e^{-\gamma(1-s)} \tag{9}$$

can, by simple transformations, be reduced to the Flory equation derived for this particular case. Equation (9) has a solution other than the trivial $(s = 1)$ only if $\gamma \geq 1$, which corresponds to values of γ at which the network can exist.

The number of molecules containing c cross linkage points, of which r are network-forming, is:

$$v(c, r) = n(c)(1-s)^r s^{c-r}\frac{c!}{r!\,(c-r)!}. \tag{10}$$

The total number of molecules in which r monomer units enter the network-forming points is found by summation of $v(c,r)$ for all values of $c(r \leqslant c < u)$:

$$v(r) = \sum_{c=r}^{u} v(r, c) = n\frac{(1-q)^u(1-s)^r}{s^r}\sum_{c=r}^{u}\left(\frac{qs}{1-q}\right)^c\frac{u!}{r!\,(c-r)!\,(u-c)!} = \tag{11}$$

$$= nq^r(1-s)^r(1-q+qs)^{u-r}\frac{u!}{r!\,(u-r)!},$$

and the total number of monomer units entering the network-forming points, by summation of $rv(r)$ for all values of r from 2 to u:

$$l' = \sum_{r=2}^{u} rv(r) = n\gamma(1-s)^2; \tag{12}$$

of these

$$l_m = \sum_{r=3}^{u}(r-2)v(r) = n(1-s)(\gamma - 2 + \gamma s) \tag{13}$$

units enter network-forming points which are not at the ends of the given molecule, and

$$l_e = 2\sum_{r=2}^{u} v(r) = 2(1-s)(1-\gamma s) \tag{14}$$

are at extreme network-forming points.

If l', l_m, and l_e are large enough (which is true even for very sparse networks), and the number of network points per molecule is small compared to the total number of such points, the probability that a given point is a middle one for the two molecules joined at it is l_m^2/l'^2. Similarly, for a point which is extreme for one and middle for the other, or extreme for both molecules, we have: $2\,l_e l_m/l'^2$ and l_e^2/l'^2. The number of points of each of these types is found by multiplication of the corresponding probability by the total number of network points $(\nu = l'/2)$.

The number of active chains contained in unit volume of the network, according to Equation (5), is:

$$N = 2\nu_{mm} + 1{,}5\,\nu_{me} = l_m^2/l' + 1.5\,l_m l_e/l' = n(\gamma - 2 + \gamma s)(\gamma + 1 - 2\gamma s)/\gamma. \tag{15}$$

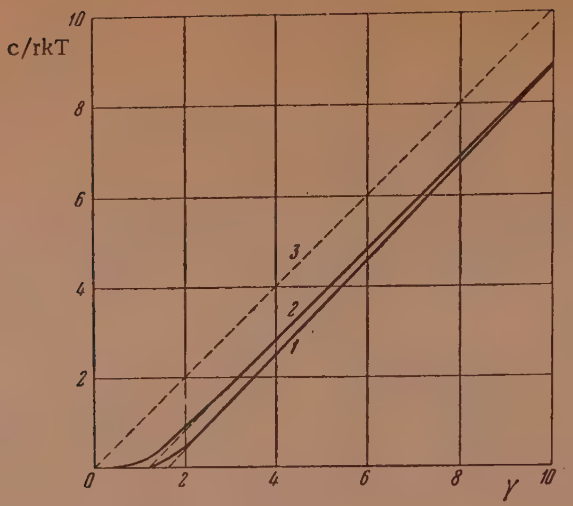

Fig. 2. Variation of the number of effective chains N with γ for a network formed in 1) a monodisperse rubber, Equation (15); 2) a rubber with a Poisson molecular weight distribution, Equation (24); 3) $N/n = \gamma$

The variation of N, a quantity proportional to the elastic constant C of the rubber, with γ, calculated by Equation (15), is shown in Fig. 2 (curve 1). It is seen that C = 0 at $\gamma = 1$, and then C gradually increases with γ, while from $\gamma \approx 2$ its increase is approximately linear. Extrapolation of this plot to the abscissa axis gives an intersection point corresponding to $\gamma \approx 1.6$. At high values of γ, Equation (15) reduces to the expression

$$N \approx n(\gamma - 1 - 2/\gamma) \approx n(\gamma - 1) \tag{16}$$

as stated at the beginning of this paper.

Network of molecules with size distribution conforming to Poisson's law. Suppose that the original rubber was formed by the random scission of an infinitely long molecule. Such a molecular weight distribution (or one similar to it) is found in real rubbers. In this case the number of molecules consisting of u monomer units is

$$m(u) = np(1-p)^{u-1} \approx npe^{-pu}/(1-p), \tag{17}$$

where n and u are the total numbers of molecules and monomer units per unit volume respectively; $p = n/u$. The rest of the notation used here is the same as before ($\gamma = q/p$).

The number of molecules containing c monomer units entering into cross links

$$n(c) = \frac{np}{1-p}\,\frac{1}{p+q-pq}\,A^c, \qquad A = (1-p)\,q/(p+q-pq) \tag{18}$$

was calculated by Charlesby [7].

From this it is not difficult to determine the number of molecules, containing r monomer units, entering the network-forming points:

$$v(r) = \sum_{c=r}^{\infty} v(c, r) = \frac{np}{1-p}\,\frac{(1-s)^r}{s^r(p+q-pq)} \sum_{c=r}^{\infty} A^c s^c \frac{c!}{r!\,(c-r)!} = \frac{np}{(1-p)(p+q-pq)}\,\frac{(1-s)^r A^r}{(1-As)^{r+1}}, \tag{19}$$

where $v(c, r)$ is expressed in terms of $n(c)$, in accordance with Equation (10).

The values of l', l_m and l_e respectively are:

$$l' = \sum_{r=2}^{\infty} rv(r) = \frac{np}{(1-p)(p+q-pq)} A(1-s)\left[\frac{1}{(1-A)^2} - \frac{1}{(1-As)^2}\right] \approx \tag{20}$$

$$\approx n\gamma(1-s)^2. \tag{21}$$

$$l_e = 2\sum_{r=2}^{\infty} v(r) = \frac{2np}{1-p}\frac{(1-s)^2}{(p+p-pq)}\frac{A^2}{(1-A)(1-As)^2} \approx 2n\gamma^2(1-s)^2 s;$$

$$l_m = l' - l_e \approx n\gamma(1-s)^2(1-2\gamma s). \tag{22}$$

As an approximation, Charlesby's equation connecting γ and $\underline{s}$ [7] was used:

$$s = \frac{1}{(1+\gamma-\gamma s)^2}, \tag{23}$$

and it was assumed that $\underline{q}$ and $\underline{p}$ were negligible relative to unity.

The total number of active chains in unit volume, according to Equations (6) and (15) is

$$N = l_m^2/l' + 1.5\, l_m l_e/l' \approx n\gamma(1-s)^2(1-2\gamma s)(1+\gamma s). \tag{24}$$

The $N - \gamma$ relationship calculated by means of Equation (24) is also shown in Fig. 2. In this case N becomes zero at $\gamma = 0.5$ and Curve 2 at small values of γ lies somewhat above Curve 1. At high values of γ, N, expressed in accordance with Equation (24), is also approximately equal to $n(\gamma - 1)$. Extrapolation of the linear portion of the plot to the abscissa axis gives an intersection at $\gamma \approx 1.2$.

Some applications of the foregoing calculations. A comparison of the experimental relationships between the elastic constant C (number of active chains) and the original molecular weight, with Equations (15) and (24) may be used to estimate the number of cross linkage points per unit volume [4]. It follows from the foregoing that it is necessary to take into account the nature of the molecular weight distribution of the original rubber.

Horikx [5] has recently shown that studies of the relationship between the sol fraction content and the number of active chains in the gel fraction at different stages of oxidative degradation of vulcanizates can be used for elucidating the mechanism of this process. By comparing experimental data with theoretical relationships, derived on the assumption that oxidative degradation is accompanied by: 1) disintegration of cross linkage points, 2) random chain rupture, and 3) chain rupture near the cross linkage points, he concluded that disintegration of the network can be caused only by one of the two latter processes.

However, the relationship used by Horikx for the third case is not quite exact, as it was based on Equation (3). A more exact relationship can easily be derived from the results of the preceding section of this paper. Random chain rupture is equivalent to a decrease of the molecular weight of the original rubber, with a Poisson molecular weight distribution. If the number of cross linkage points per 1 cc remains unchanged during degradation, then $n\gamma = 2\nu_0 = \text{const}$, while γ decreases. Referring N in Equation (24) to the relative content of the insoluble fraction $1 - s$, we find the number of active chains in 1 cc of the gel fraction:

$$N_2 = 2\nu_0(1-s)(1-2\gamma s)(1+\gamma s). \tag{25}$$

The plot of $1 - N_{22}/N_{21}$, calculated on the basis of Equation (25) (N_{22} and N_{21} are the numbers of active chains in 1 cc of the gel fraction of the degraded and original vulcanizate respectively) against $\underline{s}$ (the content of the soluble fraction) lies further away from the experimental points than the relationship calculated by Horikx. Thus, the assumption that in the oxidative degradation of natural rubber vulcanizates random chain rupture occurs is less probable than chain rupture near the cross linkage points, if the values of N_2 determined from maximum swelling can be taken as quantitatively significant.

Let us consider another application of these calculations. Chemical relaxation of stress in vulcanizates at high temperatures may in principle be determined by the same processes [9] as oxidative degradation. In this instance, in contrast to relaxation caused by rupture and rearrangement of cross links [10, 11] or by rupture of chains near cross linkage points, the relaxation resulting from random chain rupture should be nonexponential in character and should proceed at a rate inversely proportional to the density of the network. Indeed, on the assumption that rupture of monomer units is a reaction of the first order, we have:

$$p = 1 - (1 - p_0)\, e^{-kt} \approx p_0 + kt \tag{26}$$

or

$$\gamma = q/p = q_0/(p_0 + kt). \tag{27}$$

Here we confine ourselves to two terms in resolution of the exponent, as kt is always small. Substituting Equation (27) into (16), and taking into account that $n\gamma = 2\nu_0 = \text{const}$, we derive an approximate expression for N as a function of time at large values of γ (the first relaxation period)

$$N \approx 2\nu_0 \left[(1 - 1/\gamma_0) - kt/q_0\right], \tag{28}$$

where terms with the subscript "$_0$" refer to the original vulcanizate.

A more exact relationship is obtained by substitution of Equation (27) into (24). The results of numerical calculations for $q_0 = 0.02$, $\gamma_0 = 40$ are shown graphically in Fig. 3 (Curve 1). This relationship differs from that derived by Berry and Watson [11] owing to the rougher concepts regarding the network structure. Comparison with an exponential relationship (Curve 2, Fig. 3) shows that in this instance stress relaxation should be more rapid than indicated by the exponential law.

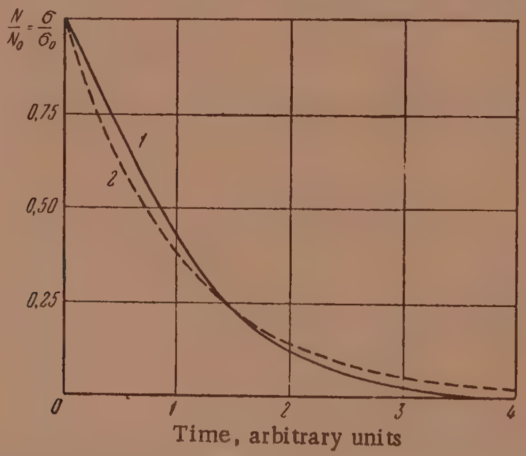

Fig. 3. Stress-time relationship during relaxation caused by random chain rupture (1), and the exponential relationship (2).

In comparisons of the equations given in this section with experimental data it should be remembered that secondary processes, which complicate the effect, may occur in oxidative degradation and chemical relaxation. We must also point out that these equations can be claimed to give only a qualitative description of the effect, as they were derived on the assumption that Equation (2) is valid, which is not the case.

SUMMARY

1. The elastic constant – initial molecular weight relationship has been calculated for monodisperse rubber and rubber with molecular weight distribution conforming to Poisson's law. It is found that the correction for the original molecular weight of the rubber depends on the type of distribution only for relatively sparse networks.

2. It is shown that Flory's calculation contains an error, and that the Flory equation $C = 2\nu_0\,(1-2\,M_c/M)$

should be replaced by $C = 2\nu_0(1 - M_c/M)$. The appropriate modifications must also be introduced into equations derived from the Flory equation.

3. Several applications of these calculations are illustrated by examples.

It is the author's pleasant duty to thank B.A. Dogadkin, who suggested the subject of this investigation.

Scientific Research Institute for the Tire Industry,
Moscow

Received April 12, 1957

LITERATURE CITED

[1] P. Flory J. Chem. Rev. 35, 51 1944.

[2] P. Flory, N. Rabjohn, M. Shaffer, J. Pol. Sci. 4, No. 3, 225 1949; Rub.Chim.Tech.19,522, 1956.

[3] A. M. Buche, J. Pol. Sci. 19, No. 92, 297 1956.

[4] P. Flory, J. Ind. Eng. Chem. 38, 417 1946; Rub. Chem. Technol. 19, 522 1946.

[5] M. H. Horikx, J. Pol. Sci. 19, No. 93, 445 1956; Rub. Chem. Technol. 29, No. 4, 1166 1956.

[6] P. Flory, J. Chem. Phys. 46, 132 1942.

[7] A. Charlesby, J. Pol. Sci. 11, No. 6, 513 1953.

[8] T. Alfrey, Mechanical Behavior of High Polymers, translation edited by M. V. Volkenshtein, (IL 1952) p. 310.

[9] A. V. Tobolsky, J. Appl. Phys. 27, No. 7, 673 1956.

[10] B. A. Dogadkin and Z. N. Tarasova, Colloid J., 15, No. 5, 347 1953.*

[11] J. P. Berry, W. F. Watson, J. Pol. Sci. 18, No. 88, 201 1955.

---

* Original Russian pagination. See C. B. translation

RECIPROCAL DISPLACEMENT OF COMPONENTS IN ION-EXCHANGE CHROMATOGRAPHY

G.V. Samsonov and V.A. Orestova

In the movement of a mixed zone of two types of exchanging ions along a column filled with an ion exchange resin, separation of this zone into zones of the individual components should conform to the theory advanced by us earlier [1, 2]. If the exchanging ions are of equal valencies (with equal ionic charges) the conditions of ion displacement are completely determined by the ion exchange constant in the equation

$$\frac{m_1}{m_2} = K\frac{c_1}{c_2}, \tag{1}$$

where m_1 and m_2 are the quantities of ions of the first and second type in the adsorbed state on the resin, and c_1 and c_2 are the concentrations of these ions in solution. If $K > 1$, ions of the second type (c_2, m_2) form the leading zone, while ions of the first type (c_1, m_1) are in the second zone. When $K < 1$, the sequence of the zones should be reversed. If $K = 1$, the mixed ion zone moves without separation into zones of the individual components. Reciprocal displacement of the components can be observed most conveniently in dynamic sorption in a three-component system. If through a column filled with one type of ions a solution is passed containing exchanging ions of second and third types, then the moving mixed zone of the latter two components should be deformed in such a way as to form a sharp boundary between the zones of the ions contained in the mixed zone. This is possible only when ions of a particular type in a mixed zone form a separate zone of this component only, situated at the boundary between the zone of the displaced ion and the mixed zone, corresponding in composition to the solution continuously entering the column. The formation of a sharp boundary within the zone of the components entering the column and separation of a pure zone of one of them must evidently be accompanied by the formation of a maximum on the elution curve for the displaced component.

The presence of maxima on the elution curves in the exchange of three types of ions in dynamic conditions, when a solution containing two types of exchanging ions is introduced into the column, has been experimentally observed in a number of cases [3-6]. One of the components entering the column was displaced and formed a pure zone of the single component. As was already stated above, the conditions for the displacement of this component, which determine that one of the two components is displaced and forms a pure zone, depend entirely on the ion exchange constant in the exchange of ions of different valencies. This has been demonstrated experimentally. It follows from our theory of the dynamics of ion exchange [1, 2] that in the exchange of ions of different valencies in dynamic conditions the formation of a sharp boundary depends on a number of variables, including the solution concentration. In a two-component system a sharp boundary between zones of two types of ions is determined by the condition:

$$c_0 > c_{cr}, \text{ when } z_1 < z_2 \tag{2}$$

or

$$c_0 < c_{cr}, \text{ when } z_1 > z_2, \tag{3}$$

where c_0 is the aggregate concentration of the two types of exchanging ions.

$$c_{cr} = m/K^{\frac{z_1 \cdot z_2}{z_1 - z_2}}, \tag{4}$$

where m is the exchange capacity of the resin; K is the ion exchange constant in the equation

$$\frac{m_1^{1/z_1}}{m_2^{1/z_2}} = K \frac{c_1^{1/z_1}}{c_2^{1/z_2}}, \tag{5}$$

where z_1 and z_2 are the ionic charges (we are considering a process in which, in the separation of a mixed zone, the second component, with c_2 and m_2, is displaced by the first).

It follows from the theory that a mixed zone of two ions of different valencies can separate into zones containing the individual components in such a way that in one and the same two ions – resin system both ions of the higher and of the lower valencies can be displaced. It all depends on the aggregate concentration of the ions in the mixture. There is a certain critical concentration, readily calculated by means of Equation (4), on the two sides of which the sequence of the components in the ion exchange columns will be different. If the total solution concentration is greater than c_{cr}, ions of the lower valency should displace ions of the higher valency; at a concentration below c_{cr} the ion zones should move in the reverse sequence.

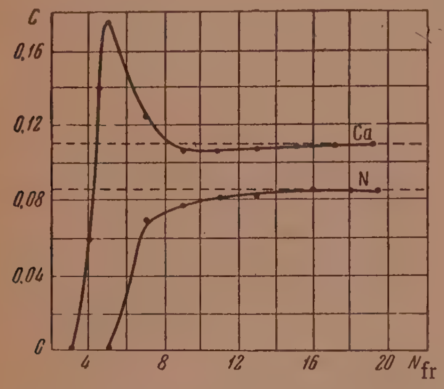

Fig. 1. Frontal sorption of calcium (Ca) and trimethylbenzylammonium (N) ions in the sodium form of SNF sulfophenolic resin at $c_0 > c_{cr}$. Initial concentrations of the ions: Ca – 0.1096 N $(CH_3)_3C_6H_5CH_2$ N – 0.0874 N; $c_0 = 0.1953$ N

The method described above was used for experimental study of the reciprocal displacement of ions of different valencies. A solution of two components with respect to exchanging ions was passed through an ion exchange column containing a definite type of ions (sodium). As the result of formation of a sharp boundary between the ion zones, one of the ions should be displaced from the mixed zone with formation of a maximum on the elution curve.

In order that the critical concentration should not be too high (otherwise Equation (5) cannot be used, and moreover it is difficult to carry out the experiments at $c_0 > c_{cr}$), according to Equation (4) the constant for the exchange of the bivalent for the univalent ion must not be large.

In other words, the univalent ions chosen must interact vigorously with the resin. It is known [7] that quaternary ammonium ions have this property. Ions of calcium and trimethylbenzylammonium (chlorides) were therefore chosen for studying the sequence of ion motion in the chromatographic column. The cation exchange resin was SNF sulfonic resin. The exchange constant for calcium and the quaternary ammonium ions was 0.086; the critical concentration was 0.026 N.

In each experiment 1 g of the resin in sodium form was used, with grain size 60-150 mesh. The volumes of the fractions taken were 5 ml in the first experiment and 50 ml in the second. The solution flow rates were 20 and 50 ml/cm^2. hour respectively.

The elution curves in Fig. 2, obtained at $c_0 > c_{cr}$ and at $c_0 < c_{cr}$, show that in the first case trimethylbenzylammonium ions displace calcium ions, and in the second the position is reversed. As was predicted from our theory, the univalent ion is the displacing ion at high concentrations, and the multivalent ion at low. This transposition of the sequence of ionic motion in ion exchange chromatography by simple alteration of the solution concentration casts doubt on the value of sorption series of ions arranged in order of their reciprocal displacing power.

The reciprocal displacement of ions on ion exchange resins has been studied previously in relation to the statistical characteristics of ion exchange [3-6, 8, 9].

The effect of solution acidity on the sequence of the ion zones in chromatography has also recently been the subject of special investigations [10, 11]. It was found that changes in the sequence of the ion zones are in accordance with changes in the ion adsorbabilities, as was to be expected in systems in which the concentration of one type of exchanging ion is many times less than the concentration of the other.

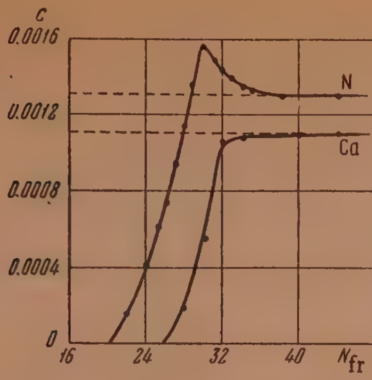

Fig. 2. Frontal sorption of calcium (Ca) and trimethylbenzylammonium (N) ions in the sodium form of SNF sulfophenolic resin at $c_0 < c_{cr}$. Initial concentrations of the ions: Ca – 0.00110 N; $(CH_3)_3C_6H_5CH_2$ N 0.00130 N; c_0 = 0.00240 N

Our results show that reciprocal displacement of ions under dynamic conditions, when the concentrations of the ions are comparable, is entirely determined by the laws of adsorption dynamics – by the conditions for the formation of sharp boundaries between the ion zones.

SUMMARY

1. It is shown that the sequence of the components in ion exchange chromatography involving ions of different valencies may change with changes in the concentration of the solution entering the column.

2. It is shown that the sequence of the ions in the column is determined by the conditions for formation of sharp ion zone boundaries.

Institute of High Molecular
Compounds, Leningrad

Received
February 9, 1957

LITERATURE CITED

[1] G. V. Samshonov, Proc. Acad. Sci. USSR, 97, 707 1954.

[2] G. V. Samsonov, in Symposium: "Chromatography" (Leningrad State Univ. Press 1956) p. 22.

[3] L. S. Aleksandrova, T. B. Gapon, N. V. Filatova, and K. V. Chmutov, Trans. Commission Anal. Chem., vol. 6 (9), 235 1955.

[4] O. Samuelson, Ion Exchangers in Analytical Chemistry (IL, 1955) p. 57.

[5] A. M. Trofimov, in Symposium: "Chromatography" (Leningrad State Univ. Press 1956) p. 15.

[6] G. V. Samsonov, S. F. Lavrentyeva, and M. P. Shesterikova, Antibiotics, No. 2 1957.

[7] T. R. Kressman, J. A. Kitscher, J. Chem. Soc. 1949, 1208.

[8] S. M. Partridge, R. C. Brimleg, Biochem. J. 44, 513 1949; S. M. Partridge, R. G. Westall, Biochem. J. 44, 418 1949.

[9] C. W. Davies, Biochem. J. 45, 38 1949.

[10] S. Yu. Elovich, Proc. Acad. Sci. USSR, 101, 293 1955.

[11] S. Yu. Elovich and L. T. Kuzmina, Colloid J., 18, 268 1956.*

---

* Original Russian pagination. See C. B. translation.

INVESTIGATION OF THE STRUCTURE OF BRANCHED POLYSTYRENE BY THE LIGHT SCATTERING METHOD

I.G. Soboleva, N.V. Makletsova and S.S. Medvedev

It was shown in the previous paper [1] that the root mean square distance h between the chain ends, when the second virial coefficient is zero, is independent of the chemical nature of the solvent and is therefore a characteristic parameter of the polymer structure. This is in agreement with views on the configuration of polymer molecules in various solvents, based on the statistical physics of polymer molecules [2, 4]. On the basis of these views it seems likely that the most promising approach to evaluation of polymer chain structure is by studies of the behavior of the polymer molecules near the precipitation point.

The purpose of the present investigation was to establish the possibility, by using polystyrene of known degree of branching, of evaluating molecular chain structure from the absolute magnitude of the polymer molecules dissolved in different media.

Radical polymerization of styrene does not result in appreciable branching of the polymer, owing to the low rate of chain transfer to the polymer [5]. Branched polystyrene was prepared by photopolymerization of styrene in presence of a narrow fraction of brominated polystyrene of high molecular weight (graft polymerization). The active centers formed in the chain as the result of bromine removal serve as origins of side chain growth [6]. This was accompanied by polymerization of styrene, initiated by bromine atoms. The average length of the side chains formed could be deduced from the average molecular weight of this polymer.

The graft polymerization was carried out in benzene solution at 40°. The amount of brominated polystyrene added (containing 1.5-3.5% bromine) was 15% on the monomer; the initial concentration of the polymer in the reaction mixture was 7-9%. The irradiation was by means of ultraviolet light of wave length 3600 A and over; the irradiation intensity, determined by means of a uranyl oxalate actinometer, was $1.4 \cdot 10^{-8}$ einstein/sec.

Control experiments in absence of monomer showed that under such conditions only slight changes take place in the molecular characteristics of the original brominated polystyrene, indicating that the reaction of recombination of the polymer radicals formed by removal of bromine atoms has little effect. However, in presence of monomer, owing to the formation of growing polymer radicals, the probability of their recombination increases. The degree of branching cannot therefore be conclusively estimated from molecular weight data. To estimate the degree of branching of polystyrene, graft polymerization was carried out with styrene containing radioactive carbon.

Tagged styrene was prepared from ethyl alcohol containing C^{14} and benzene, by the following scheme: ethyl alcohol ⟶ ethylene; ethylene + benzene ⟶ ethylbenzene ⟶ styrene. The degree of branching of the graft polymers was calculated from the results of determinations of the radioactivity of narrow fractions of the graft polymers relative to the activity of polystyrene synthesized from tagged monomer without any additions. Isolation of the narrow fractions, not contamined with low molecular radioactive polymer, was carried out by precipitation with methyl alcohol from 0.25% solution, with subsequent fractionation from 0.1% solution. The fractions so obtained were reprecipitated from 0.05% solution. Table 1 gives the results of determinations for polymer P23, prepared by graft polymerization with linear brominated polystyrene L2 containing 3.5% bromine.

The molecular weight and molecular size determinations were carried out by the light scattering method with apparatus in which the determinations could be made at three angles [7]. The calculations were done by

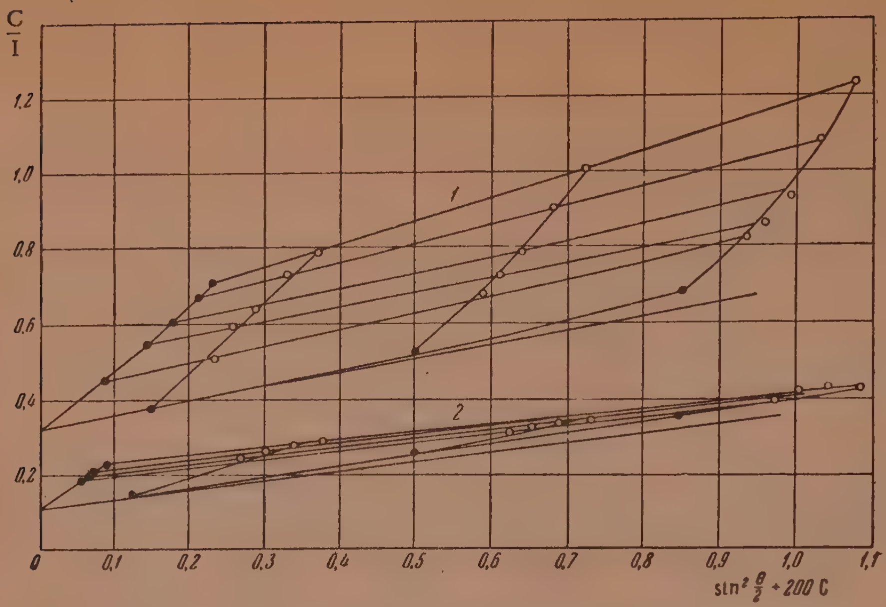

Fig. 1. Graphical determination of molecular weight and molecular size of L-1 polystyrene from light scattering data; 1) in toluene; 2) in cyclohexane; ordinate to double scale; arbitrary constant, 1.33.

TABLE 1

Relative Radioactivity and Degree of Branching of P23 Polystyrene Fractions

Fractions	Molecular wt. $M \cdot 10^{-3}$ by light scattering	Number of pulses per 3 minutes	Relative radioactivity	Wt. of branches in molecule × $\times 10^{-3}$	Number of branches per molecule
1					
2	6100	2227	0.372	2270	27.7
3	4350	1352	0.225	980	13.1
4	3250	1049	0.175	569	7.6
5	2500	1122	0.187	468	6.2
6	1600	1137	0.189	303	4.0
7	950	1832	0.305	—	—
8	620	3743	0.625	—	—
9	360	5092	0.850	—	—
10*	75	5323	0.887	—	—
Standard**	—	6000	1.000		

---

* Molecular weight determined from osmotic data.

** Polystyrene synthesized from tagged monomer.

TABLE 2

Effect of Bromine Content on the Molecular Size of Brominated Polystyrene in Solution

Bromine content of polystyrene, %	Mol. wt. $M \cdot 10^{-3}$	$h_T/M^{1/2}$* in toluene	Bromine content of polystyrene %	Mol. wt. $M \cdot 10^{-3}$	$h_T/M^{1/2}$* in toluene
0	1820	0.91	2.0	460	0.94
0	1500	0.95	3.0	1130	1.00
0	1070	0.98	5.5	1560	0.68
2.0	1060	0.93	5.5	715	0.65

---

* h_T is the root mean square distance between the chain ends.

Zimm's method [8] with approximate extrapolation to zero concentration and zero angle. The calculated data for the linear polymers did not differ from data calculated by Debye's method from the scattering asymmetry [9]. The data for the branched polymers were somewhat lower. The measurements were performed in toluene at room temperature and in cyclohexane at a temperature 3° above the precipitation point. The measurement temperature was 30-35°, depending on the molecular weight. The second virial coefficient in the osmotic pressure equation for solutions in cyclohexane was close to zero. Fig. 1 shows an example of a graphical determination of molecular weight and molecular size from light scattering data at three angles.

The intrinsic viscosity was measured in toluene, methyl ethyl ketone, and cyclohexane at the temperatures of the light scattering determinations. In order to determine the influence of molecular chain structure on the configuration of the molecules in solution, it was necessary to find the extent of the influence of the bromine present in the macromolecule on the molecular size. Table 2 gives the molecular parameters of polystyrene with different bromine contents.

TABLE 3

Molecular Characteristics of Linear and Branched Polystyrenes, Based on Light Scattering Data

Polymer	Mol. wt. $M\cdot10^{-3}$	Number of branches per 3500 monomer units of principal chain	Root mean square distance between chain ends, Å in toluene $[\eta]_T$	in cyclohexane $[\eta]_{ch}$	$\frac{h_T}{M^{1/2}}$	$\frac{h_0}{M^{1/2}}$	Second virial coefficient in toluene $B\cdot10^4$
L-1	1900	0	1900	810	0.94	0.59	1.9
L-2	1150	0	1150	670	0.92	0.64	3.6
P1-1	2400	0.5	1240	920	0.80	0.59	2.8
P2-1	2600	1.1	1200	720	0.74	0.45	3.2
P23-1	6100	3.0	1920	1130	0.78	0.46	1.2
P23-2	4350	1.3	1770	840	0.83	0.40	1.8
P23-3	3250	1.0	1300	860	0.72	0.47	1.9
P23-5	2500	1.1	1180	630	0.75	0.40	1.9
P23-6	1600	1.1	1030	570	0.82	0.45	5.0

TABLE 4

Intrinsic Viscosities of Linear and Branched Polystyrenes

Polymer	Mol. wt. $M\cdot10^{-3}$	Branches / 3500 units of chain	Intrinsic viscosity $[\eta]\frac{100\text{ ml}}{\text{g}}$			$\frac{(M\,[\eta])^{1/3}}{M^{1/2}}$		
			in toluene $[\eta]_T$	in methyl ethyl ketone $[\eta]_{mek}$	in cyclohexane $[\eta]_{ch}$	in toluene	in methyl ethyl ketone	in cyclohexane
L-1	1900	0	5.0	3.1	1.8	1.53	1.31	1.09
L-2	1150	0	4.0	2.2	1.1	1.55	1.27	1.02
P1-1	2400	0.5	4.6	—	1.4	1.44	—	0.97
P2-1	2600	1.0	4.0	2.3	1.45	1.36	1.11	0.960
P23-1	6100	3	7.0	3.8	1.70	1.43	1.16	0.90
P23-2	4350	1.3	4.5	—	—	1.29	—	—
P23-3	3250	1.0	3.9	2.5	1.5	1.295	1.12	0.94
P23-5	2500	1.1	3.4	—	1.3	1.29	—	0.93
P23-6	1600	1.1	2.65	—	1.0	1.28	—	0.92

It follows from Table 2 that an increase of the density of globularly coiled molecules is found at ~ 5% bromine content; lower contents of bromine do not affect the molecular configuration of polystyrene in solution. Therefore, with a total bromine content not greater than 3.5% in the polymers studied, small fluctuations of the bromine content as the result of partial removal in the course of photopolymerization could not influence the results of the molecular size determinations.

Table 3 contains the results of nephelometric determinations of the molecular characteristics of linear polystyrene fractions L-1 (the starting polymer used for preparation of brominated polystyrene L-2), L-2 (the starting polymer used for preparation of graft polymers P2 and P23), and branched polymers: the first fractions of polymers P1 and P2, and six fractions of polymer P23. The following three fractions of polymer P 23 were not investigated, as they were contaminated with low molecular radioactive polymer.

Examination of the data in Table 3 indicates that the parameter $h/M^{1/2}$ decreases with molecular chain branching by a factor of about 1.2 in a good solvent, and by 1.5 near the precipitation point. Further increase of the degree of branching of the polystyrene molecules could not be achieved, as increase of the bromine content led to structurization of the polymer. Jones et al. [6], in order to avoid gel formation in the synthesis of branched polystyrene, used carbon tetrachloride in graft polymerization; the rate of chain transfer to the polymer is then fairly high and indefinite amounts of chlorine were thereby introduced into the molecular chains. Naturally this made it difficult to draw conclusions concerning the influence of branching on the molecular configuration in solution.

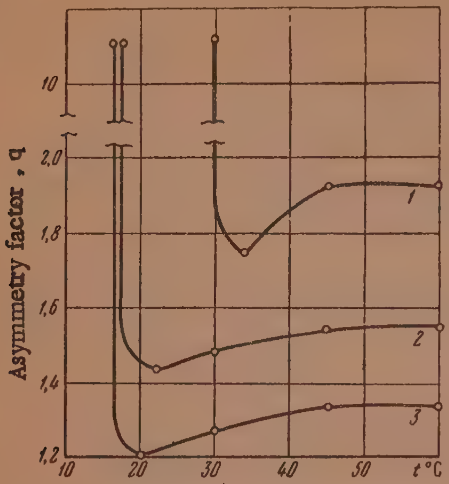

Fig. 2. Precipitation temperatures of polystyrenes with different chain structure. Solvent: toluene + 29 ml/100 ml of methyl alcohol; polymer concentration 0.02 g/100 ml; 1) linear polystyrene, $M = 3 \cdot 10^6$; 2) branched polystyrene P2 = 1, $M = 2,6 \cdot 10^6$; 3) linear polystyrene L-2, $M = 1.15 \cdot 10^6$

The viscosimetric results are given in Table 4. The ratio of $(M[\eta])^{1/3}$, proportional to the size of the molecules in solution [2], to the root of the molecular weight, like the parameter $h/M^{1/2}$, decreases with increasing chain branching. The ratio in cyclohexane decreases somewhat less, as compared with the light scattering data.

It is seen that the second virial coefficients for branched polymers in toluene solutions are somewhat higher than for linear polymers (see Table 3). A comparison of the precipitation points of linear and branched polystyrenes from toluene solutions on addition of methyl alcohol also showed that the branched polystyrene is precipitated at lower temperatures (see Fig. 2). This is understandable if it is taken into account that cross linkage points and free chain ends influence entropy changes in opposite directions.

SUMMARY

1. Branched polystyrene was synthesized by grafting of side chains containing radioactive carbon C^{14} on brominated linear polystyrene.

2. The molecular size of the branched polystyrenes in solution is less than that of linear polymers. The changes in molecular size are more prominent near the precipitation point of the polymer.

3. Viscosimetric data are in agreement with light scattering data, confirming the validity of the Flory equation for the relationship between the size of polymer molecules and the intrinsic viscosity.

The L. Y. Karpov Physicochemical Scientific
Research Institute

Received July 2, 1956.

LITERATURE CITED

[1] I. G. Soboleva, N. V. Makletsova, and S. S. Medvedev, Proc. Acad. Sci. USSR, 106, No. 2, 303 1956.

[2] P. Flory, T. Fox, J. Am. Chem. Soc. 73, 1904 1951.

[3] M. V. Volkenshtein and O. B. Ptitsyn, Progr. Phys. Sci. 4, No. 4, 501 1953.

[4] O. B. Ptitsyn, J. Phys. Chem., 29, No. 2, 396 1955.

[5] J. C. Bevington, G. M. Guzman, H. W. Melville, Proc. Roy. Soc. 221, 453 1954.

[6] M. H. Jones, H. W. Melville, W.J.P. Robertson, Nature 174, 78, 1954.

[7] I. G. Soboleva, Inst. Tech. Econ. Inf. Acad. Sci. USSR, Instruments and Stands, Theme 8, No. 2, pp. 56-449 1956.

[8] B. Zimm, J. Chem. Phys., 16, 1099 1948.

[9] N. Z. Fattakhov, V. N. Tsvetkov, and O. V. Kallistov, J. Exp. Theoret. Phys., 26, No. 3, 345 1954.

THE EFFECT OF PLASTICIZERS ON THE HYDROGEN PERMEABILITY OF POLYVINYL CHLORIDE

S.I. Sokolov, S.A. Reitlinger and R.I. Feldman

Addition of plasticizers to high polymers weakesn intermolecular bonds, with a consequent lowering of the potential barriers which restrict flexibility, and a decrease of steric obstacles to the relative displacement of the segments of the polymer chains [1-3]. It follows from this that the structural changes caused by plasticizers should lead to an increase in the gas permeability of polymer systems [4]. In fact, it has been shown in earlier investigations that plasticization results in an increase of polymer permeability [5, 6] and in changes of the permeability activation energy [7]. However, the available data mainly refer to plasticized polymers in the high elastic state.

Investigations of the gas and vapor permeability of films in the temperature range covering the transition from the glassy to the high elastic state [8-10] have shown that the transition is accompanied by changes in the relationships between the temperature and the permeability and diffusion constants. Studies of the gas permeability of plasticized polymers, in different states of aggregation according to the plasticizer content, are of definite interest. In the present investigation the hydrogen permeability of polyvinyl chloride films has been studied over a wide range of plasticizer concentrations, covering all the states from the glassy to the viscofluid.

The hydrogen permeability (P) was determined by means of a thermostatically controlled Daynes-Shakespeare apparatus [5]. The gas pressures on both sides of the films were kept equal during the tests. The diffusion constants (D) were determined by the "lag" method, and the solubility constants (σ) were calculated from the values found for P and D [4]. The hydrogen used for the tests contained 99.8% H_2.

The films were made from polyvinyl chloride prepared by emulsion polymerization and extracted with alcohol, with molecular weight $6.2 \cdot 10^4$. The film specimens, in the form of circles ~0.5 mm thick and 80 mm in diameter, were made by hot pressing between sheets of aluminum foil in a hydraulic press. For films with high plasticizer contents, the polyvinyl chloride was dissolved by warming in the plasticizer, and a film was cast from the solution on silk gauze as a support.

The gas permeability constants were expressed in cubic centimeters (at 0° and 760 mm Hg) of gas which passed through a film 1 cm^2 in area and 1 cm thick per second, with a pressure drop of 1 atmosphere / cm^2. sec. $^{-1}$. atm. $^{-1}$/; the diffusion constants were expressed in cm^2. sec. $^{-1}$, and the solubility constants in cc (at 0° and 760 mm Hg) of gas dissolved in 1 cc of the polymer under a pressure of 1 atmosphere [atm.$^{-1}$].

Fig. 1 shows variations of the hydrogen permeability of plasticized polyvinyl chloride with dimethyl phthalate content. The plasticizer concentration is expressed in mole fractions; the molecular weight of the polymeric component is taken as 62.5, the weight of one monomer unit in the polyvinyl chloride molecule. The curve has three characteristic regions, corresponding to the known thermomechanical states: the glassy, high elastic, and viscofluid states of amorphous polymers [11]. The greatest increase of gas permeability with plasticizer content in the polymer ($\Delta P/\Delta N_2$) is found in the high elastic state. The transition of polyvinyl chloride from the glassy into the high elastic state occurs at a ratio of 1:12 – 1 : 14 dimethyl phthalate molecules to polyvinyl chloride monomer units, and the transition from the high elastic to the viscofluid state at a ratio of 1:3 – 1:4; this approximately corresponds to the ratios found in mechanical tests.

The gas permeability constant of plasticized polyvinyl chloride (P_{pp}) in the region of high elasticity can be approximately expressed, like the relationship for the mechanical characteristics [12], in terms of the gas permeability constants of the polymer (P_p) and plasticizer (P_{pl}) present in the same state in the mixture

$$P_{pp} = P_{p}^{N_1} \cdot P_{pl}^{N_2}$$

where N_1 and N_2 are the respective mole fractions of polymer and plasticizer in the system, such that $N_1 + N_2 = 1$. The values of P_p and P_{pl} calculated by means of this equation are given in the Table.

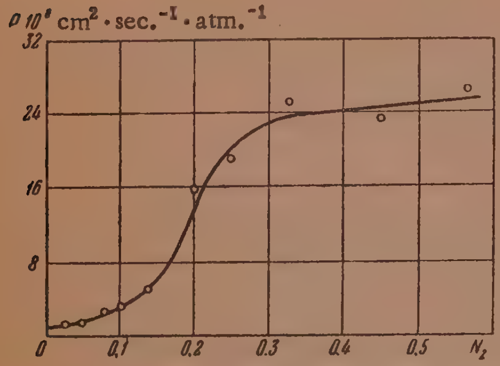

Fig. 1. Variation of the constant P with mole fraction of dimethyl phthalate N_2 in the binary system polyvinyl chloride – dimethyl phthalate at 20°.

Fig. 2 shows the results found for the constants P, D, and σ for hydrogen and polyvinyl chloride with dibutyl phthalate plasticizer. In the transition from the glassy to the high elastic state the ratio $\Delta D / \Delta N$ increases, while the solubility of hydrogen changes only slightly.

Fig. 3 shows variations of the logarithm of the permeability constant for plasticized polyvinyl chloride with contents of phthalate ester plasticizers.

The data obtained on the hydrogen permeability of films are of great interest, as they make it possible to regard gas permeability determination as a method for studying the states of aggregation of polymers [13] and variations of them under the action of plasticizers.

Plots of the gas permeability – composition relationship, if the composition of the mixture is expressed in mole fractions [14] give a clear picture of differences in the states of aggregations, which is evidence of the homogeneity of the systems in question. Essentially we are dealing with ternary systems: polymer-plasticizer-hydrogen. However, in view of the low solubility of hydrogen and of the constant permeation conditions (pressure and temperature), they may be regarded as binary polymer-plasticizer systems.

Calculated Values of P_p and P_{pl} for Polymer-Plasticizer Mixtures in the High Elastic State

Plasticizer	P_p	P_{pl}	$d \log P_{pp}/dN_2$
Dimethyl phthalate	$0.73 \cdot 10^{-8}$	$6.05 \cdot 10^{-3}$	6.00
Diethyl phthalate	$0.76 \cdot 10^{-8}$	$5.76 \cdot 10^{-1}$	7.88
Dibutyl phthalate	$0.79 \cdot 10^{-8}$	$1.86 \cdot 10^{-1}$	9.39
Diamyl phthalate	$0.75 \cdot 10^{-8}$	$1.61 \cdot 10^{3}$	11.33
Dioctyl phthalate	$0.76 \cdot 10^{-8}$	$8.52 \cdot 10^{4}$	13.05

In a binary mixture the distinction between solvent and solute is to some extent arbitrary. However, it is more rational to regard as the solvent the component which determines the state of aggregation of the mixture. If, for example, when a large amount of a crystalline substance is dissolved in a small amount of liquid a liquid solution is obtained, the second, liquid component should be regarded as the solvent. In the present instance before a mixture in the viscofluid state is obtained it is more correct to regard the polymer and not the plasticizer as the solvent.

On the other hand, after the mixture has been formed, both the components can be regarded as existing in the same state of aggregation as the mixture. The hydrogen dissolved in the mixture should be considered as being in the liquid state, despite the fact that the temperature of the mixture is considerably above its critical temperature. This may be extended to any state of aggregation, for example, the state of high elasticity [12]. Thus, both the plasticizer and the hydrogen dissolved in the mixture should be considered as if existing in the high elastic state, like the system as a whole. It follows that the values obtained by extrapolation for the pure components in the high elastic state cannot be compared with the properties which they have if taken in pure form, but not in the same state as the mixture.

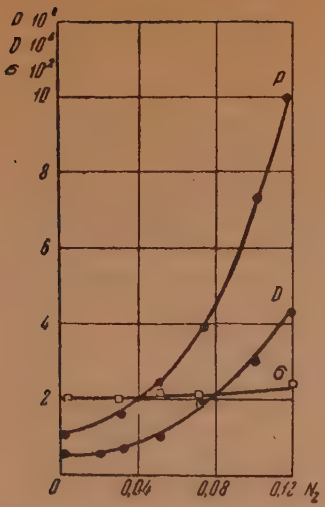

Fig. 2. Variations of the constants P, D, and σ with mole fraction of dibutyl phthalate in a system containing polyvinyl chloride, at 20°.

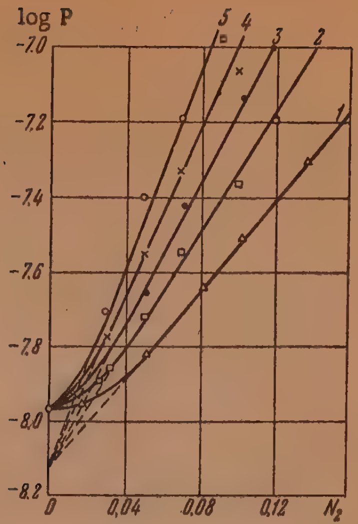

Fig. 3. Variations of the logarithm of the permeability constant for polyvynyl chloride with mole fractions of plasticizers at 20°: 1) dimethyl phthalate; 2) diethyl phthalate; 3) dibutyl phthalate; 4) diamyl phthalate; 5) dioctyl phthalate.

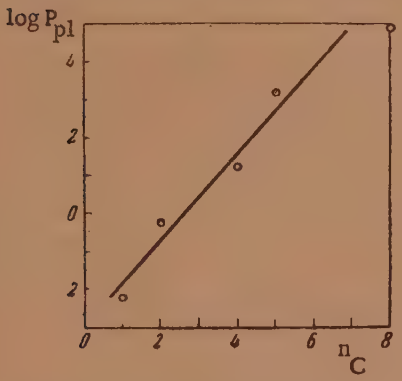

Fig. 4. Variation of the logarithms of the limiting permeabilities P_{pl} of plasticizers with n_C (n is the number of C atoms in the alkyl groups of the phthalate esters).

The large differences between the values of P_{pl} found by extrapolation for different plasticizers in the high elastic state do not correspond to the intrinsic properties of the pure plasticizers, but to the effects which they have in changing the properties of the system in the given state of aggregation. The limiting values of $P_{pl}^{N_2=1}$, found for the pure plasticizers by extrapolation, are characteristic constants, and, as Fig. 4 shows, their logarithms are a linear function of the number of carbon atoms in the alkyl groups of the phthalate esters used as plasticizers for polyvinyl chloride.

The results obtained show that additions of plasticizers to polyvinyl chloride influence the gas permeability to different extents, according to the state of aggregation of the polymer. Additions of plasticizer to the polyvinyl chloride in amounts which do not alter the glassy state have little influence on gas permeability, as the plasticizer molecules, becoming bound with individual groups along the chain, do not induce chain flexibility.

The hydrogen permeability of unplasticized polyvinyl chloride, determined experimentally at 20° (Fig. 3), is $1.06 \cdot 10^{-8}$ cm. sec.$^{-1}$, atm.$^{-1}$, as distinct from the corresponding average value $0.75 \cdot 10^{-8}$ found by extrapolation of the linear region of the plot to the ordinate axis. This discrepancy may be caused by fixation of the polymer structure at its glass transition temperature.

In the high elastic state the plasticizer molecules separate the polymer chains, with a consequent lowering of the potential barriers of chain rotation, favoring an increase of the gas permeability. It may be assumed that the action of plasticizer molecules is not confined only to interaction with polar groups, but affects a wider region of the polymer chains. Finally, in the viscofluid state an increase of the plasticizer content does not produce any significant changes in the intermolecular forces, as the separation of the chain molecules of polyvinyl chloride is largely complete. Accordingly, the viscofluid state is characterized by only a slow increase of the gas permeability of the films on addition of plasticizer.

SUMMARY

1. The rate of the increase of gas permeability of polyvinyl chloride on addition of plasticizers depend on the state of aggregation of the plasticized polymer. Additions of plasticizer within the limits of the glassy or viscofluid states of the plasticized polyvinyl chloride have no significant influence on the gas permeability, whereas in the region of high elasticity, the gas permeability increases rapidly with the plasticizer content.

2. The gas permeability of plasticized polyvinyl chloride in the high elastic state is a regular function of the mole fraction of plasticizer, similar to that found earlier for mechanical properties. The constant $P_{pl}^{N_2=1}$ which characterizes the effect of a given phthalate plasticizer, depends on the number of carbon atoms in the alkyl group of the ester.

The Moscow Technological Institute for the
Light Industries

Received November 3, 1956.

LITERATURE CITED

[1] V. A. Kargin and Yu. M. Malinsky, Proc. Acad. Sci. USSR, 73, 967 1950.

[2] P. V. Kozlov and E, F. Russkova, High Molecular Compounds, 12, 44 1952.

[3] S. I. Sokolov and R. I. Feldman, Investigations of High Molecular Compounds (Izd. AN SSSR, 1949) p. 329.

[4] S. A. Reitlinger, Progr. Chem., 20, 213 1951.

[5] S. A. Reitlinger, and L. A. Panyunina, J. Appl. Chem., 12, 886 1939.

[6] D. W. Brubaker, K. Kommermeyer, Ind. Eng. Chem. 45, 1148 1953.

[7] P. M. Doty, J. Chem. Phys. 14, 244 1946.

[8] P. Meors., J. Am. Chem. Soc. 76, 3415 1954.

[9] S. N. Zhurkov and G. Ya. Ryskin, J. Tech. Phys., 24, 797 1954.

[10] G. Ya. Ryskin, J. Tech. Phys., 24, 797 1954.

[11] V. A. Kargin and T. I. Sogolova, J. Phys. Chem., 23, 530 1949.

[12] R. I. Feldman, Proc. Acad. Sci. USSR, 97, 1033 (1954).

[13] R. I. Feldman and S. I. Sokolov, Chemistry and Physical Chemistry of High Molecular Compounds (Izd. AN SSSR, 1952) p. 159.

[14] S. I. Sokolov and R. I. Feldman, Summaries of Papers at the 3rd All-Union Conference on Physico-chemical Analysis (Izd. AN SSSR 1955) p. 160.

SPECIFIC HEATS OF AQUEOUS SOLUTIONS OF SOME SOAPS

V.I. Solnyshkin

The question of the micellar structure of colloidal soap solutions is of great theoretical significance, as definite conclusions cannot be drawn from the investigations which have been carried out in this field. Clearly defined association of molecules into micelles is observed at different concentrations of fatty acid salts.

The concentration region in which micelle formation takes place in aqueous soap solutions has been termed the "critical concentration of micelle formation" [1], below which soaps are in the ionic state, while above it colloidal solutions are formed. The work of Davies [2] on potassium n-caprylate solutions showed that measurements of the specific heats of such systems can provide additional information on micelle formation.

It was first shown by M. Fischer [3] that, in very dilute aqueous solutions, sodium salts of fatty acids are completely dissociated. Powney and Jordan [4], in a study of the hydrolysis of the salts of various fatty acids, discovered the existence of a minimum and a maximum at concentrations of the order 10^{-4} - 10^{-5} mole/liter. However, the suggested interpretation did not explain the changes in the minimum values of hydrolysis [4,5] with increasing temperature. Flockhart and and Graham [6] studied electrical conductivity and viscosity of sodium oleate solutions, and discovered sharp changes in the curves in this region. They cast doubt on the hypothesis that micelles are formed from the fatty acid molecules formed by hydrolysis of soaps, but did not examine the question in detail. The existence of aggregates of soap molecules at low concentrations is still a subject of controversy.

Hartley [1] stated that below "the critical concentration of micelle formation sodium salts of fatty acids behave like strong electrolytes" (Fig. 1, a). McBain [7] postulated the formation of ionic micelles in very dilute solutions until this concentration is reached. Ekwall discovered the existence of flat regions in electrical conductivity – concentration curves for sodium myristate solutions, while Hartley [1] postulated that this form of the conductivity curves is caused by micelle formation in the concentration region corresponding to the plateau.

It is difficult to believe that at normal temperatures the ions of a dissociated fatty acid soap, hydrated by associated water molecules and undergoing Brownian movement, can form aggregates. If this was the case, the Van-der Waals forces of the CH_2 groups would not be able to maintain such formations in equilibrium with the medium. The situation may change if the ions associate into molecules. The sharply decreasing degree of hydration would favor aggregation. Ekwall [5] and Steinsby and Alexander [8] showed that the observed changes on the hydrolysis curve [4] take place if molecular association occurs. They assumed that mixed micelles of fatty acid molecules and soap ions are formed. However, it is difficult to account for the hydrolysis minimum on this theory. If mixed micelles are formed, sodium ions remain in solution and a hydrolysis minimum cannot occur, as alkalies are completely dissociated in dilute solutions. The degree of hydrolysis corresponding to the minimum on the curve coincides with the degree of hydrolysis at high concentrations, which suggests that nonionic soap molecules are formed (Fig. 1, b). Further autoflocculation [9] of these (Fig. 1, c) leads to a sharp decrease in the concentration of soap in true solution, which naturally increases the degree of hydrolysis. The minimum value, according to the data of various authors, corresponds to the following concentrations:

Ulman [10]..........	$0.986 \cdot 10^{-3}$ M
Powney and Jordan [4]...	$0.1 \cdot 10^{-4}$ M
Flockhart and Graham [6]	$0.9 \cdot 10^{-3}$ M

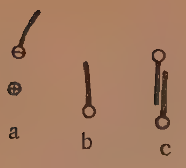

Fig. 1.

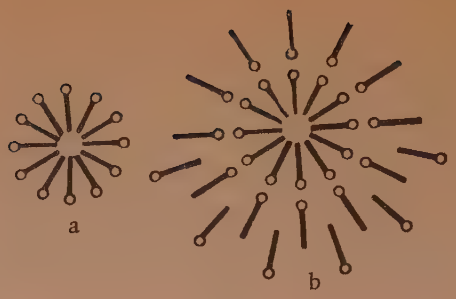

Fig. 2

However, the autoflucculated molecules are unstable and at a concentration of $1.5 \cdot 10^{-3}$ M, as indicated by the maximum on the viscosity curve for sodium oleate solutions [6], they may pass into a more stable form, which balances the van der Waals forces and confers stability to such "nuclei" in Brownian movement (Fig. 2,a). The greater the stability of such an aggregate, the higher is the degree of hydrolysis to which the maximum on the curve corresponds. The stability depends on the number of CH_2 groups in the molecular chain. The longer the molecule, the more stable is the nucleus formed and the lower is the concentration of soap in true solution. This explanation is supported by data on the hydrolysis of sodium oleate, laurate, myristate, palmitate, and stearate, as the maximum on the hydrolysis curve increases with increasing molecular length [4]. The position of the minimum on the hydrolysis curve does not remain constant with change of temperature; above 40° autoflocculates of two or three molecules may be formed, with the fatty acid playing an active role. Transition to the stable form, both at high and at normal temperatures, is associated with formation of aggregates from nonionic molecules which form layers around themselves and become the classical spherical associated micelles (Fig. 2,b).

Viscosity, electrical conductivity, and hydrolysis curves [4, 6] show that formation of initial nuclei in sodium oleate solutions at normal temperature is completed between $2.5 \cdot 10^{-3}$ and $3.0 \cdot 10^{-3}$ M. It is evident that the plateau on the conductivity curve is caused by dissociation of soap molecules together with their aggregation into autoflocculates, and hydrolysis of the soap only falls to low values again after the concentration has been reached at which nucleus formation is complete. Additions of oleic acid and caustic soda to the solutions during the determinations also indicate the predominant formation of nonionic molecules of sodium oleate. Addition of oleic acid leads to disappearance of the plateau on the conductivity curve, whereas caustic soda does not influence its course. It is evident that more nonionic molecules are formed in the first case, leading to a decrease in the degree of hydrolysis of the soap; little change in it is produced by addition of alkali.

For the specific heat determinations, sodium oleate and ricinoleate prepared by the Powney and Jordan method [4] in the form of dry neutral powders were dissolved in distilled water ($\kappa = 3.0 - 4.0 \cdot 10^{-6}$ ohm^{-1}.cm^{-1}) and then heated to 90-95°. The homogeneous solutions were cooled and analyzed by titration with 0.1 N HCl with phenolphthalein indicator [11].

The specific heats of the solutions were determined in a water-cooled adiabatic calorimeter at 20°. The heat capacity of the metallic parts of the inner calorimeter was $K_M = 47.8$ cal./deg. The specific heat was calculated by the formula:

$$c = \frac{191131\, Rg^2/\tau\Delta t - K_M}{S} \frac{\text{cal}}{\text{g}\cdot{}^\circ\text{C}},$$

where R is the resistance of the heater in ohms (8.783Ω); g is the weight of silver deposited in the platinum basin, in g; τ is the time during which the current was passed, in seconds; Δt is the difference between the thermometer readings before and after passage of the current, in deg; s is the weight of the solution in grams.

The most reproducible results under our conditions were obtained at current strengths of 0.2-0.3 amp. The results are given in Figs. 3 and 4.

In both cases a plateau is found on the specific heat curves. For sodium oleate solutions the specific heat remains constant at concentrations between 0.25 and 0.65 M, and for sodium ricinoleate the corresponding region lies between 2.25 and 2.85 M.

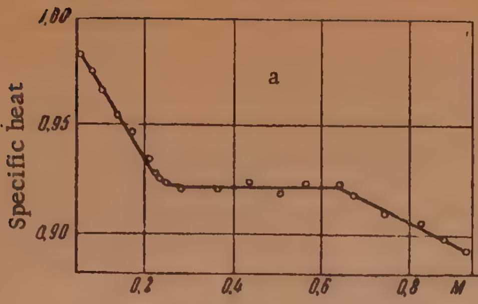

Fig. 3. Variation of specific heats of sodium oleate solutions with the molar concentration.

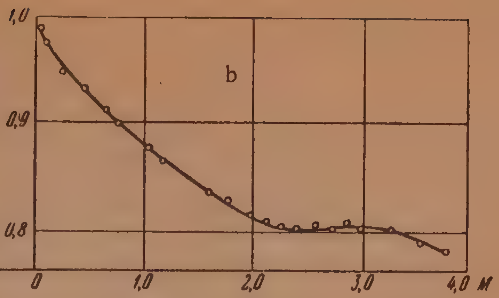

Fig. 4. Variation of specific heats of sodium ricinoleate solutions with the molar concentration.

Further growth of the nuclei into micelles does not influence the steady increase of viscosity or decrease of specific heat, but at a concentration of 8 g / 100 ml or 0.26 M of sodium oleate [12], or at 0.25 M according to our determinations, the rate of change of the specific heat with concentration decreases sharply. At these concentrations formation of asymmetric micelles of the lamellar type begins (Fig. 5). The plateaus on the specific heat curves, first discovered by Davies for potassium caprylate solutions [2], and the plateaus on the conductivity curves in dilute solutions, are caused by the characteristics of micellar growth. The spherical micelles have all their degrees of freedom, and the specific heat of the solution decreases as the result of the increase in their size and numbers. Formation of the cylindrical form disturbs the thermodynamic equilibrium of the micellar motion, leading to vigorous rotation of the spherical micelles. This transition keeps the specific heat of the solution practically constant.

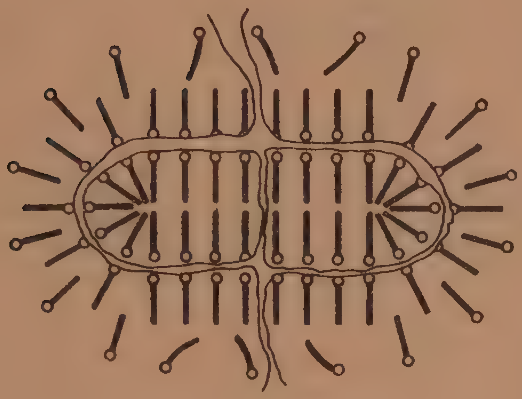

Fig. 5.

At concentrations above 0.65 M, when the transition to cylindrical micelles is complete, the formation of long micellar entanglements, causing gelation of the solution, can be postulated; the number of these increases with concentration, and in highly concentrated solutions soap crystals begin to form, consisting of oriented layers of soap molecules separated by interlayers of water. The final hydrated form of sodium oleate corresponds to the formula $NaOl \cdot 2H_2O$ [13].

In solutions of sodium ricinoleate the analogous, thermodynamically reversible process of micelle formation is shifted into the region of higher concentrations owing to the presence of a hydroxyl group in the molecular chain.

SUMMARY

1. The specific heats of aqueous solutions of sodium oleate and ricinoleate have been measured over a wide range of concentrations; plateaus have been found on the specific heat curves (Davies plateaus) in the concentration ranges from 0.25 to 0.65 M for sodium oleate solutions and from 2.25 to 2.85 M for sodium ricinoleate solutions.

2. Literature data and the experimental results are used to show the possible transition of sodium salts of fatty acids from the ionic state to the hydrated crystalline form through colloidal solutions.

Mining Institute
Academy of Sciences USSR
Beneficiation Division

Received October 12, 1956.

LITERATURE CITED

[1] G. S. Hartley, Aqueous Solutions of Paraffin-Chain Salts (Paris, 1936).

[2] D. S. Davies, J. Chem. Soc., 551 1933.

[3] M. H. Fischer, Soaps and Proteins (Moscow, 1932).

[4] I. Powney, D. O. Jordan Trans. Faraday. Soc. 34, 363 1938.

[5] P. Ekwall, Koll. Z. 101, 135 1942; Z. phys. Chem. A161, 195 1932.

[6] B. D. Flockhart, H. Graham, J. Coll. Sci. 8, 105 1953.

[7] M. N. Fineman, I. W. McBain, J. Phys. Coll. Chem. 52, 881 1948.

[8] G. Steinsby, A.E. Alexander, Trans. Faraday Soc. 45, 585 1949.

[9] B. V. Mokievsky and P. A. Rebinder, Proc. Acad. Sci. USSR, 26, 46 1940.

[10] M. Ulman, Z. phys. Chem. A182, 18 1938.

[11] I. V. Egorov, Technical Analysis (Kiev, 1926).

[12] Z. N. Markina, K. A. Pospelova, and P. A. Rebinder, Proc. Acad. Sci. USSR, 99, 121 1954.

[13] A. V. Dumansky, V. I. Solnyshkin, and P. A. Demchenko, Ukrain. Chem. J., 20, 635 1954.

LIGHT ~~SCATTERING~~ BY ~~A~~ COAGULATING AEROSOLS

O.M. Todes and A.A.Chekunov

In many investigations of the scattering of light by suspended particles [1-3] this effect has been considered mainly with reference to monodisperse aerosol systems. It is known, however, that real mists, clouds, smokes, and similar systems consist of particles of different sizes; i.e., they are polydisperse. Moreover, because of sedimenation and other processes, the particle size distribution in these systems varies continuously with time. Because of these changes the optical properties of the systems also vary and these variations may be used to study the nature of the processes taking place in aerosol systems.

The literature contains solutions of particular problems on light scattering in polydisperse aerosol systems with definite particle size distributions. This problem was solved from the meteorological aspect by Foitzik [4], and it is presented in detail in Kondratyev's monograph [5]. Foitzik assumed a Gaussian particle size distribution in clouds and mists, introduced certain empirical constants, and calculated light scattering curves. Comparison of these curves with light scattering curves for monodisperse aerosols shows significant differences. In particular, the relationship between the scattering coefficient and the average particle size is of a more complex character, while the scattering coefficients themselves can exceed the corresponding values calculated for ideal monodisperse systems.

Scattering by rain droplets of different sizes has recently been studied by Polyakova and Shifrin [6]; they assumed an empirical particle size distribution of the rain droplets, in the form

$$\frac{dn}{dr} = A_1 r^2 e^{-\beta r}, \tag{1}$$

where n is the number of particles of radius greater than r per unit volume; A_1 and β are parameters determined by measurement of the integral characteristics of the rain – its optical transparency α and total intensity f.

Particles of the order of 10^{-5} cm show the greatest scattering in the visible region of the spectrum. The sedimentation rate of such particles is negligibly small (of the order of one micron per second) and changes in the aerosol cloud are primarily determined by coagulation processes. Calculations have been reported [7, 8] of the coagulation kinetics and changes of particle size distribution in coagulating clouds. We used the results of these investigations in a theoretical and experimental study of changes in the optical properties of a coagulating aerosol.

Interpolation formula for light scattering by a monodisperse smoke. If a beam of light of intensity I passes through an aerosol layer of thickness dx, part of the light is scattered by the suspended particles and the intensity of the original beam is diminished by

$$-dI = KI\,dx, \tag{2}$$

where K is the linear coefficient of extinction due to scattering, in cm^{-1}.

We denote the particle concentration of a monodisperse aerosol by N (cm^{-3}). At low weight concentrations of the aerosol multiple scattering may be neglected, and the coefficient of extinction will be directly proportional to the particle concentraion, i.e.

$$K = FN, \tag{3}$$

where $F = K/N(\mathrm{cm}^2)$ is the effective cross section of light scattering by a single aerosol particle.

For particles the radii of which are small relative to the wave length of the scattered light $\lambda (r \ll \lambda)$, the effective scattering cross section is given by Rayleigh's law [9]:

$$F_p = \frac{24\pi^3}{\lambda^4}\left(\frac{4}{3}\pi r^3\right)^2\left(\frac{m^2-1}{m^2+2}\right)^2 = B\omega^2, \tag{4}$$

where m is the refractive index of the particle substance, $\omega = \frac{4}{3}\pi r^3$ is the volume of a particle, and B is a proportionality factor which depends on the properties of the particles (m) and of the scattered light (λ)

$$B = \frac{24\pi^3}{\lambda^4}\left(\frac{m^2-1}{m^2+2}\right)^2. \tag{5}$$

In the other extreme case, with particles large relative to the wave length ($r \gg \lambda$) purely geometrical scattering occurs by reflection of light from the particle surfaces. In this case the effective section [1] is equal to the lateral area of the front half of the particle, facing the incident light, i.e.

$$F = 2\pi r^2 = 2\pi\left({}^3/_4\,\pi\right)^{2/3}\left(\frac{4}{3}\pi r^3\right)^{2/3} = A\omega^{2/3}, \tag{6}$$

where $A = \sqrt[3]{9\pi/2}$ is a numerical term.

In the intermediate region of the greatest practical interest, with particles of a size comparable to the wave length of light ($r \approx \lambda$), diffraction scattering occurs. In this case the effective scattering cross section F_ω is a complex function of the particle volume ω, the refractive index m, and the wave length λ. To simplify the calculations, we considered it suitable to derive a simple interpolation formula for F as a function of ω, which for large particles would pass into the limiting Equation (6) of geometrical optics, and for small particles, into the Rayleigh Equation (4). In its simplest form, this interpolation relationship can be written as

$$\frac{1}{F_\omega} = \frac{1}{F_p} + \frac{1}{F_r} = \frac{1}{B\omega^2} + \frac{1}{A\omega^{2/3}}. \tag{7}$$

when $\omega \gg \left(\frac{A}{B}\right)^{3/4} \ldots\ldots \frac{1}{B\omega^2} \ll \frac{1}{A\omega^{2/3}}$ и $F_\omega \approx F_p.$

when $\omega \ll \left(\frac{A}{B}\right)^{3/4} \ldots\ldots \frac{1}{B\omega^2} \gg \frac{1}{A\omega^{2/3}} u F_\omega \approx F_r.$

Transformation of Equation (7) gives the interpolation function in explicit form

$$F_\omega = \frac{AB\omega^2}{A + B\omega^{4/3}}. \tag{8}$$

To reduce Equation (8) to a dimensionless form, we introduce scales for the volume

$$\omega_0 = \left(\frac{A}{B}\right)^{3/4} = \frac{\lambda^3}{4\pi^2\sqrt[4]{12}}\left(\frac{m^2+2}{m^2-1}\right)^{3/2} \tag{9}$$

and the effective cross section

$$F_0 = \sqrt{\frac{A^3}{B}} = \frac{\sqrt{3}}{4\pi}\lambda^2\,\frac{m^2+2}{m^2-1}. \tag{10}$$

Putting $x = \frac{\omega}{\omega_0}$ and $\frac{F_\omega}{F_0}$, we reduce Equation (8) into the final form of the universal relationship

$$y = \frac{x^2}{1 + x^{4/3}}. \tag{11}$$

Fig. 1 shows a plot of Equation (11) in logarithmic coordinates. For comparison, the broken lines in the graph represent curves for diffraction scattering, taken from Rayleigh's paper [9].

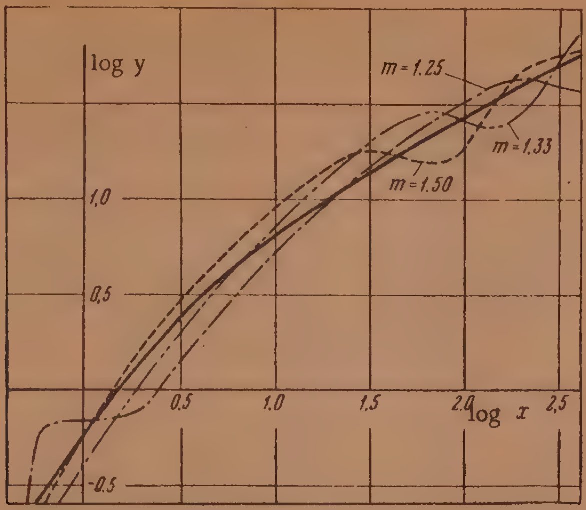

Fig. 1. Light scattering curves for a polydisperse smoke, based on diffraction scattering and Equation (11).

Fig. 1 shows that these points fit fairly satisfactorily on the plot of Equation (11). The interpolation Equation (11) is therefore suitable for approximate calculations of light scattering by monodisperse aerosols not only for the extreme cases of small and large particles, but also for the most interesting particle size range from the practical aspect, comparable with the wave length $r \approx \lambda$.

Light scattering by a coagulating aerosol. It has been shown [7, 8] that, in the coagulation of an aerosol with a fairly high initial particle concentration, a short time after the start of the process the particle size distribution function begins to vary asymptotically. We denote by dN the number of particles of size between ω and $\omega + d\omega$ per unit volume. The particle size distribution function $\rho(\omega, t)$ and dN are connected by the relationship

$$dN = \rho(\omega, t)\, d\omega. \tag{12}$$

With the coagulation process taking an asymptotic course, the function $\rho(\omega, t)$, varies with the time t according to the law

$$\rho(\omega, t) = \frac{P}{t^2}\varphi\left(\frac{Q\omega}{t}\right), \tag{13}$$

where $\varphi(u)$ is a certain function of the variable $u = Q\omega/t$, and P and Q are constants, respectively equal to

$$P = \frac{\delta}{M}\left(\frac{3\eta}{8kT}\right)^2 \text{and} Q = \frac{\delta}{M}\frac{3\eta}{8kT}, \tag{14}$$

where M is the weight concentration of the aerosol; δ is the density of the particles themselves; η is the viscosity of the surrounding medium; k is the Boltzmann constant; T is the absolute temperature.

The function $\varphi(u)$ can be found from a fairly complex differential equation to various degrees of accuracy. In the first approximation $\varphi(u)$ can be found from Smoluchowski's approximate solution [10]

$$\varphi_0(u) = 4e^{-2u}, \tag{15}$$

where e is the base of natural logarithms.

As was shown in our papers, the further refinements introduced by Phsenai-Severin [11] do not change significantly the integral characteristics of the coagulation process. Therefore in the subsequent calculations we shall only use the first approximation (15).

The linear coefficient of light scattering by a polydisperse aerosol, in accordance with Equations (3) and (12), will be given by the sum of the scattering coefficients for particles of different sizes, i.e.

$$K = \int F(\omega)\, dN = \int_{1}^{\infty} F(\omega)\, \rho(\omega, t)\, d\omega, \tag{16}$$

substituting, instead of Equations (10) and (6), their approximate values, we find

$$K = \int_{0}^{\infty} F_0 \frac{x^2}{1 + x^{4/3}} \frac{4P}{t^2} e^{-\frac{2Q\omega_0}{t} x} dx. \tag{17}$$

Putting

$$\frac{2\omega_0 Q}{t} = h \text{ and} \frac{KQ^2\omega_0}{PF_0} = \Phi(h),$$

we reduce Equation (17) to the form

$$\Phi(h) = h^2 \int_{0}^{\infty} \frac{x^2}{1+x^{4/3}} e^{-hx} dx. \tag{18}$$

When h >> 1 (small times) the function e^{-hx} diminishes very rapidly with x, and in calculations of the integral in the right hand side of Equation (18) the integrand is of primary importance at low values of x. Assuming that $\frac{x^2}{1+x^{4/3}} \approx x^2$, we can find the approximate value of the required integral

$$\Phi_1(h) \approx h^2 \int_{0}^{\infty} e^{-hx}\, dx = \frac{\Gamma(2+1)}{h} = \frac{2}{h}. \tag{19}$$

In the opposite extreme case the large values of the variable $x = 1/h$ are of primary importance in calculation of the integral. Here the integrand at large values of this variable can be replaced by an asymptotic expression, by putting $x^2/(1 + x^{4/3}) \approx x^{2/3}$; the approximate value of the required integral will then be

$$\Phi_2(h) = h^2 \int_{0}^{\infty} x^{2/3} e^{-hx}\, dx = \Gamma\left(\frac{5}{3}\right) h^{1/3} = 0{,}90\, h^{1/3}. \tag{20}$$

To find the function Φ (h) at intermediate values of the variable ($h \approx 1$) we replace it by an interpolation formula, which at large values of h passes into Equation (19), and at small values of h, into Equation (20). The simplest interpolation formula to satisfy these conditions will be an expression of the type

$$\frac{1}{\Phi(h)} = \frac{1}{\Phi_1(h)} + \frac{1}{\Phi_2(h)} = \frac{1 + 0.45 h^{4/3}}{0.90\, h^{1/3}}. \tag{21}$$

By replacing h and Φ (h) by their values (see above), Equation (21) can be reduced to the form

$$\frac{K}{M} = \frac{11.1}{\delta\lambda} \sqrt{\frac{m^2 - 1}{m^2 + 2}} \cdot \frac{\tau}{1 + \tau^{4/3}}. \tag{22}$$

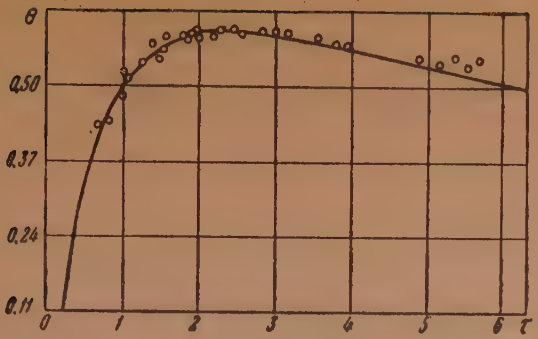

Fig. 2. Variation of the hiding power of a polydisperse aerosol with time.

The quantity K/ M represents the weakening of the light per unit length at unit weight concentration of the aerosol; it is known in the literature as the "hiding power" of a given smoke. The dimensionless time τ depends on the aerosol concentration, its optical properties at the particular wave length, and the coagulation rate; it is determined by the expression:

$$\tau = 30.2 \frac{M}{\delta} \frac{kT}{\eta \lambda^3} \sqrt{\frac{m^2-1}{m^2+2}}. \tag{23}$$

The dimensionless extinction (light weakening) coefficient, which represents the hiding power

$$\theta = \frac{K\delta\lambda}{11.1\,M} \sqrt{\frac{m^2+2}{m^2-1}} \tag{24}$$

varies with the dimensionless time τ according to the law

$$\theta = \frac{\tau}{1+\tau^{4/3}}. \tag{25}$$

a plot of which is given in Fig. 2.

It is seen in Fig. 2 and Equation (25) that the power of an aerosol first increases relatively rapidly with particle size, and then decreases slowly and gradually.

The maximum value of K/ M can be found by the usual differential calculation rules

$$\left(\frac{K}{M}\right)_{\max} = \frac{6.36}{\delta\lambda} \sqrt{\frac{m^2-1}{m^2+2}} \tag{26}$$

and the time to reach this maximum is

$$\tau_{\max} = \frac{0.0235\, \delta\lambda^3\eta}{MkT} \left(\frac{m^2+2}{m^2-1}\right)^{3/2}. \tag{27}$$

It follows from Equations (22) and (27) that the masking power (K/ M) of a particular aerosol is not a constant for the substance (one which depends only on its refractive index m at the given wave length λ), but varies continuously with time. Only the maximum hiding power of the aerosol, given by Equation (26) can be regarded as such a constant. Under otherwise equal conditions, increase of the weight concentration results in a decrease of the time required to reach the maximum K/ M and in accelerated decrease of K/ M after the maximum has been reached, as shown in Fig. 3. The maximum value of K/ M increases with the refractive index m, but the time required to reach this maximum and the duration of its existence are diminished to a greater extent, as is shown in Fig. 4.

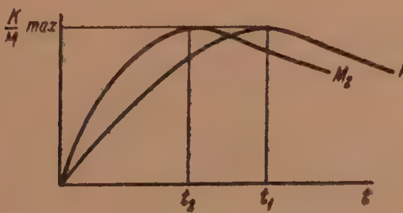

Fig. 3. Variation of the time required to reach maximum hiding power with varying aerosol concentration.

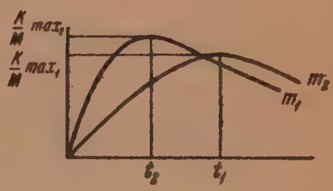

Fig. 4. Variation of maximum hiding power and of the time required to reach it with varying refractive index of a smoke.

Experimental verification of Equation (25). An experimental investigation was carried out to test the theoretically derived Equation (25). A heavy oil aerosol was prepared by the condensation method and introduced into a smoke chamber (average b.p. of the oil was 360°, density $\gamma = 0.95\ \mathrm{g/cm^2}$, refractive index $m = 1.50$). The weight concentration M of the smoke, and the light extinction coefficient K, measured by the readings I of a photocell at a distance l from a standard light source, were determined during the experiments. The extinction coefficient was calculated by the equation

$$K = \frac{2.3}{l} \log \frac{I_0}{I}. \tag{28}$$

where I_0 is the photocell reading in absence of the aerosol.

The experimental data were plotted in the form of the relationship (25) in the dimensionless coordinates θ and τ. For the experimental values of γ and $\underline{m}$ for the most perceptible wave length $\lambda = 555\ \mathrm{m\mu}$ the values of θ and τ were calculated from the expressions

$$\theta = 0.097 \frac{\mathrm{g}}{\mathrm{m}^2} \frac{K}{M}. \tag{29}$$

$$\tau = 2.10^6 \frac{\mathrm{cm}^3}{\mathrm{g\,sec}} Mt. \tag{30}$$

It was assumed in the calculations that the true value of K is 10% lower than that given by Equation (28) owing to absorption of light by the aerosol particles [12].

As is seen in Fig. 2, the experimental data fit satisfactorily on the theoretical curve for Equation (25). As a rule, at the end of the experiment the theoretical curve descends more steeply than the experimental. However, these deviations are not large, and do not exceed 30% within the limits of a 30-minute exposure. The probable cause of these systematic deviations is that coagulation is accompanied by evaporation of the oil particles; this somewhat decreases the particle size and increases the content of fractions with a higher refractive index, and therefore with better hiding properties.

SUMMARY

The optical properties of aerosols depend on the scattering of light by the particles and on the particle size distribution. A simple interpolation Equation (11), which smooths out the diffraction peaks somewhat, is given for calculation of light scattering by particles comparable in size to the wave length. On the basis of this equation and the asymptotic character of coagulation, an interpolation Equation (25) has been derived for determination of the extinction of light by aerosols; this equation was verified by an experimental study of heavy oil mist.

Leningrad Received July 9, 1956.

LITERATURE CITED

[1] K. S. Shifrin, Light Scattering by Turbid Media (State Tech. Theoret. Press, 1951).

[2] V. V. Shuleikin, Physics of the Sea (Izd. AN. SSSR, 1953).

[3] G. Mie, Ann. Phys. 25, 377 1908.

[4] L. Foitzik, Z. Meteor. 4, No. 10, 11 1950.

[5] K. Ya. Kondratyev, Radiant Energy of the Sun (Hydrometeor. Press, 1954).

[6] E. Ya. Polikova and K. S. Shifrin, Microstructure and Transparency of Rain, Trans. Main Geophysical Observatory, No. 26, 88 1951.

[7] O. M. Todes, Physical Chemistry Symposium, p. 138 1948.

[8] O. M. Todes, Problems of Kinetics and Catalysis, 7, 157 1949.

[9] Rayleigh, Phil. Mag. (5) 47, 375, 1899

[10] Smoluchowski Z. Phys. Chem. 92, 129 1917.

[11] Pshenai-Severin, Proc. Acad. Sci. USSR, 94, 865 1954.

[12] Yu. M. Veitser and G. P. Luchinsky, Chemistry and Physics of Masking Smokes (Moscow-Leningrad, 1939).

ORIENTATION OF CLAY PARTICLES DURING DEFORMATION OF A CLAY BODY

V.S. Fadeeva

When plastic clay bodies are molded into ware, in some cases a stratified structure is formed (Fig. 1), sometimes right through the thickness of the specimen and sometimes only in isolated regions. There is reason to believe that orientation of the clay particles during deformation of the body may play a part in this effect, as deformation of a disperse system is accompanied by definite spatial orientation of its particles [1-4].

In order to study the relationship between a stratified structure in a clay body and the orientation of its particles during molding of ceramic ware, we carried out a number of experiments on the deformation of a clay body based on highly plastic Chasov Yar clay with addition of 5% biotite. The biotite was first finely ground in a vibratory mill in order that the biotite particles should be of comparable size to the clay particles and undergo orientation with them. The dark biotite scales were easily distinguishable in the pale clay mass, making it possible to observe orientation of the particles during deformation of the clay body. The clay body was deformed in conditions of pure compression and under complex shearing deformation along a compression plane under the simultaneous action of compressing loads.

Three series of specimens, A, B, and C, 2 cm in height and in diameter, were made from an experimental paste with 38% moisture (the normal molding consistency). Specimens of Series A were subjected to a pressure of 1 kg/cm^2 for 24 hours; specimens of Series B were subjected to a pressure of 10 kg/cm^2 for 15 minutes; this resulted in extrusion of the body into the gap between the ring and the die. Specimens of Series C were compressed under a load of 1 kg/cm^2 for an hour (this time was sufficient to confer a uniform structure on the specimens) and were then sheared along the compression plane. The shearing was effected slowly, at 1-2 cm/minute, and was continued to various degrees of deformation, in some cases to total destruction.

Transparent sections were prepared from all three series of specimens. The sections were cut in a plane through the centers of the specimens at right angles to the base; they were dried in air and boiled in Canada balsam. Figs. 2,3 and 4 show micrographs of the sections. The structure seen in the section of a specimen of Series A (Fig. 2) is completely similar to the structure of the body before deformation, and is characterized by a random distribution of the biotite particles. The section of the specimen of Series B shows a definite orientation of the biotite particles, namely: in the region immediately under the die they tend to be oriented perpendicularly to the acting load (Fig. 3,a), and at the ring walls they tend to lie parallel to the walls, in the direction of the shearing force in the body relative to the walls (Fig.3,b). In the center of the specimen the particles of biotite had a random distribution. In the section of a specimen of Series C (Fig. 4) a tendency is seen for the biotite particles to be oriented parallel to the shear plane. In some parts of the shearing region, destruction was observed (longitudinal cracks). Investigation of the specimens of this series showed that destruction of the specimens in the shearing region does not occur before complete orientation of the particles. This is confirmed by the results of our investigations of the physicomechanical properties of plastic clay bodies based on clays of different mineralogical composition [5]. These properties were found to depend to a considerable extent on the spatial configuration of the clay mineral, determining its tendency to orientation under pressure. It may be noted that in the original body and in specimens of Series A (Fig.2) the biotite particles are larger than in the shearing region (Fig.4).

Observations were also made of the orientation of the particles in the surface layer of a specimen of the same body after sliding along a solid surface — the steel table of an instrument for determination of external friction. In this case the sections were cut in a plane perpendicular to the sliding surface (Fig. 5). Orientation

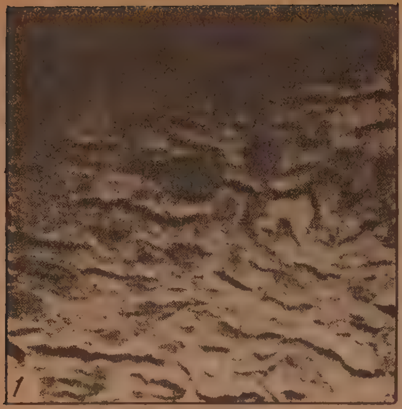

Fig. 1. Micrograph of a transparent section of a fired block molded under high pressure. The block was rejected owing to low frost resistance and nonstandard bending strength (× 56).

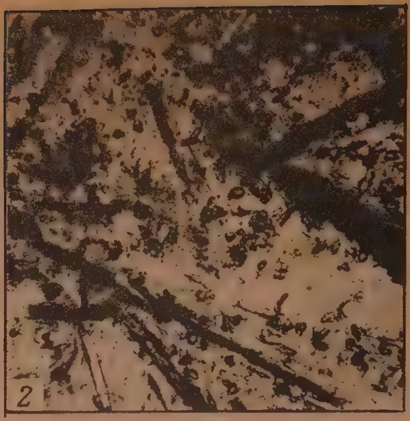

Fig. 2. Specimen after compression at 1 kg/cm^2 for 24 hours. The black elongated grains are biotite (× 56).

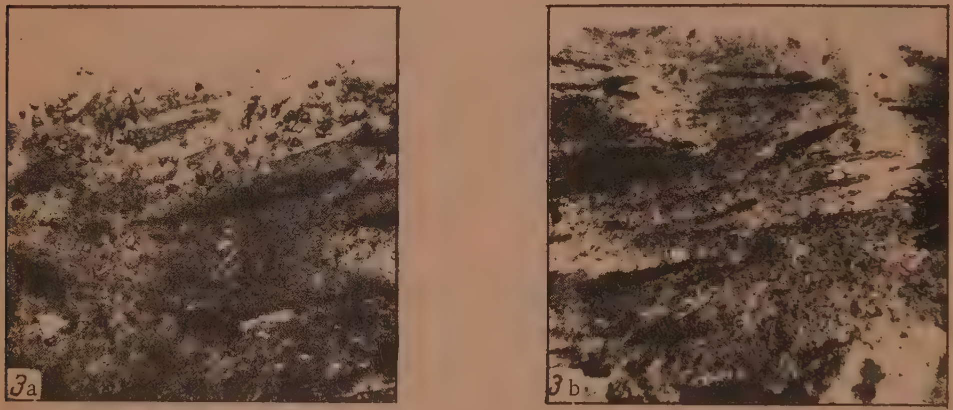

Fig. 3. Specimen after compression at 10 kg/cm^2 for 15 minutes (×56); 3a) pale field – boundary of die contact. Black elongated grains are biotite; 3b) pale field – boundary of ring walls, black elongated grains are biotite.

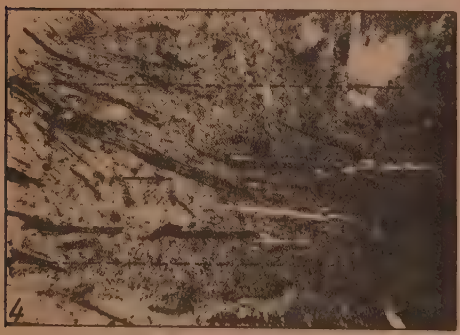

Fig. 4. Specimen after shear along a compression plane (shearing force near the limiting value) (× 56). Black elongated grains are biotite. The shearing region is marked by dotted lines. The pale stripes are cracks. The arrow indicates the direction of the shearing force.

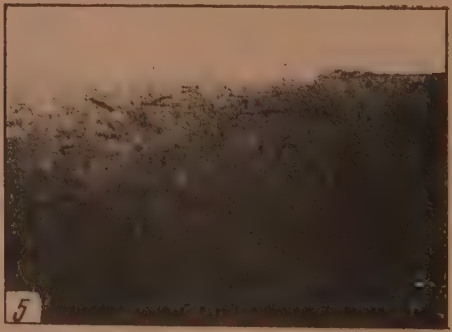

Fig. 5. Region of the friction surface of the specimen. Black lines are biotite grains. The pale field is the boundary of the friction surface (× 56).

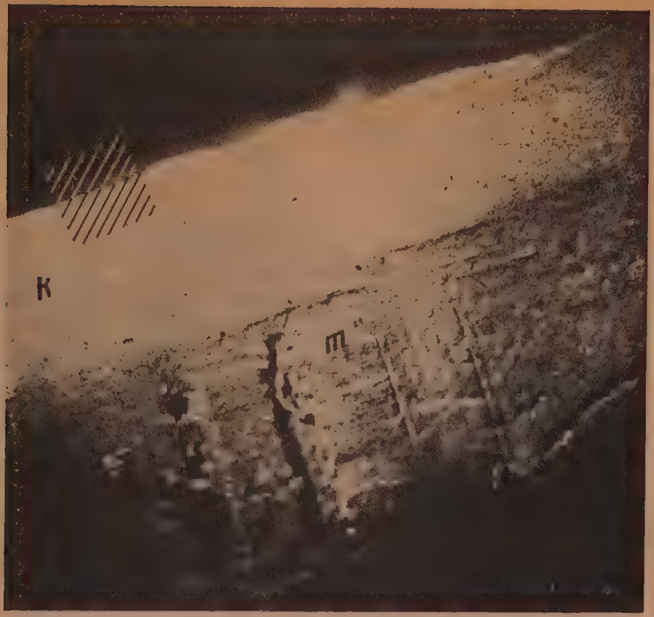

Fig. 6. Micrograph of a cross section of a clay specimen. The Zone k is a layer on the friction surface of the specimen. The square indicates the place shown in the transparent section in Fig. 5. The Zone m is the main mass of the specimen. The transverse stripes (furrows) are traces formed by sand grains during cutting of the moist specimen (x 15).

of the particles parallel to the friction surface can be seen in the photograph. The observations were hindered by the fact that sliding resulted in differentiation of the clay and biotite particles, as a result of which only the finest particles, difficult to distinguish in the prepared section, remained in the layer contiguous with the sliding plane. Examination of samples taken from the sliding surface under the electron microscope also showed them to be highly disperse. Fig. 6, which is a direct micrograph of a cross section of the specimen, shows that the surface sliding layer, Zone k, differs sharply in general strucutre from the rest of the specimen, Zone m. This accounts for the decrease of the coefficient of friction with increased normal load on the specimen, which has been observed in studies of the friction of clay specimens against solid surfaces, as the surface layer appears to act as a lubricant during movement of the specimen. It also explains why the coefficients of friction found in these investigations for bodies of molding consistency made from different clays were similar, as all clays have a highly disperse fraction which forms this layer. These results are in good agreement with Tolstoi's work [6] on the wall effect in disperse systems.

The formation of such a layer can be represented as follows: water containing minute clay particles, of colloidal dimensions passes from the interior of the specimen during its motion toward the sliding surface, which is a region under higher stress [7]; these clay particles are deposited on the sliding surface and oriented in the direction of the shearing force to form a layer consisting of very closely packed highly disperse particles. Observations showed that the friction surface of a clay specimen is similar in character to the surface of a deposit of a colloidal clay fraction on a filter; i.e., it is in the form of a dense, shining coating ("polished layer"). It is evident that the higher the pressure, the more rapidly is such a layer formed, and the higher will be its moisture content (of course, for the given sliding velocity, 2 cm/sec).

Under pure compression conditions, even under high pressures, particle orientation within a specimen of a plastic clay body occurs slowly, and probably has no appreciable influence on the formation of a stratified structure during molding of ware from these bodies. In compression with simultaneous shearing of a specimen of a plastic clay body the shearing force does not reach its limiting value (yield value) before complete orientation of the particles in the body in the shearing region. When orientation of the particles is complete further increase of the shearing force results in destruction of the specimen along the plane of the action of the maximum tangential stresses, leading to the formation of a stratified structure in the specimen. To prevent the formation of such a structure, it is necessary to vary the direction of the maximum tangential stresses during molding and not to exceed the maximum shearing stress for the given body.

When a clay specimen slides along a solid surface, a highly disperse fraction emerges toward the sliding surface, with simultaneous orientation of the particles in the direction of the frictional force. This leads to the formation of a layer, differing in structure from the rest of the specimen, on the sliding surface. Experiments showed that a similar process occurs in complex deformation of a clay specimen. Highly disperse clay fractions travel toward the planes of action of the maximum tangential stresses as these develop; this decreases the yield stress of the body and favors the formation of a heterogeneous stratified structure in the specimen. Each individual layer of such a structure is probably similar to the specimen shown in Fig. 6. The number of layers will depend on the homogeneity of the body, its degree of dispersion, and also on the homogeneity of stress distribution in it during deformation. It seems likely that the microstratified structure formed in clay specimens during molding is the result of the action of tangential stresses near or equal to the yield value of the body in these specimens; this is in agreement with the modern views on the destruction processes in such materials.

SUMMARY

1. Deformation of plastic clay bodies is accompanied by spatial orientation of the particles, mainly in the direction of the maximum shearing force. This is accompanied by differentiation of the particles in the body by size, with liberation of water containing minute particles (of colloidal dimensions) toward the shearing region.

2. Particle orientation precedes destruction of plastic clay body specimens.

3. Particle orientation and differentiation effects in plastic clay bodies occur also during slippage of specimens along solid surfaces; in consequence, the coefficient of surface friction of clays is a variable quantity.

We wish to express our gratitude to Prof. M. P. Volarovich for valuable advice in the course of this investigation.

Scientific Research Institute
for Construction Ceramics
Moscow

Received July 3, 1956

LITERATURE CITED

[1] A. Nadai, Plasticity (ONTI, 1933).

[2] K. Tertsagi, Building Mechanics of Soils on the Basis of their Physical Properties (State Constr. Press, 1933).

[3] M. P. Volarovich, Bull. Acad. Sci. USSR, Div. Math. Nat. Sci., 599 1938.

[4] M. P. Volarovich and I. S. Erokhin, J. Phys. Chem., 12, No. 2-3 1938.

[5] V. S. Fadeeva, Trans. Sci. Res. Inst. Constr. Ceramics No. 8, (Ind. Press, 1953).

[6] D. M. Tolstoi, Colloid J., 10, No. 2 1948.

[7] N. A. Nasedkin, J. Tech. Phys., 8, No. 3 1938.

EFFECTS OF THE TYPES OF RUBBER AND CARBON BLACK ON THE FORMATION OF CARBON-RUBBER GELS

Z.V. Chernykh and V.G. Epshteǐn

Addition of carbon black to rubber mixtures results in increased modulus and higher tensile, tearing, and abrasion strength. This effect is evidently determined to a considerable extent by the bonds formed between the rubber and carbon in the mixture.

In a number of recent investiagtions the bonding between rubber and carbon black has been studied by determinations of the so-called carbon-rubber gel, which is the portion of the nonvulcanized rubber mix insoluble in benzene. According to Dogadkin and Feldhstein [5], the proportion of the insoluble fraction depends on the activity of the filler. It has also been shown that the amount of carbon-rubber gel depends on the molecular weight of the rubber [1, 2], the type of carbon black (mainly its degree of dispersion) [2, 4], and on the compounding temperature [3, 6].

It is believed that the formation of a carbon—rubber gel is the result of formation of a carbon network (as was proved by Dogadkin [7]), of the considerable energy of intermolecular interaction between the rubber and the carbon, and of the entanglement of the flexible molecular chains of the rubber [1].

The formation of a carbon-rubber gel has been associated with rubber reinforcement in a number of papers [1, 2, 6, 8]. It has been shown that an increase in the amount of carbon-rubber gel corresponds to an increase in the modulus and the abrasion resistance of vulcanizates [6, 7].

Carbon-rubber gel determinations are not particularly accurate, but they may be used for estimating bond strengths in rubber-carbon black mixtures. For determining the nature of these bonds, we studied the formation of carbon-rubber gels in mixtures of natural and synthetic rubber with various carbon blacks, and estimated gel stability under various extraction conditions.

EXPERIMENTAL

The following rubbers were taken for the investigation: natural rubber (NR) (smoked sheet), SKB 50, SKBM 50, thermally plasticized SKS-10 and SKS-30 A with plasticity 0.5, and the following carbon blacks: channel, acetylene, nossle furnace, and thermal.

The molecular weights of the rubbers were calculated from viscosimetric data by the formulas:

For NR . . . . $[\eta] = 5.02 \cdot 10^{-4} . M^{0 \cdot 67}$;
For SKS. . . . . $[\eta] = 4.4 \cdot 10^{-4} . M^{0 \cdot 67}$; [11]
For SKB and SKBM $[\eta] = 2.7.10^{-4} . 10M^{0 \cdot 725}$ [12]

the values veing 126,000 for NR, 85,500 for SKB, 106,200 for SKBM, 172,600 for SKS-10, and 102,000 for SKS-30A.

The characteristics of the carbon blacks are given in Table 1.

The mixtures were milled on laboratory rolls, with roll diameter 160 mm, at 20–30°, in the following formulation:

Rubber	100	parts by weight
Stearic acid	3.0	" " "
Rubrax	5.0	" " "
Carbon	from 10 to 180	" " "

The compounding time increased with the carbon black content, and ranged from 10 to 20 minutes.

TABLE 1
Characteristics of the Carbon Blacks [10]

Type of carbon	Average particle diameter, Å	pH	Oil adsorption, ml/g
Channel	280	3.5—4.5	1.4
Acetylene	400	6.5—7.0	2.8
Furnace	640	9—10	0.8
Nozzle	1100	9—10	3.0
Thermal	1880	7—8	0.3

The compounded mixtures were left for 24 hours, and the rubber-carbon gel contents were then determined as follows: a weighed sample of 2.0 g of the finely shredded mixture was placed in a weighed textile cartridge. The cartridge was placed in a wide-necked Erlenmeyer flask and covered with benzene or carbon tetrachloride. The extraction was continued for 24 and 48 hours at 20°, and for 18 hours in boiling benzene at 78°. At the end of the extraction the solvent was decanted, the cartridge was washed once with ligroine, and dried in a thermostat at 60° to constant weight. The carbon-rubber gel content was determined as the ratio of the weight of the dry gel to the weight of the sample. The reproducibility of the results was within 2-3%. The carbon content of the carbon-rubber gels was determined by the method used for determination of carbon black in vulcanizates (by decomposition of the gel in nitric acid sp. gr. 1.37). The fraction of the rubber bound with carbon was calculated from the results.

The results of the carbon-rubber gel determinations for NR, SKB and SKS-30A rubbers are shown in the diagram. The following comments may be made on the results.

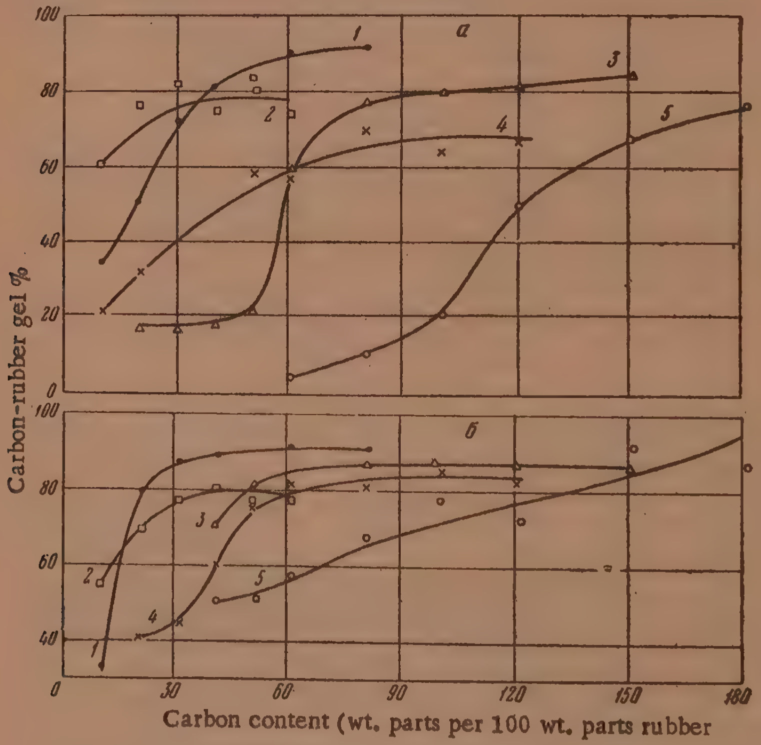

Contents of carbon-rubber gel in mixtures based on NR (a) and SKS-30A (b) with different carbon contents: 1) channel black; 2) acetylene black; 3) furnace black; 4) nossle black; 5) thermal black.

TABLE 2

Variations of Carbon-Rubber Gel Contents in Mixtures Based on NR with the Extraction Conditions

Type of carbon black	Wt. parts of carbon to 100 wt. parts rubber	Carbon–rubber gel, content, %			
		Benzene			CCl_4
		24 hrs. 20°	48 hrs. 20°	18 hrs. 78°	48 hrs. 20°
Channel	30	83.0	74.0	68.0	80.0
	80	92.0	83.0	82.0	—
Acetylene	20	77.0	67.0	63.0	79.0
	50	81.0	72.0	62.0	72.0
Furnace	80	79.0	78.0	72.0	84.0
Nozzle	80	70.0	61.0	60.0	75.0
Thermal	180	77.0	73.0	72.0	73.0

TABLE 4

Contents of Carbon Black and Rubber Bound with Carbon in Carbon-Rubber Gels in Mixtures Based on NR

Type of carbon black	Wt. parts carbon to 100 wt. parts rubber	Benzene				CCl_4	
		48 hrs. 20°		18 hrs. 78°		48 hrs. 20°	
		carbon content in gel, %	amount of rubber bound with carbon %	carbon content in gel, %	amount of rubber bound with carbon %	carbon content in gel, %	amount of rubber bound with carbon %
Channel	30	31.7	69.8	32.4	60.0	23.6	84
	80	68.5	48.0	57.6	64.0	48.6	—
Acetylene	20	47.0	45.4	32.5	44.3	27.0	52.0
	50	69.1	34.0	54.5	40.6	54.5	82.6
Furnace	80	77.6	33.0	62.0	48.3	63.4	72.2
Nozzle	80	84.0	18.5	75.5	26.2	56.0	51.6
Thermal	180	90.0	21.8	83.7	33.3	83.5	35.3

TABLE 3

Variations of Carbon-Rubber Gel Contents in Mixtures Based on SKB with the Extraction Conditions

Wt. parts carbon to 100 wt. parts rubber	Channel			Acetylene			Furnace			Nozzle			Thermal		
	Benzene		CCl_4	Benzene		CCl_4	Benzene		CCl_4	Benzene		CCl_4	Benzene		CCl_4
	24 hrs.	48 hrs.	48 hrs.	24 hrs.	48 hrs.	48 hrs.	24 hrs.	48 hrs.	48 hrs.	24 hrs.	48 hrs.	48 hrs.	24 hrs.	48 hrs.	48 hrs.
10	69.0	42.0	—	82.0	59.0	58.0	—	44.0	—	43.0	43.0	—	—	—	—
20	86.0	75.0	83.5	89.0	65.0	71.0	57.0	56.0	—	64.0	43.0	—	—	—	—
30	81.0	74.0	—	—	—	—	65.5	52.0	—	87.0	66.0	60.5	—	40.8	—
40	86.0	70.0	83.5	—	—	—	76.0	62.0	—	—	—	78.0	58.0	46.0	—
50	—	88.0	—	—	—	—	87.0	64.0	68.0	80.0	77.0	76.0	62.0	54.0	—
60	86.0	86.0	82.0	85.0	66.0	78.0	87.0	66.0	—	90.0	76.0	79.0	83.0	60.0	—
80	—	—	—	—	—	—	89.0	75.0	74.0	—	—	—	83.0	68.0	58.0
100	—	—	—	—	—	—	82.0	73.0	74.0	—	—	—	—	69.0	62.0
120	—	—	—	—	—	—	—	—	—	—	—	—	82.0	69.0	71.0
180	—	—	—	—	—	—	—	—	—	—	—	—	86.0	73.0	73.0

The carbon-rubber gel content increases with the amount of carbon black added. For example, thermal black, which does not form a gel when added in small amounts, forms a large amount of gel when added in 150-180 parts by weight. The carbon-rubber gel content for a definite amount of carbon depends on the type of carbon black added. At contents of 20-40 parts by weight, the carbons form the following sequence: acetylene, channel, nozzle, furnace, thermal. The carbon-rubber gel content depends on the type of rubber. In synthetic rubbers (SKB, SKS-30A) gel formation occurs to a greater extent and with smaller additions of carbon black than in natural rubber, despite the somewhat lower molecular weight of these rubbers.

The variations of the carbon-rubber gel content with extraction conditions are given in Tables 2 and 3.

It follows from Tables 2 and 3 that the more harsh conditions of benzene extraction (boiling, or increase of extraction time) do not cause decomposition of the carbon-rubber gel, but only decrease its content somewhat; this effect is more prominent in mixtures with small amounts of carbon black.

The amounts of gel formed when the mixtures are dissolved in carbon tetrachloride are somewhat greater than when they are dissolved in benzene for mixtures containing channel and acetylene blacks, approximately the same for mixtures with furnace and nozzle blacks, and less for mixtures with thermal black.

Table 4 contains data on the contents of carbon black in the carbon-rubber gels for different extraction conditions and types of carbon. These results show that: 1) the content of carbon in the gel increases with increasing amount of carbon added to the mixture; 2) in mixtures containing furnace and nozzle blacks, with a lower gel content (see Table 2) the carbon content of the gel is higher than in mixtures containing carbon black; 3) more harsh extraction conditions – the use of a more active solvent (CCl_4) or boiling – lead to a decrease of the carbon black content in the gel, i.e., carbon black is removed to a greater extent than rubber.

TABLE 5

Effects of Mastication on the Contents of Carbon-Rubber Gel and of Carbon in the Gel (Benzene Extraction for 24 hours at 20°)

Type of rubber	Type of carbon black	Wt. parts carbon to 100 wt. parts rubber	Contents of carbon–rubber gel, %		Contents of carbon in carbon–rubber gel, %	
			before treatment	after 20 minutes of mastication	before treatment	after 20 minutes of mastication
NK	Channel	60	92.0	83.0	43.6	46.0
	Furnace	100	86.0	86.0	53.0	57.3
SKB	Channel	60	89.0	90.0	40.0	40.7
	Furnace	100	90.0	88.0	60.0	53.5
SKBM	Channel	60	90.0	88.0	48.0	—
	Furnace	100	92.0	87.0	52.0	56.7
SKS-10	Channel	60	94.0	91.0	39.8	39.0
	Furnace	100	95.0	91.0	64.0	—
SKS-30A	Channel	60	95.0	91.0	—	40.9
	Furnace	100	86.0	85.0	56.3	61.0

The contents of carbon-rubber gel in mixtures based on various rubbers before and after additional mastication are given in Table 5. The mixture was masticated for 20 minutes on laboratory rolls at 20-30°. The gel contents are not appreciably affected by changes in the type of synthetic rubber (increased contents of butadiene residues in the 1-4 position or decreased contents of styrene residues). In the case of a mixture of NR with channel black the amount of gel decreases after mastication; this is possibly caused by degradation of the rubber. This effect is slight for other types of rubbers.

DISCUSSION OF RESULTS

The view has been put forward in a number of papers [2, 6] that formation of carbon-rubber gels can be largely attributed to the high stability of the bonds between the rubber molecules and the carbon black. It was considered that only active blacks form carbon-rubber gels [6]. It had also been suggested that chemical bonds may be formed between the rubber and the carbon black [9].

It is known that carbon blacks differ in their tendency to form carbon structures. Channel and acetylene blacks readily form continuous structures in rubber mixtures, consisting of chains of carbon particles. This property is not found in furnace and especially in thermal blacks [7]. According to our results, the ease of formation of a carbon-rubber gel depends on the tendency of the carbon black to form structures. In mixtures containing acetylene or channel blacks, appreciable amounts of gel are formed at lower carbon contents than in mixtures containing nozzle furnace, or thermal blacks. Acetylene black, which has a greater tendency to structure formation, forms large amounts of gel at lower contents than channel black, although the latter is highly disperse. The same applies to nozzle black. Though the particle size of nozzle black is greater than that of furnace black; the former forms appreciable amounts of gel at lower contents than does furnace black. On the other hand, on increase of the amount of semiactive or inactive (furnace or thermal) black, a gel is still formed. Therefore it may be assumed that all carbon blacks can form continuous structures when added in definite, large or small amounts.

Studies of the strength and stability of carbon-rubber gels, based on increasing the time and raising the temperature of extraction, or on using a more active solvent (carbon tetrachloride) showed that more harsh extraction conditions do not result in total disappearance or a substantial decrease of the carbon-rubber gel content. Moreover, it was found that on extraction with carbon tetrachloride or boiling benzene the gel contains less carbon black and more rubber than on extraction with benzene at 20°. Thus the amount of rubber bound with carbon increases in such conditions. Consequently, the action of a more active solvent or increase of temperature intensifies the separation of the carbon black particles from each other, with their subsequent elution, rather than the separation of rubber molecules from carbon particles. The action of carbon tetrachloride becomes more pronounced with decreasing strength of the bonds between the carbon particles (with decreasing tendency to structure formation). Therefore it seems probable that the strength of the bonds between the carbon black particles is one of the main factors in the stability of carbon-rubber gels.

The carbon black structure is reinforced with increasing carbon black content. At the same time the differences between the amounts of carbon-rubber under different extraction conditions decrease. Thus, in mixtures of SKB with 20 parts by weight of channel black the differences between the amounts of gel obtained by extraction with cold and with hot benzene is 11%, whereas with 60 parts by weight there is no longer any difference. This confirms once again that the gel stability depends on the formation of a carbon black structure at high loadings.

It should also be noted that formation of a carbon structure increases the cohesion between the rubber and the carbon. The carbon-rubber gel contains less carbon and more rubber in the case of structural blacks (channel and acetylene) than in the case of nonstructural blacks (furnace and thermal) (Table 4).

It is at present difficult to say what the nature of the forces is between the carbon black particles and between the carbon and the rubber. Further investigation is also needed of the reasons for the increased strength of the bonds between the rubber and the carbon if a structure is formed. The higher content of gel in synthetic rubbers as compared with natural rubber is of great interest. It is possible that the explanation lies in the larger cohesion forces between the molecules of natural rubber, associated with a tendency to crystallization, hindering adsorption of the rubber molecules on the carbon particles. The higher gel contents of synthetic rubber mixtures probably account for the higher abrasion resistance, reported in the literature, of synthetic rubber vulcanizates in comparison with natural rubber, despite the lower tensile strength of the former.

The results of our investigation show that the formation of a carbon-rubber gel is closely related to formation of carbon networks, i.e., the cohesion between the carbon black particles. The amount of carbon-rubber gel may be a measure of the tendency to carbon structure formation.

It is known that the carbon-rubber gel content determines the abrasion resistance and other properties of a vulcanizate. The fact that the gel content depends on the tendency to carbon structure formation indicates that there is a link between such structures and rubber reinforcement.

SUMMARY

1. Carbon-rubber gels are formed in mixtures containing all the types of carbon black tested (channel, acetylene, nozzle, furnace, thermal) and not only active carbons.

2. The amount of carbon-rubber gel formed depends on the amount of carbon black added. With carbon blacks which readily form continuous carbon structures (channel, acetylene) the amounts of gel are greater than with nonstructural blacks, for the same amount of black added.

3. The amount of gel is greater in synthetic than in natural rubber mixtures.

4. More harsh extraction conditions do not cause disappearance of the gel, but increase the amount of bound rubber and decrease the amount of carbon in the gel.

5. The carbon-rubber gels formed from structural carbons contain larger amounts of bound rubber.

6. It is suggested that bond stability between carbon black particles (characterized by the formation of a carbon black structure) is one of the basic causes of carbon-rubber gel formation.

Yaroslav Technological Institute Received October 12, 1956.

LITERATURE CITED

[1] A. S. Novikov, M. B. Khaikina, T. V. Dorokhina, and M. I. Arkhangelskaya, Colloid J., 15, No. 1, 51 1953.*

[2] J. Duke, W. K. Taft, J.M. Kolthoff, Rubb. Chem. Techn. 25, No. 3, 500 1952.

[3] C. W. Sweitzer, W.C. Goodrich, K. A. Burgess, Rubb. Age (NJ) 65, No. 6, 651 1949.

[4] C. W. Sweitzer, Rubb. Age (NJ) 72, No. 1, 55 1952.]

[5] B. A. Dogadkin and M. S. Feldshtein, Caoutchouc and Rubber, No. 12, 12 1939.

[6] L. R. Sperberg, J.F. Svetlik, Ind. Eng. Chem. 41, No. 8, 1641, 1949.

[7] B. A. Dogadkin, K. A. Pechkovskaya, and V. V. Kuriyanova, Investigations of the Physics and Chemistry of Caoutchouc and Rubber (Goskhimizdat, 1950), p. 103.

[8] S. D. Gehman, Ind. Rubb. World. 128, No. 2, 129 1953.

[9] W. F. Watson, Ind. Eng. Chem. 47, 1281 1955.

[10] V. P. Zuev and V. V. Mikhailov, Production of Carbon Black (Goskhimizdat, 1953) p. 15.

[11] T. Alfrey, Mechanical Behavior of High Polymers (IL, 1950) p. 484.

[12] I. I. Zhukov, I. Ya. Poddubnyi, and A. V. Lebedev, Investigations in the Field of High Molecular Compounds (Izd. AN SSSR, 1949) p. 250.

---

* Original Russian pagination. See C. B. translation.

~~THE~~ STRUCTURE ~~OF~~ GEL~~S~~

~~11. EFFECT~~ OF ~~THE~~ FORMATION CONDITIONS OF GELATIN FILMS ON BONDING STRENGTH

S.A. Shreiner and P.I. Zubov

It was shown in a study of the mechanism of protein gel formation that the physicochemical properties of such systems depend very largely on the conditions of the formation of their structure [1]. Since protein solutions are widely used for impregnation and gluing of various materials, it was of interest to determine how the formation conditions of an adhesive film (glue layer) affect the strength of the bond. The effects of the drying rate of the glue layer, concentration of the adhesive solution, and presence of low-molecular additives on bonding strength were studied.

The bonding strength was measured in terms of the average shearing force required to break down the bond between two overlapping optically polished steel plates, 10 mm thick and 20 mm wide, glued together.

The amount of gelatin in the glue layer was determined from the weights of the specimens, weighed on an analytical balance, before and after gluing, and the thickness of the layer was found by calculation. The plates were fixed in the dynamometer by means of a self-centering device. Before being joined, the plates were washed thoroughly in alcohol-ether mixture, dried, and rubbed with finely powdered active charcoal.

The adhesive solutions were prepared as follows. Weighed amounts of gelatin were mixed in flasks (with ground glass stoppers) with water, or with solutions of urea or acetamide, or other substances of known composition by weight, and after 4 hours of swelling were heated at 60° on a water bath until the gels were completely dissolved. A definite amount of the solution was then applied from a pipet to the surface of the plate intended to form the joint, and this was covered by the other plate. The joined plates were placed in holders and pressed in a spring screw press at 5-20 kg (according to the concentration of the adhesive solution and the thickness of the layer); they were left in this state during the whole hardening period of the adhesive layer. The very first experiments showed that the bonding strength depends on the rate of drying; the bonding strength is always less after rapid than after slow drying. Since slow drying is very inconvenient in experimental work, the rate of drying was accelerated by gradual increase of temperature as the solvent was removed.

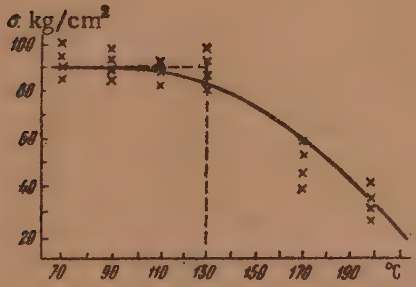

Fig. 1. Effect of temperature on the average shearing force (σ) required to separate glued polished steel surfaces.

The following drying procedure was adopted, as giving the most reproducible results in our experimental conditions. The drying was performed for three days at 30°, and for three days at 35°, with final drying of 8-hour periods at 60, 80, and 100°. It was found that with small amounts of water in the adhesive layer the drying can be done at even higher temperatures. Degradation of the adhesive film becomes appreciable only above 130° as can be seen from the experimental data in Fig. 1, where the average destroying shearing force is plotted against the drying temperature. The reproducibility of parallel experiments is indicated by the scatter of the experimental points in this and the other figures.

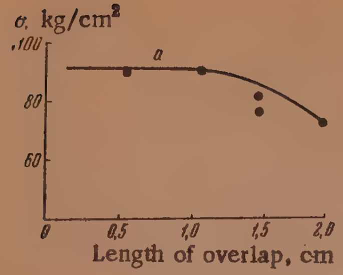

Fig. 2. Effect of length of overlap (in cm) of a joint glued by 20% gelatin solution on the average destroying force σ; thickness of adhesive layer $5 \cdot 10^{-4}$ cm.

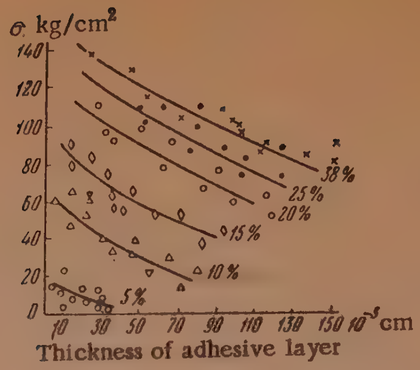

Fig. 3. Effect of thickness of adhesive layer and concentration of adhesive gelatin solution on bonding strength.

Fig. 2 shows the variation of the destroying force with the length of the overlap. It is seen in Fig. 2 that with overlaps up to ~ 1 cm the average destroying force is practically constant. Similar results have been obtained by others [2]. An overlap of 0.9 cm was used in the subsequent experiments.

Some workers found [3, 4] that bonding strength depends on the thickness of the adhesive layer. This was found to be the case in our experiments also; Fig. 3 shows that the bonding strength depends not only on the thickness of the adhesive layer, but also on the concentration of the adhesive solution. Under equal drying conditions and with equal layer thicknesses, the bonding strength increases with gelatin concentration. Change of concentration from 5 to 30% more than doubles the bonding strength.

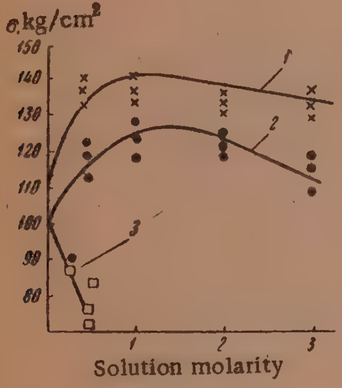

Fig. 4. Effect of additives on the bond strength between two steel plates glued by 20% gelatin solution based on solutions of different concentrations of: 1) urea, 2) acetamide, 3) sodium sulfate.

This effect, which is of interest and of practical importance, is in our opinion associated with the kinetics of relaxation of the internal stresses which arise during removal of solvents from dilute and concentrated adhesive solutions. As is known [1], relaxation effects and the nature of the internal stresses depend not only on gel concentration but also on the number of local intermolecular bonds. Increase of intermolecular interaction should retard while weakening accelerates relaxation processes [5]. The experimental data in Fig. 4 show that this is the case during formation of a glue layer. The curves in Fig. 4 show that the highest adhesive strength is found in adhesive films containing urea (Curve 1); this is probably because urea, by weakening intermolecular interaction, accelerates the relaxation processes. In presence of acetamide, which is a less active plasticizer, although the bond strength increases (Curve 2), the increase is considerably less than with urea.

Addition of sodium sulfate, which increases intermolecular interaction in gelatin solutions, decreases the bonding strength.

SUMMARY

1. The bonding strength between two lapped polished steel plates depends on the formation conditions of the adhesive film and the concentration of the gelatin solution.

2. Additives of low molecular weight, which weaken interaction between the polymer chains, increase the bonding strength; additives which intensify interaction between the macromolecules decrease it.

The L. Ya. Karpov Physicochemical Institute
The Leningrad Technological Institute
for the Food Industry

Received January 12, 1957

LITERATURE CITED

[1] P. I. Zubov, Z. N. Zhurkina, and V. A. Kargin, Colloid J. No. 2, 109 1947.

[2] N. A. de Bruyne, Aircraft Eng. 16, 115 140 1940.

[3] I. W. Mc Bain, W. B. Lee, J. Phys. Chem. 31, 1675 1927.

[4] O. Gerngross, Z. ang. Chem. 37, 847, 1924; 44, 232 1931.

[5] P. I. Zubov, Z. N. Zhurkina, and V. A. Kargin, Colloid J., 16, 109 1954.*

---

* Original Russian pagination. See C. B. translation.

~~LETTER TO THE~~ EDITOR

THE TENSILE STRENGTH OF MIXTURES ~~OF~~ POLYETHYLENE ~~AND~~ POLYISOBUTYLENE

R.I. Feldman and A.K. Mironova

In studies of the mechanical properties [1, 2] and gas permeability [3] of systems consisting of polymers and low-molecular plasticizers, we established relationships between the conventional modulus conventional tensile strength, and gas permeability of mixtures in the high-elastic state, the corresponding characteristics of the constituents, and the composition expressed in mole fractions. The characteristics of the components were calculated in the form of limiting values by extrapolation of the linear plots of the logarithm of the property against the composition of a given system. It was reported [1] that for a system polymer I – polymer II the values of these characteristics at suitable temperatures can be found experimentally. The present communication deals with a study of the conventional (nominal) tensile strength of the system polyethylene-polyisobutylene in which polyisobutylene can be regarded as a polymeric plasticizer for polyethylene. Mixtures of the two polymers in different proportions were prepared by mixing on rolls with subsequent pressing. The polymers and mixtures were extended to break in a Polanyi dynamometer at 20° ± 0.5. The uniaxial extension rate was constant at 2 mm/minute.

Conventional Tensile Strengths of Polyethylene-Polysobutylene Mixtures, Determined Experimentally and Calculated by Equation (1). Extension Rate 2 mm/minute, t = 20°

Composition in mole fractions		Conventional tensile strength in kg/mm²	
polyethylene	polyisobutylene	experimental	calculated by Equation (1)
1.000	0	1.140	—
0.886	0.114	0.685	0.666
0.825	0.175	0.402	0.497
0.747	0.253	0.353	0.344
0.666	0.334	0.234	0.234
0.572	0.418	0.202	0.157
0.461	0.539	0.085	0.089
0.333	0.667	0.038	0.048
0.183	0.817	0.028	0.024
0	1.000	0.010	—

Plots of the logarithms of the conventional tensile strengths of the mixtures against the composition on mole fractions are linear. The mole fractions of polyethylene (N_{pe}) and polyisobutylene (N_{pib}) were calculated from the molecular weights of the monomer units C_2H_4 and C_4H_8 ($N_{pe} + N_{pib} = 1$).

The C_2H_4 group was taken as the unit in polyethylene, as the polyisobutylene unit corresponds to two carbon atoms in the principal macromolecular chain.

If the plot of log σ as a function of N is linear then the conventional tensile strengths of various polyethylene-polyisobutylene mixtures (σ_m) can be expressed in terms of the conventional tensile strengths of polyethylene (σ_{pe}) and polyisobutylene (σ_{pib}), in the first approximation as follows:

$$\sigma_m = \sigma_{pe}^{N_{pe}} \cdot \sigma_{pib}^{N_{pib}} . \qquad (1)$$

The Table gives the experimental values of σ_m and values calculated by Equation (1).

Because of the fairly good agreement between σ_m^{calc} and σ_m^{exp}, it is possible to calculate the conventional tensile strength of a mixture from experimentally determined tensile strengths of the constituent polymers for given extension conditions. The composition of a mixture of given properties can also be calculated.

The Moscow Technological Institute
for the Light Industry

Received June 2, 1957

LITERATURE CITED

[1] R. I. Feldman, Proc. Acad. Sci. USSR, 97, No. 6, 1033 1954.

[2] R. I. Feldman and A. K. Mironova, Colloid J., 17, No. 6, 465 1955.*

[3] S. I. Sokolov, S. A. Reitlinger and R. I. Feldman, Colloid J., 19, 624 1957.*

---

* Original Russian pagination. See C. B. translation.

COLLOID JOURNAL OF THE U.S.S.R. IN ENGLISH TRANSLATION

September-October, 1957

TABLE OF CONTENTS

	Page	Russ. Page
1. Development of Colloid Chemistry in the USSR	531	529
2. Antifrictional Properties of Disperse Phases of Metal Organosols. M. L. Barabash and E. M. Natanson	535	534
3. Modification of Polyamide Properties by the Inclusion Method. A. N. Bykov, M. I. Ivanova and A. B. Pakshver	543	542
4. Studies of Electroosmosis in Binary Powder Mixtures Consisting of Particles of Different Chemical Nature. O. N. Grigorov and K. P. Tikhomolova	549	548
5. The Influence of Intermolecular Interaction on the Properties of Rubber Solutions. V. E. Gul and V. A. Berestnev	553	552
6. The Possibility of Surface Activation and Passivation of Nuclei in Water Vapor Condensation. G. I. Izmailova, P. S. Prokhorov and B. V. Deryagin	557	556
7. Adsorption of Water Vapor by Silica and Hydration of its Surface. A. V. Kiselev and G. G. Muttik	563	562
8. Influence of Pore Size and Surface Hydration of Silica on Adsorption of Nitrogen Vapor. A. V. Kiselev and E. V. Khrapova	573	572
9. The Specific Heat of Bound Water. O. D. Kurilenko	585	584
10. Variations of the Specific Volume of Rubber During Stretching. A. B. Kusov, V. I. Trofimova and Yu. I. Nilova	587	587
11. Effect of the Nature of the Emulsifier on the Thermal Decomposition of Cumene and 1,1-Diphenylethane Hydroperoxides in an Aqueous Medium. R. V. Kucher and S. D. Kazmin	591	592
12. The Structure of Thin Copper Sulfide Films at the Solution–Gas Interface. S. G. Mokrushin, Yu. D. Tkachev and O. K. Shabalina	595	597
13. The Effect of Structure on the Viscosity of Butadiene–Styrene Rubbers. A. S. Novikov and F. S. Tolstukhina	599	599
14. Dependence of the Elastic Constant of a Vulcanizate on the Molecular Weight of the Original Rubber. L. S. Priss	607	607
15. Reciprocal Displacement of Components in Ion Exchange Chromatography. G. V. Samsonov and V. A. Orestova	615	615
16. Investigation of the Structure of Branched Polystyrene by the Light Scattering Method. I. G. Soboleva, N. V. Maktletsova and S. S. Medvedev	619	619
17. The Effect of Plasticizers on the Hydrogen Permeability of Polyvinyl Chloride. S. I. Sokolov, S. A. Reitlinger and R. I. Feldman	625	624
18. Specific Heats of Aqueous Solutions of Some Soaps. V. I. Solnyshkin	629	629
19. Light Scattering by a Coagulating Aerosol. O. M. Todes and A. A. Chekunov	633	633

(Continued on inside back cover)

COLLOID JOURNAL OF THE U.S.S.R. IN ENGLISH TRANSLATION

September-October, 1957

TABLE OF CONTENTS (continued)

	Page	Russ. Page
20. Orientation of Clay Particles During Deformation of a Clay Body. V. S. Fadeeva	641	640 3
21. Effects of the Types of Rubber and Carbon Black on the Formation of Carbon–Rubber Gels. Z. V. Chernykh and V. G. Epshtein	645	644
22. The Structure of Gels. 11. Effect of the Formation Conditions of Gelatin Films on Bonding Strength. S. A. Shreiner and P. I. Zubov	651	651

Letter to the Editor

	Page	Russ. Page
23. The Tensile Strength of Mixtures of Polyethylene and Polyisobutylene. R. I. Feldman and A. K. Mironova	655	654 2

SUBSCRIPTION PRICES SLASHED ON SOVIET CHEMISTRY TRANSLATIONS

Consultants Bureau is pleased to announce a major achievement in our program to reduce the prices of our cover-to-cover translations of Soviet scientific journals.

An arrangement with the National Science Foundation has made possible reductions of up to 90% in the annual subscription prices of 3 major Soviet chemical journals in complete translation. These price slashes, effective with the first issues of 1957, put these cover-to-cover translations well within the reach of even the most limited library and research laboratory budgets.

The journals affected are:	(Former price)	New price*	Non-profit research and academic institutions*
Journal of General Chemistry (*Zhurnal Obschei Khimii*). Oldest and major Soviet chemical journal—theoretical and experimental reports in organic, analytical and physical chemistry. 12 issues per year, approximately 3600 pages.	$170.00	**$90.00**	**$30.00**
Journal of Applied Chemistry (*Zhurnal Prikladnoi Khimii*). All aspects of applied chemical research. Reports from research institutes and USSR factory laboratories. 12 issues per year, approximately 2000 pages.	95.00	**60.00**	**20.00**
Bulletin of the Academy of Sciences USSR, Div. Chem. Sci. (*Izvestiya Akad. Nauk SSSR, Otdel. Khim. Nauk*). Research reports in all fields of chemistry, by leading members of the Soviet Academy of Sciences. General, organic, inorganic, physical and biological chemistry. 12 issues per year, approximately 1500 pages.	150.00	**45.00**	**15.00**

*Foreign subscriptions—$5.00 higher.

These cover-to-cover translations by Consultants Bureau bilingual chemists are clearly reproduced by the multilith process from IBM cold-type composition. All tabular material, diagrams and photographs are reproduced, integal with the text. Each issue is staple bound and is mailed to subscribers immediately on publication.

CONSULTANTS BUREAU, INC.

227 West 17th Street, New York 11, N. Y.
Telephone: ALgonquin 5-0713 **Cable: CONBUREAU NEWYORK**